1992

Organometallic and reactor studies of the thiophene hydrodesulfurization mechanism

John William Benson
Iowa State University

Order Number 9311477

Organometallic and reactor studies of the thiophene hydrodesulfurization mechanism

Benson, John William, Ph.D.

Iowa State University, 1992

U·M·I
300 N. Zeeb Rd.
Ann Arbor, MI 48106

Organometallic and reactor studies of the thiophene hydrodesulfurization mechanism

by

John William Benson

A Dissertation Submitted to the

Graduate Faculty in Partial Fulfillment of the

Requirements for the Degree of

DOCTOR OF PHILOSOPHY

Department: Chemistry
Major: Inorganic Chemistry

Approved:

Signature was redacted for privacy.

In Charge of Major Work

Signature was redacted for privacy.

For the Major Department

Signature was redacted for privacy.

For the Graduate College

Iowa State University
Ames, Iowa

1992

DEDICATION

To Jill, Dad and Mom

TABLE OF CONTENTS

GENERAL INTRODUCTION. MECHANISMS OF THIOPHENE HYDRODESULFURIZATION

Preface

This dissertation contains results of research in two different areas: organometallic synthesis and microreactor studies. First, in the organometallic studies, thiophene coordination to metal complexes is studied. Of the different possible modes of thiophene coordination to organotransition metal centers (and possibly an active site on the catalyst surface), the $\eta^1(S)$-bound mode has been rarely studied due to the weak interaction of the thiophene S atom with transition metal centers. Therefore, one goal of this research is to study the $\eta^1(S)$-bound thiophenes and use the results to establish the plausibility of thiophene binding to the catalyst in this manner.

Second, the 1,3-butadiene from thiophene deuterodesulfurization in a flow-microreactor at 400 °C over $PbMo_{6.2}S_8$ is examined by mass and ^2H NMR spectrometries for its deuterium content and the postion of incorporation. The goal of this study is to determine which of the mechanisms in the literature are supported by the deuterium uptake under these reaction conditions. This work was done in collaboration with Professor Glenn L. Schrader of the Chemical Engineering Department at Iowa State University.

This dissertation contains a general introduction and four papers. The general introduction is a review of the mechanisms of thiophene HDS as proposed in the literature. The following four papers contain the results of my research as it was submitted for journal publication. Literature citations, tables and figures pertain only to the papers in which they are included. Included with the final paper is an appendix detailing the operation of the microreactor that will not be published. Following the appendix is a general summary and additional references for the general introduction.

Introduction

Hydrodesulfurization (HDS) is a heterogeneous catalytic process which removes sulfur from crude oil and coal liquids.[1] HDS ranks as one of the largest catalytic processes performed in 1992; 27.2 million barrels of oil are treated each day worldwide.[2] This pretreatment of petroleum feedstocks is necessary for a number of reasons. First, sulfur must be removed, as it poisons the precious metal catalysts used in catalytic reforming. Second, even the least reactive sulfur containing compounds, which form sulfur oxides during the combustion of the fossil fuels must be removed, due to increasingly strict air quality regulations. Third, HDS is increasingly important in a time of dwindling oil reserves, as it becomes necessary to process heavy crude oil residua (b. pt. > 350 °C), which contain as high as 5 - 10 % sulfur,[3] into cleaner burning fuels. HDS is also used to remove the pungent odor from feedstocks.

The organosulfur compounds shown in Figure 1, typical of those found in petroleum feedstocks, are listed in approximate order of decreasing HDS activity.[1a] The thiols, sulfides and disulfides, usually found in the lighter fractions, are among the easiest to desulfurize requiring milder conditions than thiophenes. The aromatic thiophenic compounds, especially thiophene, benzo[b]thiophene and dibenzothiophene, are much more difficult to desulfurize. Due to their lower reactivity, they are often used as models for studying the HDS process. The HDS reaction of the most widely studied organosulfur compound, thiophene, is shown in equation 1.

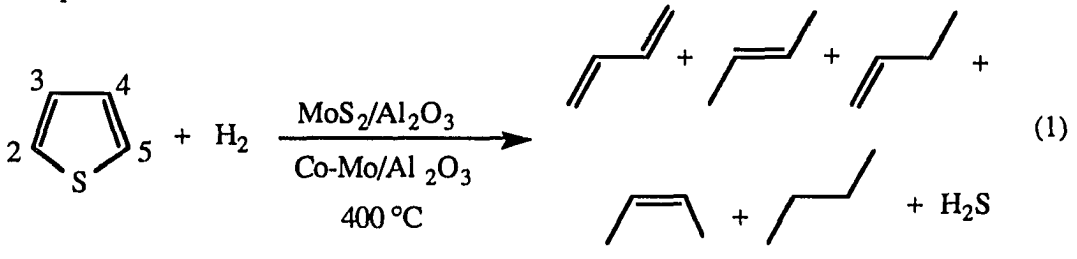

(1)

Compound Class	Structure
Thiols (mercaptans)	R–S–H
Sulfides	R–S–R'
Disulfides	R–S–S–R'
Thiophenes	
Benzo[b]thiophenes	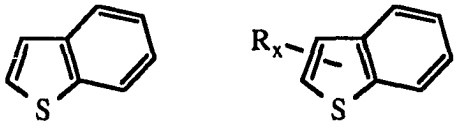
Dibenzothiophenes	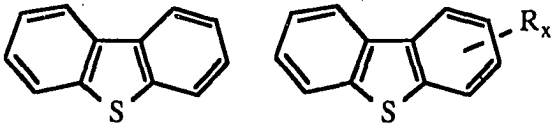
Benzonaphthothiophenes	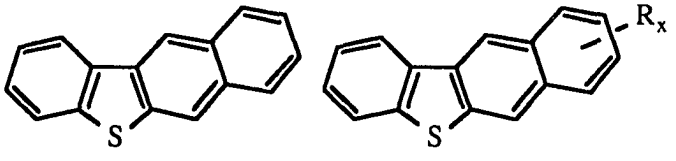
Benzo[*def*] dibenzothiophenes	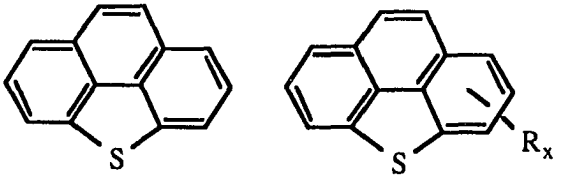

Figure 1. Organosulfur compounds typically found in petroleum.

Industrially, desulfurization reactions are run at temperatures of 340 - 425 °C and at pressures of 55 - 170 atmospheres.[4] Under these conditions, HDS is an exothermic, essentially irreversible process. The catalysts used for this process and the other related hydrotreating processes, hydrogenation, hydrodenitrogenation (HDN), hydrodeoxygenation (HDO) and hydrodemetalation (HDM) are supported sulfides of molybdenum and tungsten on alumina promoted with cobalt and nickel. Generally, these catalysts are quite complex. Although the catalyst has been probed by different spectroscopic techniques, such as EXAFS,[5] *in situ* raman,[6] X-ray diffraction,[7] XPS[8] and Mössbauer[9] spectroscopies, the nature of the active sites as well as the exact role of the promoter are as of yet not well understood.

Despite the research that has been carried out on thiophene HDS, the exact mechanism, or mechanisms of this process are still not clear. Although a number of mechanisms have been proposed, they all follow either of two general pathways: initial hydrogenation of the thiophene followed by desulfurization, or initial C-S bond cleavage followed by partial or complete hydrogenation of the hydrocarbon fragment. The initial step in any HDS mechanism is the adsorption of thiophene to an active site on the catalyst surface. A number of possible binding modes have been demonstrated in several organometallic complexes containing thiophene as ligands.[10] These complexes, their reactions, as well as numerous reactor studies, provide the basis for these mechanisms. A number of reviews of HDS have been written recently.[4, 11] The following section is a summary of HDS mechanisms published by 1992. The mechanisms published prior to 1986 have been reviewed in detail by Sauer[12] and will be reviewed only briefly here. After 1986, four mechanisms have been published, and they will be examined in greater detail.

Hydrodesulfurization Mechanisms

Hydrogenation Mechanisms

One of the first mechanistic studies of thiophene HDS was reported by Moldavski and Prokoptscuk[13] in 1932. These early studies of thiophene HDS over MoS_2 at 350 °C produced butane as the major product. In later work by Griffith, Marsh and Newling,[14] however, using a continuous flow reactor at atmospheric pressure over MoS_2 and Ni_2S_3, butenes were detected as the major hydrocarbon product. No THT or n-BuSH was observed. A partial hydrogenation mechanism (eq 2) for HDS was suggested by

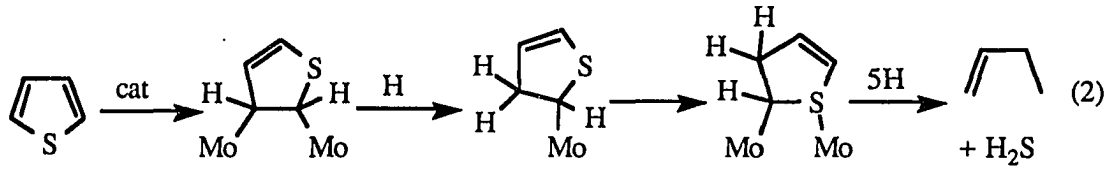

(2)

Griffith et al. that begins with two-point thiophene adsorption to two neighboring Mo atoms. One H atom is added to thiophene to partially hydrogenate one double bond, followed by attachment of the S atom to another Mo that activates the thiophene to undergo C-S bond cleavage to give 1-butene and H_2S.

Kieran and Kemball[15] studied the HDS of thiophene, THT and straight-chain thiols over MoS_2 and WS_2; THT was detected from thiophene HDS. They found thiophene was the hardest to desulfurize, followed by THT and then the thiols. From their evidence they proposed a reaction scheme for thiophene HDS that occurred in three stages: hydrogenation of the thiophene ring, ring cleavage and desulfurization and isomerization and desorption of desulfurized products.

Kwart, Schuit and Gates[16] reviewed the inconsistencies in the one-point mechanism proposed by Lipsch and Schuit (*vide infra*). Citing work by Daudel et al.,[17] who estimated the electron density of the S atom and the C-C double bonds, they proposed a mechanism in which the thiophene is initially bound through the C2-C3 double bond, since it has the highest electron density. Their mechanism describes in detail the addition of two H atoms to the double bond to give an η^1(S)-coordinated 2,3-dihydrothiophene intermediate. This intermediate can undergo β-elimination of H with C-S bond cleavage to give an η^1(S)-butadiene thiolate. Two paths are possible for cleaving the second C-S bond: either the second olefin is coordinated and hydrogenated followed by a β-elimination step which cleaves the second C-S bond to give 1,3-butadiene, or the first olefin remains coordinated, is then hydrogenated as the second C-S bond cleaves to desorb 1-butene.

C-S Cleavage Mechanisms

Hydrogenolysis of thiophene over vanadium oxide catalyst,[18] using a flow-reactor at 350 - 400 °C produced 1,3-butadiene in detectable amounts along with butenes and butane. From this work by Komarewski and Knaggs, a mechanism was suggested in which the thiophene is adsorbed to two neighboring V atoms similar to that of Moldavski and Prokoptscuk (*vide ante*), except through the C-S bond, which is cleaved step wise to give 1,3-butadiene and H_2S (eq 3). Subsequent hydrogenation of 1,3-butadiene gives butenes and butane.

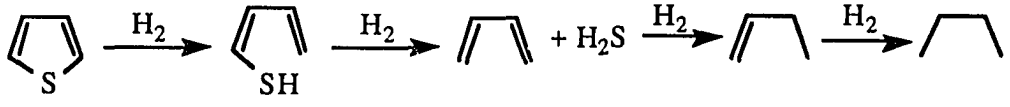

(3)

In the early 1960's, Owens and Amberg[19] published a mechanism based on their flow reactor studies of thiophene HDS over Co-Mo/Al_2O_3 and chromia/Al_2O_3 catalysts. Under atmospheric hydrogen pressure, 1,3-butadiene was detected over the chromia catalyst. They also observed that 1-butene was always produced in amounts greater than the calculated equilibrium distribution for butenes. It was concluded that C-S cleavage is the first step in the mechanism to give 1,3-butadiene followed by hydrogenation of 1,3-butadiene to 1-butene. The 1-butene isomerizes to give the detected distribution of butenes. In an extension of this work, the kinetics of the HDS of thiophene, 2-methylthiophene, 3-methylthiophene and tetramethylthiophene were examined by Desikan and Amberg.[20] Their results indicated that C-S cleavage is the rate determining step in the mechanism. The work was also supported by Kolboe and Amberg,[21] who also detected 1,3-butadiene from thiophene HDS at atmospheric pressure over MoS_2, Co-Mo/Al_2O_3 and chromia catalysts.

Kolboe[22] investigated the HDS of thiophene, tetrahydrothiophene and n-BuSH over MoS_2, Co-Mo/Al_2O_3 and chromia/Al_2O_3 catalysts. He observed that more 1,3-butadiene was produced from THT than from thiophene and that the overall product distibutions were different in each case. The desulfurization of n-BuSH produced mainly 1-butene and butane. He concluded that the intermediates in the HDS of thiophene, THT and n-BuSH were not the same. Based on his observations, he proposed a thiophene HDS mechanism that begins with dehydrosulfurization (eq 4), where C-S bond cleavage occurs stepwise to give H_2S and 1,3-butadiyne, a pathway analogous to alcohol dehydration. The adsorbed 1,3-butadiyne, which is not observed, is quickly hydrogenated to give 1,3-butadiene. The reaction of THT gives 1,3-butadiene directly by a similar mechanism in which β-hydrogens are lost as the C-S bonds cleave. This mechanism for thiophene HDS is supported by IR studies[23] of thiophene decomposition on MoS_2 films which exhibited a band between 3140 and 3160 cm^{-1} that was

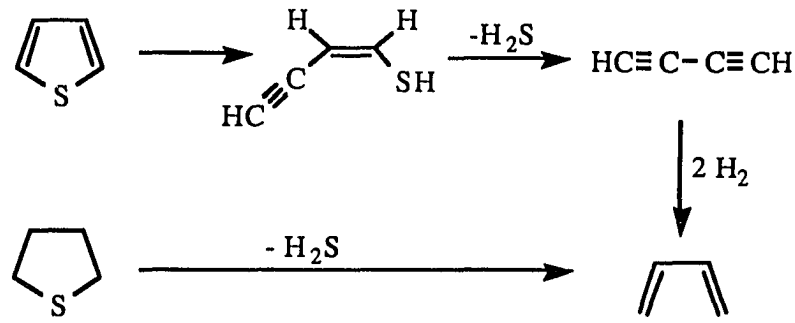

(4)

assigned to the asymmetric stretch of an acetylene species on the surface and supported the idea that thiophene decomposes through an acetylenic intermediate.

In 1969, Lipsch and Schuit[24] described adsorption and reactivity studies of thiophene over Co-Mo/Al_2O_3. Based on this work and the previous work by Kolboe, Amberg, and Nickolson,[25] they proposed a detailed mechanism for thiophene HDS, which included a description of the adsorption mode of thiophene and the active site on the catalyst (eq 5). In

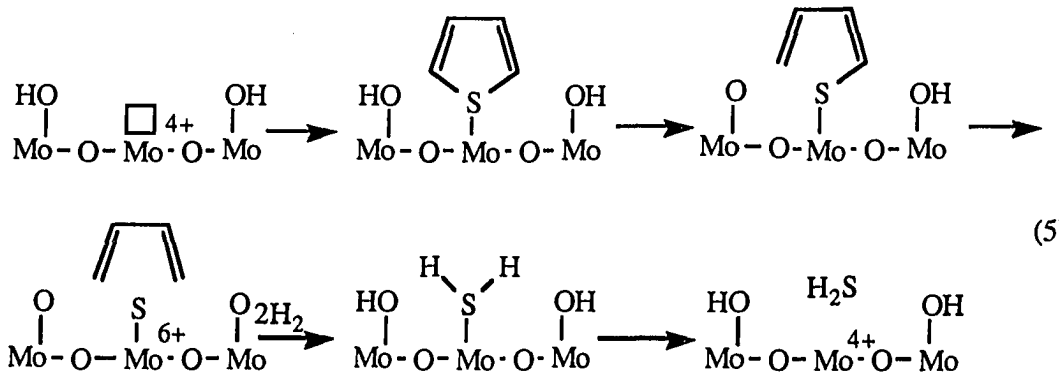

(5)

their "One Point" mechanism, thiophene was proposed to be bound through the sulfur atom in an η^1(S)-fashion through one of its lone pairs to an anion vacancy. This thiophene surface interaction was thought to weaken the C-S bond. Transfer of H atoms from neighboring

-OH groups cleave the C-S bonds to give 1,3-butadiene and an adsorbed S atom. Addition of two equivalents of H_2 gives H_2S and regenerates the active site.

Although Kolboe does not explicitly identify the origin of the hydrogen in the product H_2S, Mikovsky, Silvestri and Heineman[26] interpreted his mechanism as to include an intramolecular β-elimination, whereby H in the H_2S comes from the β-positions on thiophene. Thus, examining the D content of the H_2S produced during thiophene deuterodesulfurization (DDS) (using D_2 instead of H_2) would differentiate between the mechanisms proposed by Kolboe and Amberg (eq 6). They observed the isotopic content

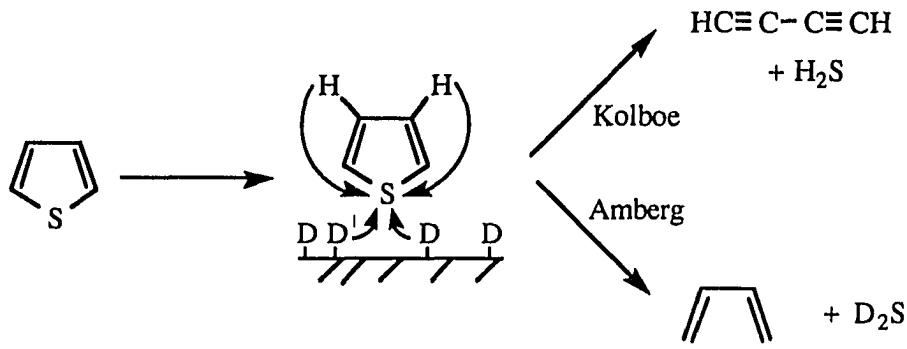

(6)

of the H_2S (H_2S, HSD and D_2S) from thiophene DDS over Co-Mo/Al_2O_3 to be nearly all H at low conversion. Their results suggested that the hydrogen on H_2S comes from thiophene, not from the surface, supporting Kolboe's mechanism. Their results are similar to those of McCarty and Schrader[27] who observed 96% H_2S from thiophene DDS. McCarty and Schrader postulated, however, that the H atoms came from H "pools" on the surface created by thiophene exchange, not the intramolecular reaction.

Cowley[28] also investigated the isotopic distribution of H_2S from the DDS of 2,5-dideuterothiophene over Co-Mo/Al_2O_3. In contrast to the results of Mikovski and McCarty, he found a majority of D_2S (44%) and HDS (39%) and concluded that the Kolboe mechanism was not the route for thiophene HDS. Similarly, Blake, Eyre, Moyes and

Wells[29] found 91% D_2S and 9% HSD at 5% conversion of thiophene over MoS_2 in a static reactor at 365 °C. Based on his results, Cowley proposed a mechanism that begins with initial π-adsorption of the thiophene ring to a metal site. This π-adsorption, also proposed by Zdrazil,[30] was believed to disrupt the ring aromaticity, making it susceptable to C-S bond cleavage. While π-bonded, the sulfur associates with surface hydrogen, and C-S bond cleavage occurs by addition of H from nearby -SH groups.

Dual Path Mechanism

Devanneaux and Maurin[31] studied HDS of thiophene and benzo[b]thiophene over Co-Mo/Al_2O_3 in order to look at the discrepancies between the C-S cleavage and hydrogenation mechanisms. At higher reaction pressure, approaching those of commercial processes, THT and butenes were detected, prompting them to propose a dual path mechanism for both thiophene C-S bond cleavage and hydrogenation. From kinetic analysis of these reactions, the existence of two separate catalytic sites for hydrogenation and desulfurization were proposed. Supporting a mechanism involving hydrogenated surface species, Zdrazil[32] in examining C-S bond strengths, found that direct cleavage of the aromatic C-S bond would be difficult. Disruption of the thiophene aromaticity by hydrogenation destroys any double bond character of the C-S bond, making it easier to desulfurize.

New Mechanisms

Hydrogenation Mechanism Proposed by Sauer, Markel, Schrader and Angelici.[33]

In recent years, organotransition metal complexes containing thiophene as ligands have provided models of thiophene binding modes and reactivities which may be similar to the types of reactions occurring on the catalyst surface. Microreactor studies and reactions of organometallic complexes containing thiophene are used as the basis for the mechanism in Figure 2.[33] The mechanism begins with adsorption of thiophene to a surface metal site in the η^5-binding mode. This binding mode has been observed in a number of organometallic complexes: $CpM(\eta^5\text{-}T)^+$ ($Cp = \eta^5\text{-}C_5H_5$; T = thiophene; M = Fe,[34] Ru[35]), $(CO)_3Cr(\eta^5\text{-}T)$,[36] $(CO)_3Mn(\eta^5\text{-}T)^+$ [37] and $Cp^*M(\eta^5\text{-}T)^{2+}$ ($Cp^* = \eta^5\text{-}C_5Me_5$; M = Rh, Ir)[38] and $(\eta^5\text{-}T)M(PPh_3)_2^+$ (M = Rh, Ir).[39] Reactions[37b] of $(CO)_3Mn(\eta^5\text{-}T)^+$ with metal hydride complexes $HFe(CO)_4^-$ and $HW(CO)_5^-$ (eq 7) add H^- to the 2-position on thiophene,

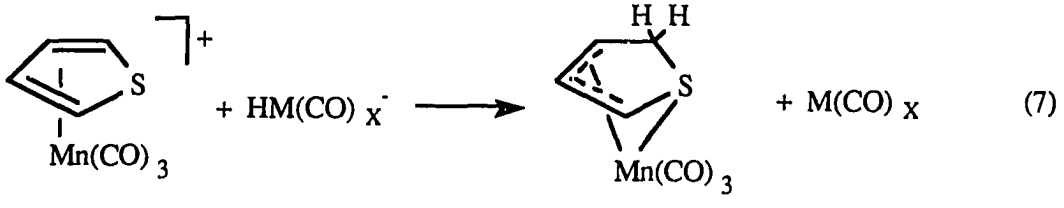

(7)

$M(CO)_X = Fe(CO)_4$ or $W(CO)_5$

breaking the thiophene aromaticity and forming an allyl sulfide intermediate. Thus, it is likely that H^- from a nearby metal hydride on the catalyst surface transfers to the 2-position (step *a*) (Figure 2) of the π-bound thiophene.

In step *b*, an H^+ from a nearby -SH group adds to the 3-position on the thiophene,

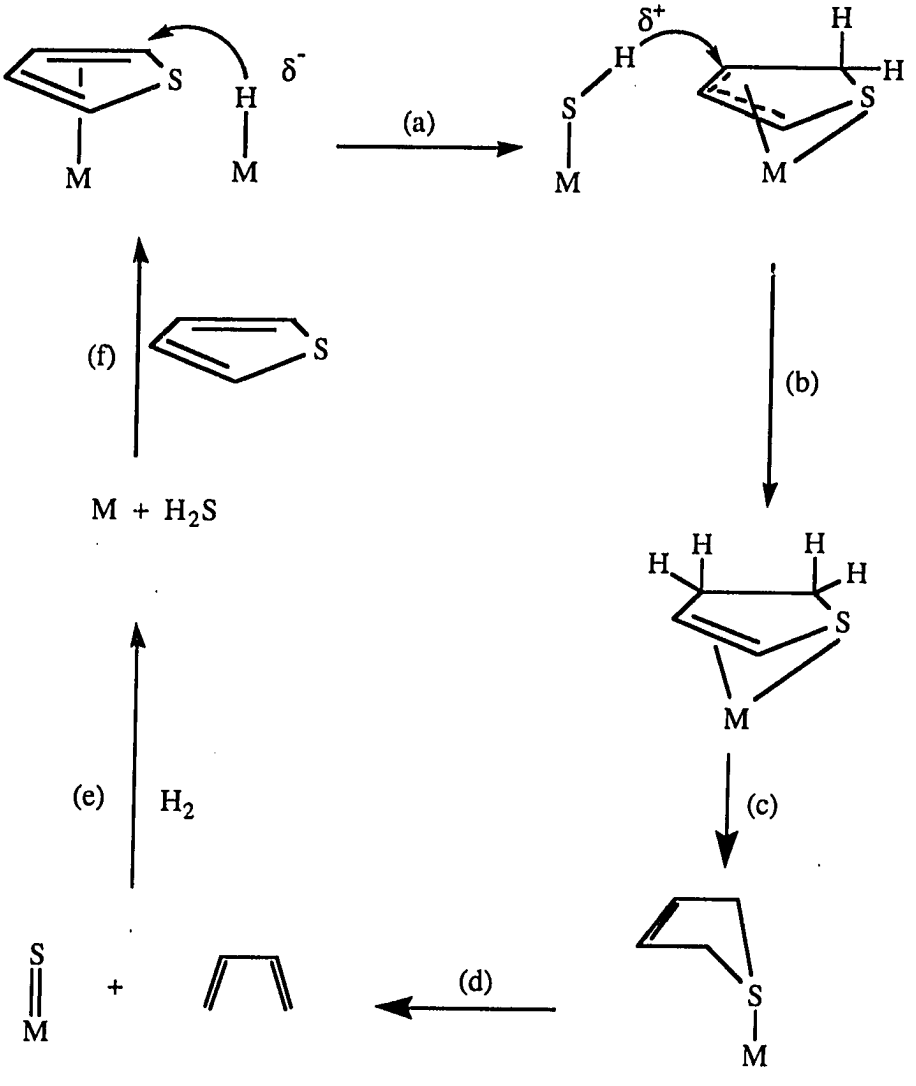

Figure 2. Hydrogenation mechanism proposed by Sauer, Markel, Schrader and Angelici.[33]

forming a 2,3-dihydrothiophene (2,3-DHT) species on the catalyst surface. This step is based on the reactions of the organometallic complex, $(CO)_3Mn(\eta^4\text{-}T\cdot H)$,[37b] with strong acids in which the 3-position of the thiophene ring is protonated (eq 8) to give 2,3-DHT. It is

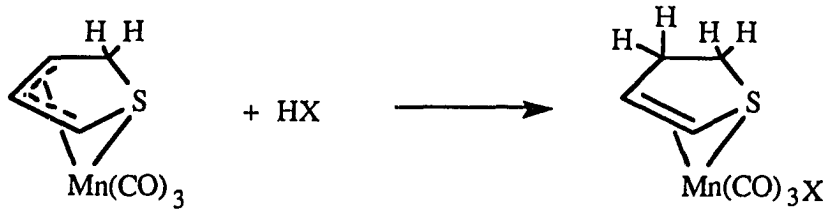

(8)

HX = HCl, CF_3SO_3H or CF_3CO_2H

unclear as to whether the 2,3-DHT species will be bound through both the S atom and the olefin, or through just the S. The structure of this Mn complex could not be determined as it was too unstable for an X-ray experiment. However, 2,3-DHT was displaced from the complex with MeCN. Other complexes containing only the S-bound 2,3-DHT are known.[40]

Step *c* (Figure 2) is an isomerization step converting the 2,3-DHT to the thermodynamically more stable 2,5-dihydrothiophene (2,5-DHT). This isomerization was observed in reactor studies in which 2,3-DHT was converted to 2,5-DHT over Re/Al_2O_3 at 300 °C.[41] Likewise, the reverse reaction was observed when 2,5-DHT was passed over the same catalyst under the same conditions. Although the exact nature of this isomerization is unknown, 1,3-H shifts are well known in organic chemistry as are olefin isomerizations in heterogeneous and homogeneous catalysis.[42] Finally, as the 2,5-DHT intermediate is coordinated to a metal atom, sulfur is abstracted and 1,3-butadiene is desorbed (step *d*) leaving a metal sulfide which is subsequently hydrogenated to give H_2S (step *e*). This decomposition of 2,5-DHT was observed over Re/Al_2O_3. Likewise, decomposition of 2,5-DHT complexes of metal carbonyls, $(CO)_4Fe$(2,5-DHT),[33b] $(CO)_5W$(2,5-DHT) and

$(CO)_9Re_2(2,5\text{-DHT})$[43] at 120 °C occurs rapidly to give 1,3-butadiene, 2,5-DHT and a residue that is likely to be the metal sulfides.

The mechanism in Figure 2 leads to just 1,3-butadiene formation. The observed hydrogenated hydrocarbons, butenes and butane (eq 1), are likely produced directly from 1,3-butadiene hydrogenation, rather than from thiophene by a separate pathway. Reactor studies[21, 27] indicate that as conversion of thiophene decreases, the relative amount of 1,3-butadiene increases. Also, the amount of 1-butene is in excess of its equilibrium value , indicating that 1,3-butadiene is the first desulfurized product, which is rapidly hydrogenated.

C-S Cleavage Mechanism Proposed by Chen and Angelici[44]

A second mechanism derived from reactions involving organometallic complexes is shown in Figure 3.[44] This mechanism begins with η^4-coordination of the thiophene C-C double bonds to a metal site on the catalyst surface. In the η^4-mode, which has been observed in organometallic model complex, $Cp^*Ir(\eta^4\text{-}2,5\text{-}Me_2T)$,[44] (2,5-$Me_2$T = 2,5-dimethylthiophene) the sulfur atom is bent out of the plane of the thiophene ring as is seen in the structure of the complex (eq 9). Base catalyzed C-S bond cleavage using Et_3N, basic Al_2O_3 or "Red-Al" $[(CH_3OCH_2CH_2O)_2AlH_2^-]$ converts the η^4-thiophene to the ring-opened form, $Cp^*Ir(C,S\text{-}2,5\text{-}Me_2T)$ (eq 9), at room temperature. This is the basis for step *a*

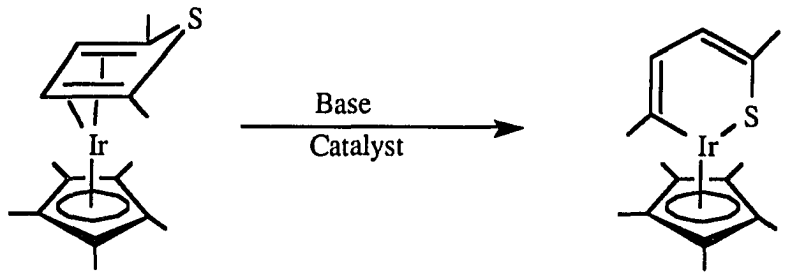

(9)

$Cp^*Ir(\eta^4\text{-}2,5\text{-}Me_2T)$ $\qquad$ $Cp^*Ir(C,S\text{-}2,5\text{-}Me_2T)$

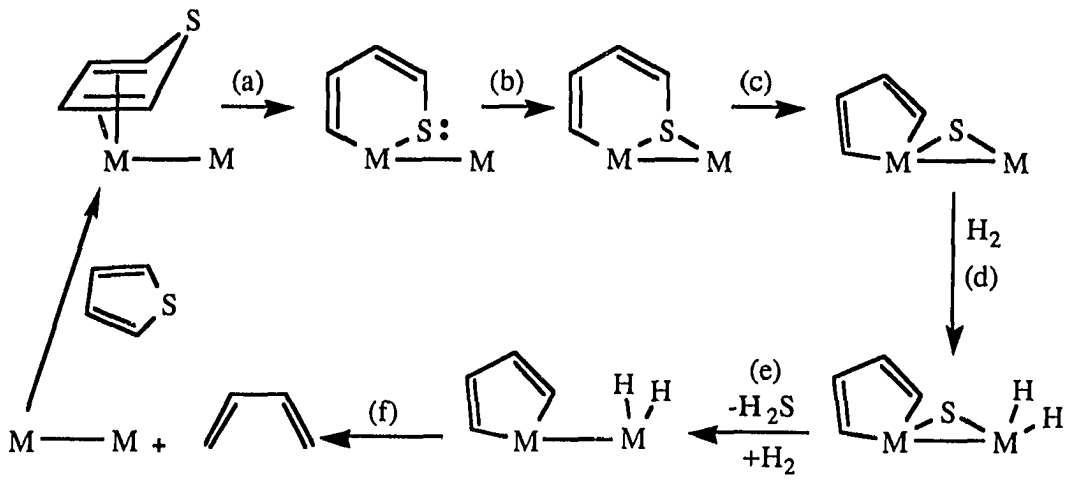

Figure 3. C-S cleavage mechanism proposed by Chen and Angelici.[44]

(Figure 3) in which the C-S bond in the η^4-thiophene cleaves to form a six-membered ring on the surface. Other complexes, $Cp^*Rh(PMe_3)(C,S\text{-}Th)$[45] (Th = T, 2,5-$Me_2$T, 2-methylthiophene [2-MeT], 3-methylthiophene [3-MeT], benzo[b]thiophene [BT] and dibenzothiophene [DBT]), $Cp^*Rh(C,S\text{-}Me_4T)$[46] (Me_4T = tetramethylthiophene) and $Cp^*_2Co_2(\mu_2\text{-}C,S\text{-}T)$[47] are known in which the metal atom inserts into the C-S bond. A nearby metal may interact with the thiophene S atom, as in step *b*, which cleaves the second C-S bond forming a bridging metal sulfide and a five-membered metallacyclopentadiene ring.

The surface species formed in step *b* is based on an organometallic complex isolated from the reaction of Cp*Ir(η^4-2,5-Me_2T) and $Fe(CO)_5$ in THF (eq 10). Although the exact structure

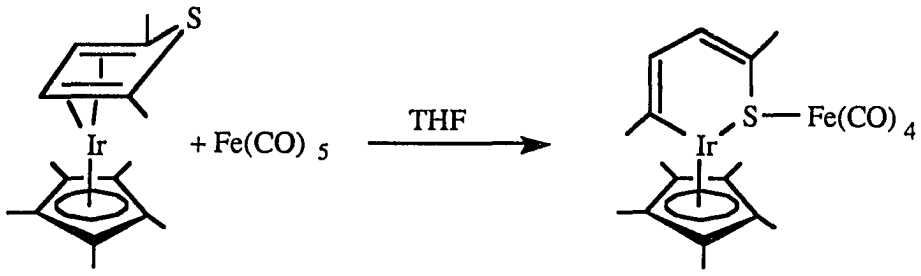

(10)

of the product of equation 10 was not established by X-ray, the figure drawn is consistant with spectroscopic data. The structures of the intermediates formed in steps *c* and *e* (Figure 3) are based on similar reactions of both Cp*Ir(η^4-2,5-Me_2T) and Cp*Ir(C,S-2,5-Me_2T) with $Fe_2(CO)_9$ and $Fe_3(CO)_{12}$ in THF (eq 11).[44] In both cases, these reactions give the

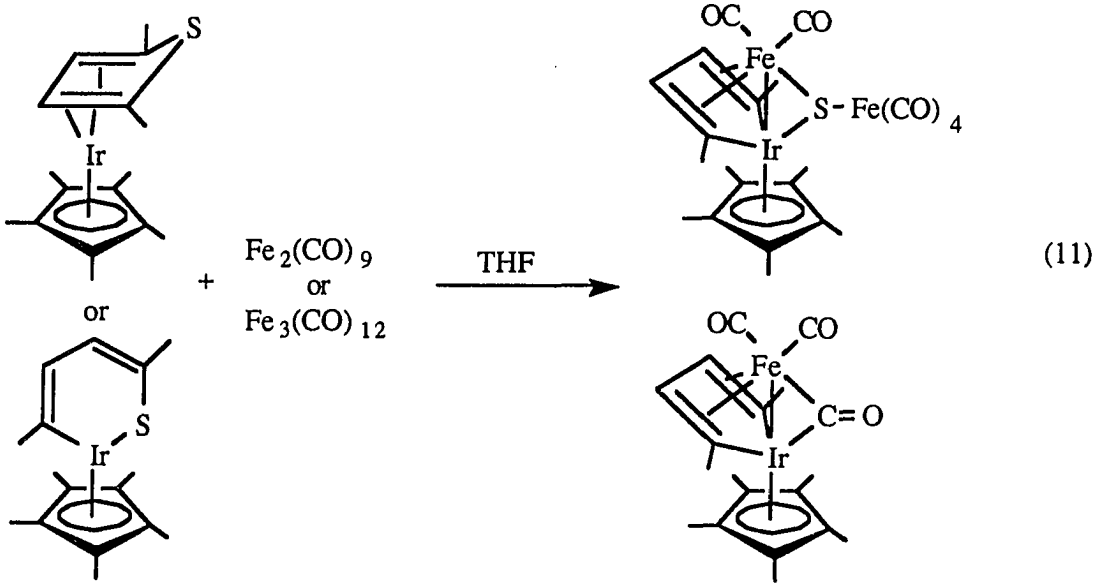

(11)

metallacyclopentadiene complexes shown in equation 11. These reactions provide a pathway for sulfur abstraction from thiophene without prior hydrogenation of the thiophene ring. Following the formation of the 5-membered ring (step *c*, Figure 3), the S atom and the C_4 fragment could be abstracted as H_2S and 1,3-butadiene by reaction with surface hydrogen. Although just 1,3-butadiene is produced by this mechanism, it is likely that subsequent hydrogenation gives the distribution of C_4 products

Mechanism Proposed by Curtis and Coworkers

Curtis and coworkers[48] proposed the HDS mechanism shown in Figure 4. In their study, two catalysts were prepared by depositing the cluster compounds, $Cp'_2Mo_2Fe_2S_2(CO)_8$ and $Cp'_2Mo_2Co_2S_3(CO)_4$, ($Cp' = \eta^5$-C_5H_4Me) on alumina. Heating the supported clusters under He or H_2 evolves CO, C_5H_5Me, CO_2, CH_4 and H_2S or Me_2S, producing an active catalyst for both HDS and CO hydrogenation. The HDS activities of thiophene and THT as well as the hydrogenation activities of 1,3-butadiene and 1-butene were measured in a differential flow reactor at 300 °C using both reduced and sulfided forms of the catalyst.

In their mechanism (Figure 4), thiophene is initially hydrogenated to either 2,5-DHT (step *a*), a likely intermediate in the formation of 1,3-butadiene or to 2,3-DHT (step *b*) as an intermediate in the formation of 1-butene. The small amounts of 1,3-butadiene detected in their reactions prompted their proposal of a separate, minor pathway for its formation. Separate formation of 2,3-DHT is described as the major reaction pathway as 1-butene (step *c*) is always in excess of the equilibrium values for butenes. Dual path formation of hydrocarbons, however, is contrary to other proposals which suggest that 1-butene results from direct hydrogenation of 1,3-butadiene.[27] This second pathway to 2,3-DHT also leads to cracking (step *d*) of the hydrocarbon fragment to give propene, methane and methanethiol.

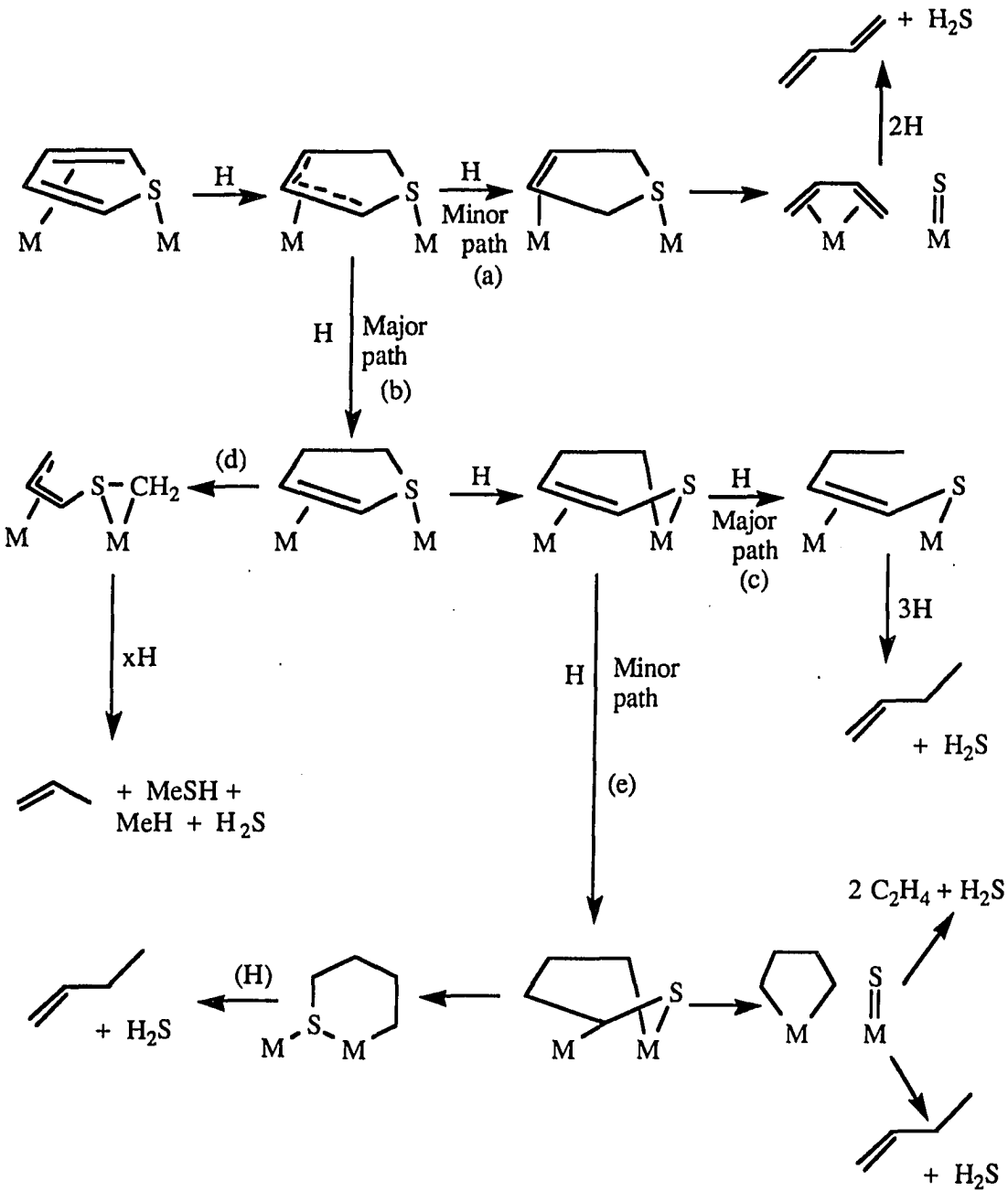

Figure 4. HDS mechanism proposed by Curtis from reactions of thiophene over $CoMoS/Al_2O_3$ and $FeMoS/Al_2O_3$ catalysts at 300 °C.[48]

Since cracking was not detected with control reactions of 1,3-butadiene or 1-butene, it was proposed to occur while the S atom is still attached to the C_4 fragment. Insertion of the metal atom into the C-S bond (step *e*) of 2,3-DHT may also lead to the formation of a metallacyclopentane, which may produce either ethylene as a cracked hydrocarbon, or a metallathiocyclohexane to give 1-butene.

Mechanism Proposed by Delmon and Dallons[49]

Delmon and Dallons[49] reviewed the HDS literature and published a mechanism which explains the results published thus far. Their mechanism, shown in Figure 5, takes into account the nature of the catalyst while remaining consistent with known mechanisms in organic chemistry. They suggest that the reaction is concerted and can be extended to O and N heterocycles as well.

In step *a*, the carbons in thiophene are π-adsorbed to a coordinatively unsaturated Mo atom through both double bonds in an η^4-binding mode, while the thiophene S atom interacts with neighboring -SH groups by partial donation of the surface -SH lone pairs to the thiophene S atom. Although the nature of this interaction is not described (i.e. which orbitals on thiophene accept the donation from the surface S atoms), this interaction is unlikely as the sulfur in η^4-thiophene organometallic complexes[50] is a strong Lewis base, rather than a Lewis acid. They suggest, however, that this initial interaction increases the adsorption strength over just π-adsorption and makes this mechanism universal to other 5-membered aromatic heterocyclic rings (furan, pyrrole). The second step in the mechanism (step *b*) is hydrogenation of C3 and C4. As this hydrogenation takes place, C2 and C5 form bonds with the surface Mo atom. This is based on the fact that partial hydrogenation is necessary to break the aromaticity of the ring and weaken the C-S bond.

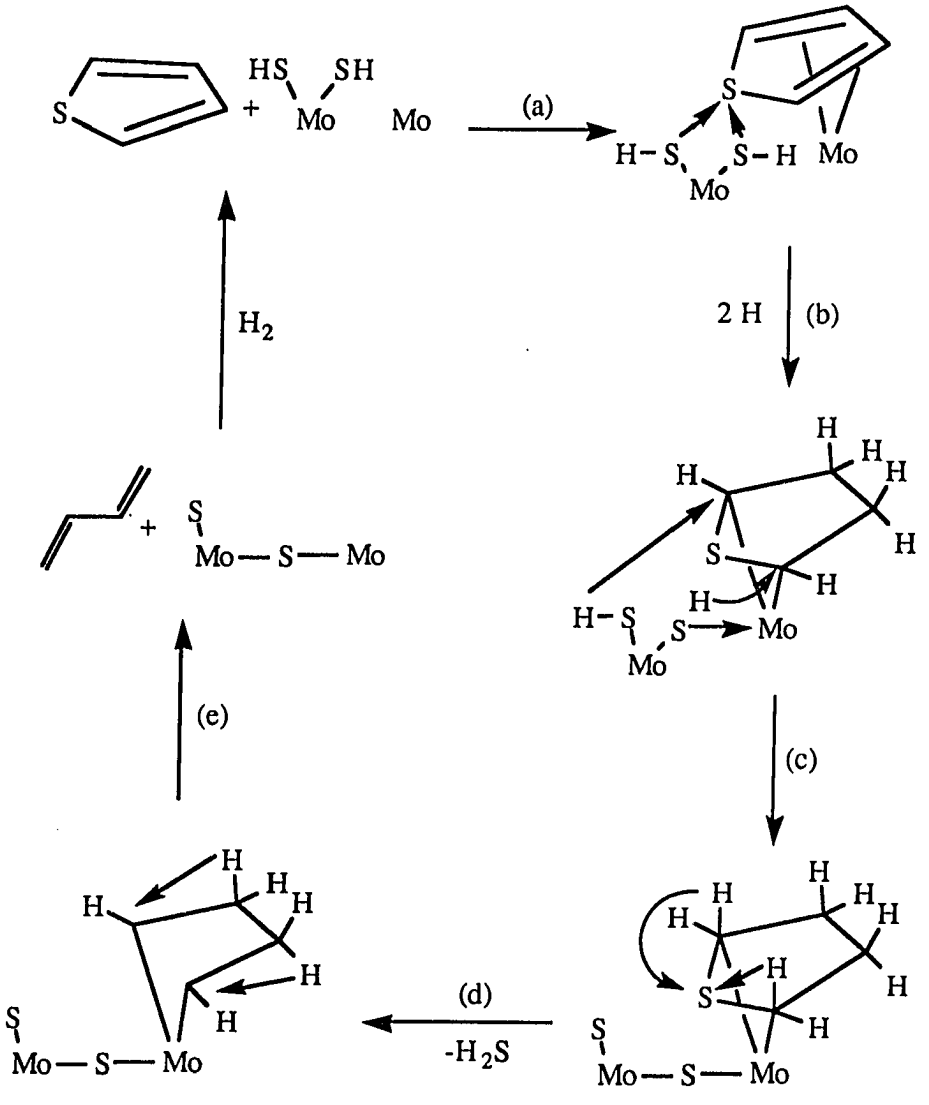

Figure 5. HDS mechanism to give 1,3-butadiene proposed by Delmon and Dallons.[49]

Steps *c*, *d* and *e* are proposed to occur simultaneously. The surface -SH groups each transfer H atoms (step c) to C2 and C5 forming hypervalent carbons similar to those found in S_N2 type transition states which weaken the thiophene C2-H and C5-H bonds; the thiophene H's transfer to the thiophene S atom to form H_2S, which is desorbed (step *d*). This step accounts for the formation of H_2S rather than D_2S during the deuterodesulfurization thiophene (using D_2 gas instead of H_2) as seen by Mikovski[26] and McCarty and Schrader,[27] and the D_2S observed by Cowley.[28] Under low concentrations of hydrogen (i.e. low H_2 pressure), H atoms from C3 and C4 migrate to C2 and C5 and 1,3-butadiene is desorbed (step *e*) from the surface. Higher concentrations of H_2 reform the -SH groups which subsequently hydrogenate the C_4 fragment to give butenes and butane.

PAPER I. EQUILIBRIUM STUDIES OF THE DISPLACEMENT OF $\eta^1(S)$-THIOPHENES (Th) FROM $Cp(CO)(PPh_3)Ru(\eta^1(S)\text{-}Th)^+$, 1

ABSTRACT

The reactions of $Cp(CO)(PPh_3)RuCl$ ($Cp = \eta^5\text{-}C_5H_5$) with Ag^+ and thiophenes (Th) produce the stable sulfur-bound ($\eta^1(S)$-) thiophene complexes $Cp(CO)(PPh_3)Ru(\eta^1(S)\text{-Th})^+$ (Th = T, 2-MeT, 3-MeT, 2,5-Me_2T, Me_4T, BT and DBT). Equilibrium constants, K', for the displacement of thiophene (T) by methyl-substituted thiophenes, benzo[b]thiophene (BT) and dibenzothiophene (DBT), $Cp(CO)(PPh_3)Ru(\eta^1(S)\text{-T})^+ + Th' \rightleftharpoons Cp(CO)(PPh_3)Ru(\eta^1(S)\text{-Th}')^+ + T$, increase in the following order: T(1) < 2,5-Me_2T(2.76) < 2-MeT(4.11) < 3-MeT(6.30) < BT(29.9) < Me_4T(57.4) < DBT(74.1). In general, methyl groups on thiophene increase K', but a-methyl groups reduce the stabilities of complexes with 2-MeT, 2,5-Me_2T and Me_4T ligands due to a steric interaction with the PPh_3 group. The ligands tetrahydrothiophene (THT) and MeCN have K' values ($> 7.1 \times 10^6$) which are much higher than any of the thiophenes, while MeI (K' = 2.0) is a slightly better ligand than T. An x-ray structure determination of $[Cp(CO)(PPh_3)Ru(2\text{-MeT})]BF_4$ is also reported.

INTRODUCTION

An important step in the mechanism(s) of thiophene (T) hydrodesulfurization (HDS) on heterogeneous catalysts is its adsorption to a metal site on the catalyst surface. Results of heterogeneous studies[2] indicate that methyl-substituted thiophenes bind more strongly to a Co-Mo/Al_2O_3 catalyst than thiophene itself; the adsorption equilibrium constants (in parentheses) decrease in the order: 2,5-dimethylthiophene (2,5-Me_2T) (2.5) > 3-methylthiophene (3-MeT) (1.7) ≈ 2-methylthiophene (2-MeT) (1.6) > T (1.0). The same trend is observed for η^5-thiophene binding in the complexes $CpRu(\eta^5\text{-Th})^+$;[3] equilibrium constants (K') for equation (1) decrease with different methyl-substituted thiophenes Th' in

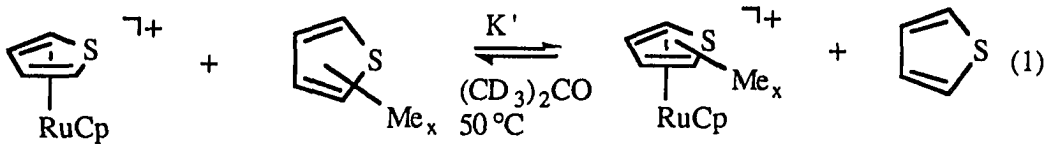

(1)

the order: Me_4T > 2,5-Me_2T > 3-MeT > 2-MeT > T (where Me_4T is tetramethylthiophene). These similar trends are consistent with η^5- binding of thiophene on the catalyst surface. The well-known reactivity[4] of η^5-thiophene in its metal complexes also supports such an adsorption mode on HDS catalysts.

The other common mode of thiophene coordination in transition metal complexes is h^1(S) through the sulfur.[5] Complexes exhibiting this mode of thiophene binding are as follows: $Ru(NH_3)_5(T)^{+2}$,[6] $Cp(CO)_2Fe(T)^+$,[7] $CpFe(NCMe)_2(2,5\text{-}Me_2T)^+$,[8] $W(CO)_3(PCy_3)_2(T)$,[9] $(C_5H_4CH_2C_4H_3S)Ru(PPh_3)_2^+$,[10] $Cp^*(CO)_2Re(T)$,[11] $MX_2(L')$ (M = Pd, X = Cl, Br, I, SCN; M = Pt, X = Cl),[12a] $[CuCl_2(L')]_2$,[12b] Pd(h^3-allyl)(L') [12c] (L' = 2,5,8-trithia[9](2,5)thiophenophane), $[RuClL_2]BF_4$ [13] (L = 6-(2-thienyl)-2,2'-bipyridine) and $Cp(CO)_2Fe(2,5\text{-}Me_2T)^+$.[14] Kinetic studies[15] of the replacement (eq 2) of methyl-

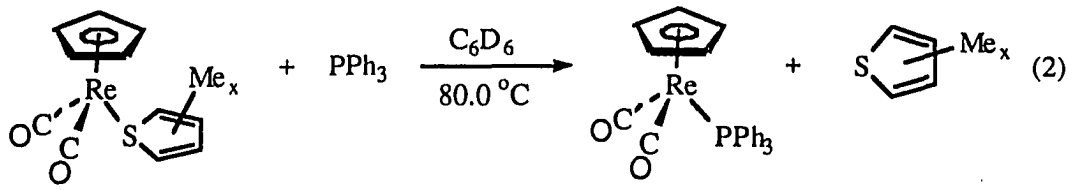

(2)

substituted thiophenes in $CpRe(CO)_2(\eta^1(S)\text{-Th})$ show that the rate of thiophene dissociation decreases in the order (rate constants, 10^7 s^{-1}, in parentheses): T(3000) > 3-MeT(1200) > 2-MeT(91) > 2,5-Me_2T(13) > Me_4T(2.7) > DBT(1.6). This trend suggests that Me groups on the thiophene strengthen its coordination to the Re, and there is no evidence of steric repulsion between the Me groups in the 2- and 5-positions with the other ligands around the Re; such a repulsion would be expected to weaken the M-S bond if the ligand were bound perpendicularly to the metal. However, structures of S-bound thiophenes indicate that the S is pyramidal,[5,7b,16,17] so that the Me groups in the 2- and 5-positions pose less of a steric problem. The above trend in rates of thiophene dissociation suggests that methyl-substitution of thiophenes would strengthen bonding to metal sites on HDS catalysts. However, no studies of the relative equilibrium binding strengths of $\eta^1(S)$-thiophenes have been reported.

In this study, we present the synthesis and characterization of a new series of stable $\eta^1(S)$-thiophene complexes $Cp(CO)(PPh_3)Ru(Th)^+$ where Th = T, 2-MeT, 3-MeT, 2,5-Me_2T, Me_4T, BT and DBT; structures and numbering systems of benzo[b]thiophene, BT, and dibenzothiophene, DBT, are shown below:

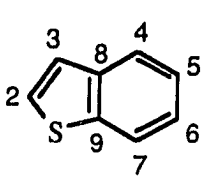

BT

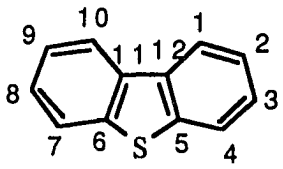

DBT

Also, the X-ray-determined structure of $Cp(CO)(PPh_3)Ru(2\text{-}MeT)^+$ and equilibrium constants, K', for the thiophene displacement reactions shown in equation 3 are reported.

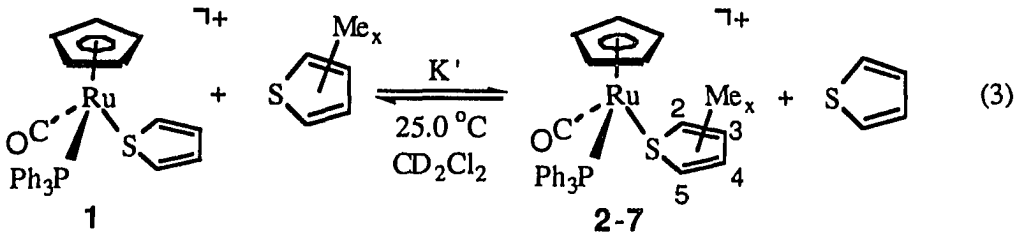

1 2-7 (3)

Th: 2-MeT (**2**), 3-MeT (**3**), 2,5-Me $_2$T (**4**), Me $_4$T (**5**), BT (**6**), DBT (**7**)

EXPERIMENTAL

General Procedures

All reactions were performed under a nitrogen atmosphere in reagent grade solvents using standard Schlenk techniques.[18] Diethyl ether was distilled under nitrogen from Na/benzophenone; CH_2Cl_2 was distilled from CaH_2. Solvents were stored over 4-Å molecular sieves under nitrogen. The ^1H and $^{13}C\{^1H\}$ NMR spectra were obtained on Nicolet NT-300 or Varian VXR-300 spectrometers using CD_2Cl_2 as the solvent and the internal lock. Fast atom bombardment (FAB) spectra were obtained in a CH_2Cl_2-3-nitrobenzyl alcohol matrix with a Kratos MS-50 mass spectrometer; infrared spectra of the compounds were taken in CH_2Cl_2 solvent with a Nicolet 710 FT-IR spectrometer. Elemental analyses were performed by Galbraith Laboratories, Inc., Knoxville, TN.

The starting material, $Cp(CO)(PPh_3)RuCl$, was prepared according to a literature procedure.[19] Thiophene was purified as previously described.[20] 2-MeT, 3-MeT, 2,5-Me_2T, BT, DBT and $AgBF_4$ were purchased from Aldrich and used without further purification. Me_4T was prepared by a literature method.[21]

General Procedure for the Preparation of the $[Cp(CO)(PPh_3)Ru(Th)]BF_4$ Complexes (1-7)

To a solution of 0.103 g (0.209 mmol) of $Cp(CO)(PPh_3)RuCl$ and 1.04 mmol of the thiophene, Th, in 25 mL of CH_2Cl_2 was added 0.056 g (0.288 mmol) of solid $AgBF_4$. The mixture was stirred at room temperature for 1 h, during which time the solution turned cloudy and the color changed from orange to yellow. The solution was filtered through Celite, and the volatiles were removed under vacuum. The residue was dissolved in a minimum amount of CH_2Cl_2 (the BT and DBT reaction residues were first washed with two 5-mL portions of

Et_2O to remove the excess thiophene), and the solution was layered with Et_2O. The products (**1-7**) crystallized overnight at -20°C as yellow powders or pale orange crystals in 65-85% yields.

Characterization of 1-7

[Cp(CO)(PPh_3)Ru(T)]BF_4 (**1**): ^1H NMR δ 7.21 (m, 2H) and 7.12 (m, 2H), T; 4.98 (s, Cp); 7.60-7.30 (m, PPh_3). $^{13}C\{^1H\}$ NMR δ 137.95 (d, $^3J_{CP}$ = 2.11 Hz, C2, C5) and 132.12 (s, C3, C4), T; 88.14 (d, $^2J_{CP}$ = 1.5 Hz, Cp); 200.17 (d, $^2J_{CP}$ = 18.3 Hz, CO); 133.41-129.67 (PPh_3), [a typical pattern for the PPh_3 resonances in all of the complexes **1-7** is 133.41 (d, J_{CP} = 11.23 Hz), 132.64 (d, J_{CP} = 51.6 Hz), 132.09 (d, J_{CP} = 2.79 Hz) and 129.67 (d, J_{CP} = 10.71 Hz)]. IR υ(CO) 1999 cm^{-1}(s).

[Cp(CO)(PPh_3)Ru(2-MeT)]BF_4 (**2**): ^1H NMR δ 6.98 (m, H4), 6.92 (m, H3), 6.52 (d, J = 1.1 Hz, H5) and 2.42 (d, J = 1.2 Hz, Me), 2-MeT; 4.95 (s, Cp); 7.62-7.22 (m, PPh_3). $^{13}C\{^1H\}$ NMR δ 152.02 (d, $^3J_{CP}$ = 3.7 Hz), 134.44 (s), 132.36 (s), 129.35 (s) and 14.43 (s, Me), 2-MeT; 88.35 (d, $^2J_{CP}$ = 1.5 Hz, Cp); 200.74 (d, $^2J_{CP}$ = 18.6 Hz, CO); 133.38-129.71 (PPh_3). IR υ(CO) 1996 cm^{-1} (s). Anal. Calcd. for $C_{29}H_{26}BF_4OPRuS$: C, 54.30; H, 4.09. Found: C, 54.00; H, 4.24.

[Cp(CO)(PPh_3)Ru(3-MeT)]BF_4 (**3**): ^1H NMR δ 7.02 (m, H2, H5), 6.60 (m, H4) and 2.22 (d, J = 1.2 Hz, Me), 3-MeT; 4.99 (s, Cp); 7.60-7.28 (m, PPh_3). $^{13}C\{^1H\}$ NMR δ 143.70 (s), 137.84 (d, $^3J_{CP}$ = 2.2 Hz), 135.22 (s), 130.99 (d, $^3J_{CP}$ = 2.1 Hz) and 16.38 (s, Me), 3-MeT; 88.14 (d, $^2J_{CP}$ = 1.5 Hz, Cp); 200.35 (d, $^2J_{CP}$ = 18.6 Hz, CO); 133.4-129.6 (PPh_3). IR υ(CO) 1997 cm^{-1} (s).

[Cp(CO)(PPh_3)Ru(2,5-Me_2T)]BF_4 (**4**): ^1H NMR δ 6.62 (s, 2H) and 2.07 (s, Me), 2,5Me_2T; 4.96 (s, Cp); 7.59-7.32 (m, PPh_3). $^{13}C\{^1H\}$ NMR δ 148.71 (d, $^3J_{CP}$ = 0.9 Hz), 129.33 (s) and 14.81 (s, Me), 2,5-Me_2T; 88.14 (d, $^2J_{CP}$ = 1.5 Hz, Cp); 200.17 (d, $^2J_{CP}$ =

19.5 Hz, CO); 133.4-129.7 (PPh_3). IR υ(CO) 1996 cm^{-1} (s). FAB: m/e 569.0 (M^+), 456.9 (M^+-2,5-Me_2T). Anal. Calcd. for $C_{30}H_{28}BF_4OPRuS$: C, 54.97; H, 4.31. Found: C, 55.00; H, 4.23.

[Cp(CO)(PPh_3)Ru(Me_4T)]BF_4 (**5**): ^1H NMR δ 1.97 (s, Me) and 1.93 (s, Me), Me_4T; 4.93 (s, Cp); 7.56-7.30 (m, PPh_3). $^{13}C\{^1H\}$ NMR δ 139.28 (s), 137.45 (d, $^3J_{CP}$ = 1.5 Hz), 13.78 (s, Me) and 12.60 (s, Me), Me_4T; 88.13 (d, $^2J_{CP}$ = 1.5 Hz, Cp); 201.60 (d, $^2J_{CP}$ = 20.1 Hz, CO); 133.4-129.6 (PPh_3). IR υ(CO) 1992 cm^{-1} (s).

[Cp(CO)(PPh_3)Ru(BT)]BF_4 (**6**): ^1H NMR δ 7.86 (m, 1H), 7.73 (m, 1H), 7.41 (d, J = 5.7 Hz, 1H), 6.40 (d, J = 5.7 Hz, 1H) BT; 7.61-7.34 (m, PPh_3); 4.84 (s, Cp). $^{13}C\{^1H\}$ NMR δ 146.10 (d, $^3J_{CP}$ = 3.4 Hz), 139.53 (s), 132.45 (d, $^3J_{CP}$ = 1.0 Hz), 131.15 (s), 128.88 (s), 127.81 (s), 126.48 (s) and 124.05 (s), BT; 88.68 (d, $^2J_{CP}$ = 1.5 Hz, Cp); 200.76 (d, $^2J_{CP}$ = 18.6 Hz, CO); 133.4-129.7 (PPh_3). IR υ(CO) 1994 cm^{-1} (s). Anal. Calcd. for $C_{32}H_{26}BF_4OPRuS$: C, 56.73; H, 3.87. Found: C, 57.14; H, 3.91.

[Cp(CO)(PPh_3)Ru(DBT)]BF_4 (**7**): ^1H NMR δ 8.11 (d, J = 7.5 Hz, 1H) and 7.67-7.28 (m, 22 H) DBT and PPh_3; 4.76 (s, Cp). $^{13}C\{^1H\}$ NMR δ 142.15 (d, $^3J_{CP}$ = 2.19 Hz), 136.61 (s), 129.47 (s), 129.39 (s), 124.77 (s) and 123.44 (s), DBT; 88.96 (d, $^2J_{CP}$ = 1.5 Hz, Cp); 200.95 (d, $^2J_{CP}$ = 19.23 Hz, CO); 133.38-129.76 (PPh_3). IR υ(CO) 1993 cm^{-1} (s). FAB: m/e 641.0 (M^+), 457.0 (M^+-DBT). Anal. Calcd. for $C_{36}H_{28}BF_4OPRuS{\cdot}0.8CH_2Cl_2$: C, 55.56; H, 3.75. Found: C, 55.82; H, 3.91. The solvating CH_2Cl_2 was identified in ^1H NMR spectra of **7** in CD_2Cl_2 solvent.

Preparation of [Cp(CO)(PPh_3)Ru(THT)]BF_4 (8)

Solid $AgBF_4$ (40.1 mg, 0.206 mmol) was added to a solution of Cp(CO)(PPh_3)RuCl (59.2 mg, 0.120 mmol) in 20 mL of CH_2Cl_2. The resulting solution was stirred for 5 min during which time the solution turned cloudy. Tetrahydrothiophene, THT (55 ml, 0.62

mmol) was added, and the mixture was stirred for 30 min. The reaction was worked up as for complexes **1-7** to give **8** as a light green powder (40.1 mg, 52.8% yield). ^{1}H NMR δ 2.73 (m) and 2.00 (m), THT; 5.18 (s, Cp); 7.54-7.30 (m, PPh_3). IR υ(CO) 1984 cm^{-1}(s). Anal. Calcd. for $C_{28}H_{28}BF_4OPRuS \cdot 0.54\ CH_2Cl_2$: C, 50.60; H, 4.33. Found: C, 50.98; H, 4.58. The solvating CH_2Cl_2 was identified in ^{1}H NMR spectra of **8** in CD_2Cl_2 solvent.

X-ray Diffraction Study of [Cp(CO)(PPh_3)Ru(2-MeT)]BF_4 (2)

A single crystal of **2** suitable for an x-ray diffraction study was obtained by slow evaporation of a CD_2Cl_2 solution under nitrogen at room temperature and mounted on a glass fiber. Data collection and reduction information are given in Table I. The cell constants were determined from a list of reflections found by an automated search routine. Lorentz and polarization corrections were applied. A correction based on a decay in the standard reflections of 0.2% was applied to the data. An absorption correction based on a series of psi-scans was applied. The agreement factor for the averaging of observed reflections was 1.7% based on F. The positions of the Ru, S and P atoms were determined from a Patterson map.[22] All remaining non-hydrogen atoms were found in one successive Fourier map. All non-hydrogen atoms were refined with anisotropic thermal parameters. After the least-squares converged, all hydrogen atoms were placed at calculated positions, 0.95 Å from the attached atom with isotropic temperature factors set equal to 1.3 times the isotropic equivalent of that atom. The hydrogen atom positions were not refined in the final least-squares cycle. Bond distances, angles, and atomic positional parameters for **2** are given in Tables II-III. An ORTEP drawing of the cation in **2** is shown in Fig. 1.

Table I. Crystal and Data Collection Parameters for $[Cp(CO)(PPh_3)Ru(2\text{-}MeT)]BF_4$ (2)

Formula	$[RuPSOC_{29}H_{26}]^+[BF_4]^-$
Formula weight	646.47
Space Group	$P\bar{1}$
a, Å	9.441(1)
b, Å	10.4858(6)
c, Å	14.281(2)
α, deg	87.690(8)
β, deg	82.14(1)
γ, deg	89.01(1)
V, Å3	1399.(3)
Z	2
d_{calc}, g/cm3	1.534
Crystal size, mm	0.12 x 0.10 x 0.10
$\mu(MoK_\alpha)$, cm^{-1}	7.2
Data collection instrument	Enraf-Nonius CAD4
Radiation (monochromated in incident beam)	
	$MoK_\alpha(\lambda = 0.71073$ Å)
Orientation reflections,	
number, range (2θ)	25, $18.2 < \theta < 35.2$
Temperature, °C	22.0(10)
Scan method	θ-2θ

Table I (continued)

Data col. range, 2θ, deg.	4.0-55.0
No. data collected:	6427
No. unique data, total:	5065
with $F_o^2 > 3\sigma(F_o^2)$:	4218
Number of parameters refined	343
Trans. factors, max., min. (ψ-scans)	0.999, 0.949
R^a	0.038
R_w^b	0.045
Quality-of-fit indicator[c]	1.11
Largest shift/esd, final cycle	0.00
Largest peak, e/Å^3	0.70(5)

[a] $R = \Sigma||F_o|-|F_c||/\Sigma|F_o|$

[b] $R_w = [\Sigma w(|F_o|-|F_c|)^2/\Sigma w|F_o|^2]^{1/2}$; $w = 1/\sigma^2(|F_o|)$

[c] Quality-of-fit = $[\Sigma w(|F_o|-|F_c|)^2/(N_{obs} - N_{parameters})]^{1/2}$

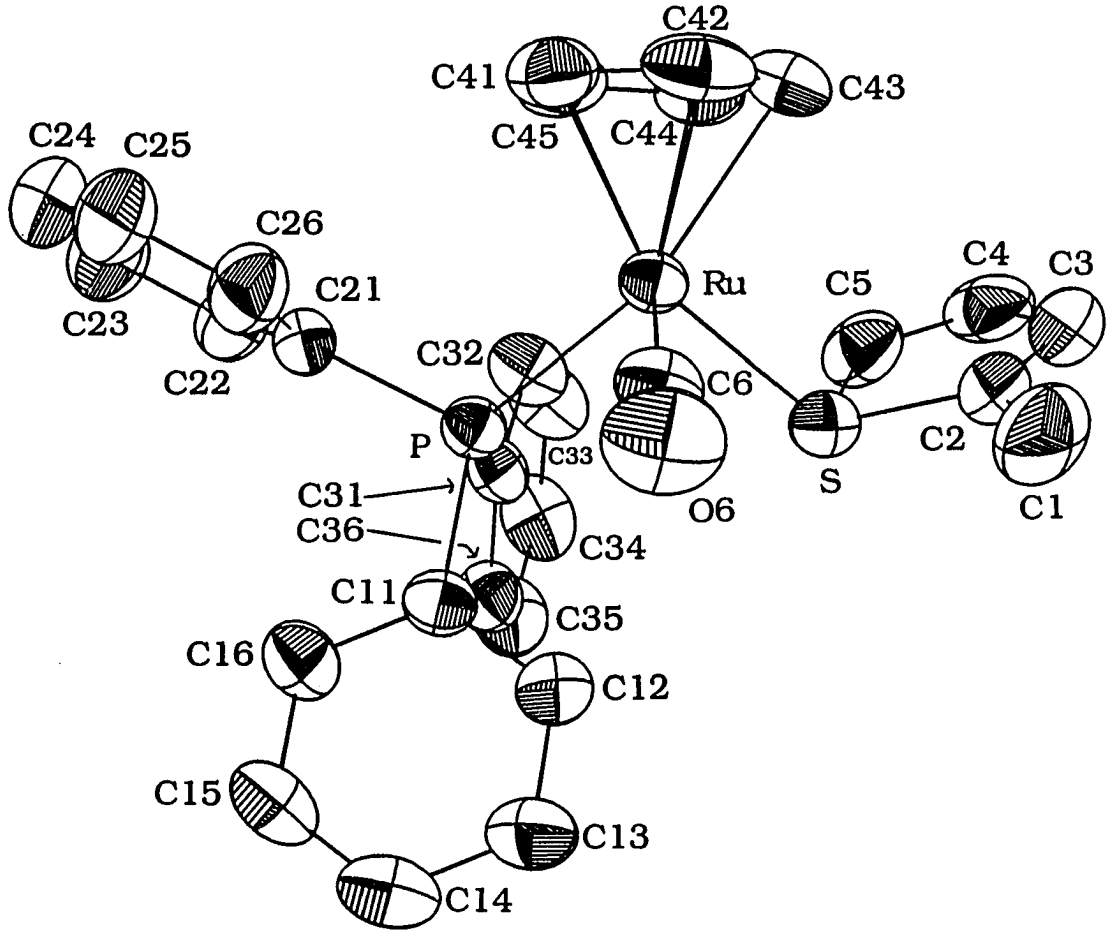

Figure 1. ORTEP drawing of the cation in $[Cp(CO)(PPh_3)Ru(2\text{-}MeT)]BF_4$ (2).

Table II. Bond Distances (Å)[a] and Angles (deg)[a] for [Cp(CO)(PPh$_3$)Ru(2-MeT)]BF$_4$ (2)

Atom	Distance	Atom	Distance
Ru-S	2.392(1)	S-C(2)	1.753(5)
Ru-C(6)	1.869(4)	S-C(5)	1.756(5)
Ru-P	2.332(1)	C(1)-C(2)	1.489(7)
Ru-C(41)	2.196(4)	C(2)-C(3)	1.350(7)
Ru-C(42)	2.204(4)	C(3)-C(4)	1.417(8)
Ru-C(43)	2.222(4)	C(4)-C(5)	1.329(7)
Ru-C(44)	2.241(4)	C(6)-O(6)	1.143(5)
Ru-C(45)	2.238(4)		

Atom	Angle	Atom	Angle
S-Ru-C(6)	95.2(1)	C(2)-S-C(5)	92.3(2)
S-Ru-P	91.67(4)	S-C(2)-C(1)	120.6(4)
C(6)-Ru-P	91.1(1)	S-C(2)-C(3)	109.2(4)
Ru-S-C(2)	108.8(2)	S-C(5)-C(4)	109.4(4)
Ru-S-C(5)	110.6(2)	Ru-C(6)-O(6)	173.3(4)
Ru-S-Mid Pt	119.11(6)		

[a] Numbers in parentheses are estimated standard deviations in the least significant digits.

Table III. Positional Parameters for [Cp(CO)(PPh_3)Ru(2-MeT)]BF_4 (2)

Atom	x	y	z	B(Å2)[a]
Ru	0.19915(3)	0.77508(3)	0.15332(2)	2.938(6)
S	0.0757(1)	0.6348(1)	0.06499(8)	3.86(2)
C(1)	0.2897(7)	0.6204(6)	-0.0926(4)	7.0(2)
C(2)	0.1402(6)	0.6574(4)	-0.0555(3)	4.7(1)
C(3)	0.0343(7)	0.7062(5)	-0.1013(4)	6.0(1)
C(4)	-0.0961(6)	0.7273(5)	-0.0418(4)	6.2(1)
C(5)	-0.0932(5)	0.6984(5)	0.0494(4)	5.1(1)
C(6)	0.3735(5)	0.6866(4)	0.1339(3)	4.2(1)
O(6)	0.4863(4)	0.6438(4)	0.1198(3)	6.9(1)
P	0.1304(1)	0.6567(1)	0.29341(7)	3.01(2)
C(11)	0.2255(4)	0.5066(4)	0.3118(3)	3.33(8)
C(12)	0.2630(5)	0.4271(4)	0.2368(3)	4.3(1)
C(13)	0.3328(6)	0.3115(5)	0.2499(4)	5.2(1)
C(14)	0.3641(6)	0.2741(5)	0.3392(4)	5.3(1)
C(15)	0.3257(5)	0.3514(5)	0.4137(4)	4.9(1)
C(16)	0.2567(5)	0.4668(5)	0.4005(3)	4.2(1)
C(21)	0.1522(5)	0.7465(4)	0.3969(3)	3.61(9)
C(22)	0.0404(6)	0.7689(5)	0.4687(3)	4.9(1)
C(23)	0.0632(8)	0.8403(6)	0.5451(4)	6.8(2)
C(24)	0.1960(8)	0.8899(6)	0.5499(4)	7.3(2)

Table III (continued)

Atom	x	y	z	B(Å2)[a]
C(26)	0.2872(5)	0.7961(5)	0.4025(4)	5.2(1)
C(31)	-0.0571(4)	0.6095(4)	0.3114(3)	3.33(8)
C(32)	-0.1610(5)	0.7022(5)	0.2988(4)	4.5(1)
C(33)	-0.3049(5)	0.6688(5)	0.3086(4)	5.3(1)
C(34)	-0.3441(5)	0.5458(6)	0.3318(4)	5.4(1)
C(35)	-0.2432(5)	0.4538(5)	0.3445(4)	5.1(1)
C(36)	-0.0991(5)	0.4852(4)	0.3341(3)	4.1(1)
C(41)	0.2642(5)	0.9623(4)	0.1950(4)	5.0(1)
C(42)	0.3048(5)	0.9529(5)	0.0962(4)	5.6(1)
C(43)	0.1814(6)	0.9417(4)	0.0542(4)	5.4(1)
C(44)	0.0619(5)	0.9456(4)	0.1268(4)	4.7(1)
C(45)	0.1136(5)	0.9603(4)	0.2115(4)	4.8(1)
B	0.6466(6)	1.0167(6)	0.2117(5)	5.4(1)
F(1)	0.5622(4)	0.9823(4)	0.2933(3)	7.7(1)
F(2)	0.7737(4)	1.0545(6)	0.2271(3)	12.4(2)
F(3)	0.6729(5)	0.9114(4)	0.1568(3)	10.4(1)
F(4)	0.5774(4)	1.1006(4)	0.1588(3)	8.8(1)

[a] Anisotropically refined atoms are given in the form of the isotropic equivalent displacement parameter defined as: $(4/3)[a^2B(1,1) + b^2B(2,2) + c^2B(3,3) + ab(\cos \gamma)B(1,2) + ac(\cos \beta)B(1,3) + bc(\cos \alpha)B(2,3)]$.

Exchange Reactions. Equilibrium constants (K) for the displacement (eq 4) of

$$Cp(CO)(PPh_3)Ru(Th)^+ + Th' \underset{25.0^\circ C}{\overset{K}{\rightleftharpoons}} Cp(CO)(PPh_3)Ru(Th')^+ + Th \qquad (4)$$

one thiophene (Th) by another (Th') were determined by integration of ^1H NMR signals of the reactants and products. About 0.020 mmol of a $[Cp(CO)(PPh_3)Ru(Th)]BF_4$ complex was placed in an NMR tube, dissolved in 0.5 mL of CD_2Cl_2 under nitrogen and mixed with an equimolar amount of a different thiophene (Th'). The solution was frozen in liquid nitrogen, and the tube was flame sealed under vacuum. The solution was thawed, and the tube was kept in a 25.0°C temperature bath. Spectra of the solution were recorded on a Varian VX-300 NMR spectrometer thermostated at 25.0°C using CD_2Cl_2 as the internal lock and reference (d 5.32). A 38 sec pulse delay between scans allowed all protons to relax.[23] The NMR spectra were followed with time to establish that all of the reactions reached equilibrium; this occurred within 24 h.

The equilibrium constants, K, for eq (4) were calculated using eq 5 where I'_{Cp} and

$$K = \frac{\left(\frac{I'_{Cp}}{5}\right)^2}{\left(\frac{I_{Cp}}{5}\right)\left(\frac{I_{Me}}{x}\right)} = \frac{[Cp(CO)(PPh_3)Ru(Th')^+][Th]}{[Cp(CO)(PPh_3)Ru(Th)^+][Th']} \qquad (5)$$

I_{Cp} are the Cp peak integrals of $Cp(CO)(PPh_3)Ru(Th')^+$ and $Cp(CO)(PPh_3)Ru(Th)^+$, respectively; I_{Me} is the integral of the Me peak of Th' and x is 3 (for Th' = 2-MeT, 3-MeT, MeI) or 6 (for Th' = $2,5\text{-Me}_2$T, Me_4T). The K values in Table IV are averages of two

independent determinations for most reactions. The error limits in Table IV are average deviations from the median value. The solutions were stable for at least 6 weeks.

Table IV. Equilibrium Constants, K, for the Exchange Reactions (Eq 4) of $Cp(CO)(PPh_3)Ru(Th)^+$ with Th' in CD_2Cl_2 at 25.0°C

Reaction No.	Th	Th'	K, 25°C
1	T	3-MeT	6.30 (8)
2	T	2-MeT	4.11
3	T	2,5-Me_2T	2.76 (3)
4	T	Me_4T	57.4(40)
5	2-MeT	2,5-Me_2T	0.658(8)
6	2-MeT	3-MeT	1.46(2)
7	3-MeT	2,5-Me_2T	0.461
8	Me_4T	2,5-Me_2T	0.0483
9	BT	2,5-Me_2T	0.0918
10	BT	Me_4T	1.85
11	DBT	2,5-Me_2T	0.0375
12	DBT	Me_4T	0.740(2)
13	Me_4T	THT	$> 1.3 \times 10^5$
14	BT	NCMe	$> 1.3 \times 10^5$
15	T	MeI	2.0

RESULTS AND DISCUSSION

Syntheses of the $Cp(CO)(PPh_3)Ru(Th)^+$ Complexes 1-7 and $Cp(CO)(PPh_3)Ru(THT)^+$ (8)

The $\eta^1(S)$-coordinated thiophene complexes **1-7** are synthesized by Ag^+ abstraction of Cl^- from $Cp(CO)(PPh_3)RuCl$ in the presence of excess thiophene, benzothiophene or dibenzothiophene, giving air-stable compounds in good yields (eq 6). The air and thermal

$$Cp(CO)(PPh_3)RuCl + Th \xrightarrow[CH_2Cl_2]{Ag^+} Cp(CO)(PPh_3)Ru(Th)^+ + AgCl \quad (6)$$

1: Th = T
2: Th = 2-MeT
3: Th = 3-MeT
4: Th = 2,5-Me_2T
5: Th = Me_4T
6: Th = BT
7: Th = DBT
8: Th = THT

stability of these complexes in solution and as solids is quite remarkable since the corresponding bis-phosphine complex, $Cp(PPh_3)_2Ru(\eta^1(S)\text{-T})^+$,[10] loses its phosphine ligands and converts to the η^5-T complex $CpRu(\eta^5\text{-T})^+$. This stability is most likely due to the smaller CO ligand which reduces the steric bulk around the metal and makes the metal a better Lewis acid toward the electron-donor S-atom of the thiophene. The alkyl and aryl iodide complexes, $Cp(CO)(PPh_3)Ru(I\text{-R})^+$ (where R= alkyl or aryl), also seem to be more stable than their bis-phosphine and dicarbonyl counterparts.[24]

In the IR spectra of complexes **1-7**, the υ(CO) band is about 35 cm^{-1} higher than that in $Cp(CO)(PPh_3)RuCl$. In the ^1H NMR spectra of these compounds, the thiophene resonances are shifted slightly (0.04 - 0.4 ppm) upfield from those of the free thiophene; this trend was also observed for $Cp(CO)_2Re(\eta^1(S)\text{-Th})$,[11b] but it is opposite that for $Cp(CO)_2Fe(\eta^1(S)\text{-Th})^+$,[7b] in which these resonances are shifted slightly downfield of the

free thiophene. If the thiophene ligands were bound through one of the double bonds, one would expect the proton resonances of the coordinated carbons to shift much farther upfield, as in complexes with η^2-coordinated olefins,[25b,c] η^2-selenophene[25a,d] and η^2-thiophene[26]. In complexes **1, 4** and **5**, the thiophene exhibits only two ^{1}H NMR absorptions at room temperature, indicating the existence of a dynamic process which equilibrates the 2 and 5 positions and the 3 and 4 positions. Low temperature (198 K) spectra of **4** and **5** in CD_2Cl_2 show two separate signals for the diastereotopic a-methyl groups (in **4** at δ 2.39 and 1.52 ppm and in **5** at δ 2.23 and 1.44 ppm) due to the slowing of the stereochemical inversion at the sulfur. The free energy of activation ($\Delta G^{\neq}$) calculated[27] for this process at the coalescence temperature (213 K) in CD_2Cl_2 is 40 kJ/mol.. A similar $\Delta G^{\neq}$ of inversion (39 kJ/mol at 190 K) was obtained by Goodrich et. al.[7b] for $Cp(CO)_2Fe(\eta^1(S)\text{-BT})^+$.

In the ^{13}C NMR spectra of complexes **1-7**, the thiophene signals are slightly downfield (5-12 ppm) from those of the free thiophene. Similar small shifts were observed in $Cp(CO)_2Fe(\eta^1(S)\text{-Th})^+$ (where Th = T, BT and DBT)[7b] and $Cp(CO)_2Re(\eta^1(S)\text{-Th})$.[11b] The α-C signal, but not the β-C, of each compound is split into a doublet by coupling to the phosphorus ($^3J_{CP}$= 0.9 - 3.7 Hz); this supports the $\eta^1(S)$-mode of thiophene coordination in these complexes, which is confirmed by an X-ray structure analysis of **2**.

The synthesis of **8** is a slight modification of that for $Cp(CO)(PPh_3)Ru(Th)^+$. For the more strongly binding tetrahydrothiophene (THT), the Ag^+ is added to the $Cp(CO)(PPh_3)RuCl$ solution prior to the addition of THT in order to prevent reaction between Ag^+ and THT. The υ(CO) value (1984 cm^{-1}) of **8** is slightly lower than those (1999-1992 cm^{-1}) of compounds **1-7**. The ^{1}H NMR spectrum shows two broadened multiplets (δ 2.73, 2.00 ppm) for THT that are shifted upfield from the free ligand (δ 3.23, 2.13 ppm).

Structure of $[Cp(CO)(PPh_3)Ru(2\text{-}MeT)]BF_4$ (2)

The cation of **2** is shown in Figure 1. It contains a planar thiophene ring (± 0.005 Å for each C and ± 0.001 Å for S) bound to the Ru atom through a pyramidal S atom. The Ru-S distance (Table II) of 2.392(1)Å is similar to that in the thienyl complex $(PPh_3)_2Ru(C_5H_4CH_2C_4H_3S)^+$ (2.408(1)Å) [10] but is longer than the corresponding distances found in $Cp(PMe_3)_2Ru(2,5\text{-}DHT)^+$ (2.330(1)Å)[28] (where 2,5-DHT is 2,5-dihydrothiophene), and $Cp(PPh_3)_2Ru(n\text{-}PrSH)^+$ (2.377(2)Å);[29] this longer Ru-S bond in **2** perhaps reflects weaker bonding to thiophene than to DHT or n-PrSH. The coordinated thiophene in **2** is distorted from its uncoordinated geometry. The C2-S and C5-S bonds of 1.753(5) and 1.756(5)Å are slightly longer than the 1.714(1)Å in free thiophene,[30] but very similar to those in $(PPh_3)_2Ru(C_5H_4CH_2C_4H_3S)^+$ [11] (1.754(6) and 1.736(6)Å); although the error limits are larger in $Cp(CO)_2Re(\eta^1(S)\text{-}T)$,[11b] the C-S distances (1.72(1) and 1.73(1)Å) are similar. The C2-C3 (1.350(7)Å), C3-C4 (1.417(8)Å) and C4-C5 (1.329(7)Å) distances in **2** are all slightly shorter than the corresponding distances in free thiophene (1.370(2), 1.424(2) and 1.370(2)Å), but the short-long-short pattern is the same. This same pattern (1.344(8), 1.409(8), 1.339(8)Å)[10] was also observed in $(PPh_3)_2Ru(C_5H_4CH_2C_4H_3S)^+$, another structure with small standard deviations for its bond distances. However, in structures where the standard deviations are larger, this pattern is not always observed.[5] The C2-S-C5 angle of 92.3(2)° is the same as in the free ligand (92.2(1)°). The Ru-S-Midpt (where Midpt is the midpoint of the C2-C5 vector) angle is 119.11(6)° indicating the pyramidal nature of the thiophene. The sum of the angles around the S is 311.7°, which is much less than the 360° required for a trigonal planar S atom. The three other structurally characterized η^1(S) thiophene complexes also contain a pyramidal S atom (Table V); however, the geometry around the S as measured by the M-S-Midpt angle and sum of the angles around S does vary from one complex to another.

Table V. Structural Data on $\eta^1(S)$-Thiophene Complexes.

Complex	M-S-Midpt Angle	Sum of Angles Around S
$Cp(CO)(PPh_3)Ru(T)^+$	119.11(6)	311.7
$Cp^*(CO)_2Re(T)$[a]	140.4	333.6
$Cp(CO)Fe(DBT)^+$[b]	119.4(2)	309.8
$Cp(Cl)_2Ir(DBT)$[c]	128.0	317.9

[a] ref 11b

[b] ref 7b

[c] ref 17

Equilibrium Studies

The equilibrium constants, K, for the exchange reaction (eq 4) were calculated according to eq 5 and are shown in Table IV. At least three NMR spectra of each reaction were taken over a period of 28 days. During this time, the solution color did not change, nor did any new peaks appear in the NMR spectra to indicate that the compounds were decomposing. Equilibrium constants were also obtained for reactions 1, 2, 3, 5, 6, 9, and 11 (Table IV) at 15 and 35.0°C but the values were found to be within experimental error of those at 25°C. Thus, the ΔH values for these exchange reactions are small (less than 1 kcal/mol).

In order to put the K values in Table IV on the same scale, equilibrium constants (K', Table VI) for the displacement (eq 3) of T from $Cp(CO)(PPh_3)Ru(T)^+$ by the methyl-substituted thiophenes, BT and DBT were calculated from the K values. The results in Table

V allow the K' values to be calculated independently from different data sets. For example, the K (4.11) for reaction 2 multiplied by the K (0.658) for reaction 5 gives a K' value of 2.70 for the displacement of T with 2,5-Me_2T. The K value for this reaction measured directly (reaction 3) is 2.76. All the values calculated in this manner are in extremely good agreement (within 5%), ensuring the validity of each experimental K value.

The K' values (Table VI) give the following trend in binding abilities of the thiophenes: T < 2,5-Me_2T < 2-MeT < 3-MeT < BT < Me_4T < DBT.
This is the same trend as that obtained in a kinetic study[15] of thiophene substitution by PPh_3 (eq 2), with the exception that the 2,5-Me_2T, 2-MeT, 3-MeT order is reversed; as discussed below, this reversal appears to be due to repulsion between 2-methyl groups in the thiophene and the bulky PPh_3 ligand in the $Cp(CO)(PPh_3)Ru(Th)^+$ complexes. In both the equilibrium studies (eq 3) and the kinetic studies (eq 2), all of the methyl-substituted thiophenes bind more strongly than thiophene itself; presumably the electron-donating methyl groups make the thiophene sulfur a stronger donor ligand. In the $Cp(CO)_2Re(\eta^1(S)$-Th) kinetic studies 2-MeT dissociates more slowly than 3-MeT; this is in contrast to the equilibrium studies where 3-MeT binds more strongly than the sterically involved 2-MeT. The addition of another a-methyl group to 2-MeT to give 2,5-Me_2T reduces the K' value still further, from 4.11 to 2.76; on the contrary, the dissociation of 2,5-Me_2T is 13 times slower than that of 2-MeT in $Cp(CO)_2Re(\eta^1$(S)-2,5-Me_2T).[15] This difference is also most likely due to a steric interaction between the thiophene Me's and the phenyl groups of the phosphine ligand in **4**. In the structure of **2** (Fig. 1), the Me group of 2-MeT is oriented toward the carbonyl ligand and away from the bulky phosphine. A computer generated model of $Cp(CO)(PPh_3)Ru(\eta^1(S)$-2,5-$Me_2T)^+$ (**4**) using the structural data of **2** shows that it is impossible to add the 5-Me group because it interferes with a Ph group of the PPh_3; therefore the 2,5-Me_2T ligand must adopt a different orientation in **4** than 2-MeT does in **2**. The addition of 2 more Me groups in

Table VI. Relative Equilibrium Constants, K', for the Reactions of $Cp(CO)(PPh_3)Ru(T)^+$ with Th' (Eq 3) in CD_2Cl_2 at 25.0°C

Th	K'
T	1.00
MeI	2.0
2,5-Me_2T	2.76(3)
2-MeT	4.11
3-MeT	6.30(8)
Me_4T	57.4(40)
BT	29.9(1)
DBT	74.1(10)
THT	$> 7.1 \times 10^6$
NCMe	$> 7.1 \times 10^6$

the 3 and 4 positions to give Me_4T strengthens the M-S bond (K' = 57.4) as expected. Thus, except for specific steric interactions, the binding of thiophenes in $Cp(CO)(PPh_3)Ru(Th)^+$ is enhanced by electron-donating methyl groups in the thiophene ring.

With a K' value of 29.9, BT is a weaker ligand than Me_4T, but DBT is the most strongly bound (K' = 74.1) of all of the thiophene ligands that were studied.

Despite the stability of complexes **1-7**, the thiophenes are still very weakly bound. Other more strongly coordinating ligands, such as tetrahydrothiophene (THT) and NCMe, completely displace the thiophene ligands. The exchange equilibrium where Th = Me_4T and

Th' = THT was studied in both directions. There was no change in the NMR spectrum during one week when **8** was mixed with equimolar Me_4T; on the other hand, there was complete displacement of Me_4T by THT within 24 h when **5** was reacted with THT. Likewise, BT is completely displaced from **6** by equimolar NCMe within the same time period. Based on the sensitivity of the ^1H NMR instrument used in the equilibrium studies, we estimate that K is greater than 1.3×10^5 for these reactions (reactions 13 and 14, Table V), which means that K' is greater than 7.1×10^6. Thus, THT and NCMe are much more strongly coordinating ligands than any of the thiophenes.

Methyl iodide, a weakly binding ligand, is known to form stable complexes with the $Cp(CO)(PPh_3)Ru^+$ fragment.[24] A study of the reaction of **1** with equimolar MeI conducted under the same conditions as the thiophene reactions, after 24 h, gives an equilibrium constant of 2.0 according to eq 5. This value, however, is less accurate than the others since a small amount of decomposition of $Cp(CO)(PPh_3)Ru(MeI)^+$ to other Cp-containing products occurs with the liberation of free MeI.[24] Thus, the equilibrium constant (Table VI) for MeI is between those of T and 2,5-Me_2T. The weak $\eta^1(S)$-coordinating ability of thiophene is demonstrated by its K' value (1.00), which is even less than that (2.0) of MeI toward $Cp(CO)(PPh_3)Ru^+$.

Relevance To Thiophene Adsorption On HDS Catalysts

In an effort to gain insight into the nature of the adsorption of thiophene on HDS catalysts, we have measured equilibrium constants for the binding of methyl-substituted thiophenes as η^5-ligands[3] in $CpRu(\eta^5\text{-Th})^+$ (eq 1) and as $\eta^1(S)$-ligands in $Cp(CO)(PPh_3)Ru(\eta^1(S)\text{-Th})^+$ in the present study (eq 3). Relative equilibrium constants, K', for η^5- and $\eta^1(S)$-coordination are compared in Table VII with relative adsorption coefficients (K_{rel}) for thiophenes[2] on a sulfided Co-Mo/Al_2O_3 HDS catalyst at 350 °C.[31] It is

clear from the Table that the trend (T < 2-Me < 3-Me < 2,5-Me_2T) in equilibrium constants for adsorption (K_{rel}) and η^5-coordination (K') in $CpRu(\eta^5\text{-Th})^+$ is the same. It was this comparison and several reactivity studies[4] of η^5-Th complexes that led us to propose η^5-Th adsorption as a mode of thiophene activation that leads to thiophene HDS by two possible mechanisms.[4a,32,33] Taken together, these results offer the most complete explanation for thiophene adsorption and its HDS.

On the other hand, the data in Table VII also offer some support for η^1(S) adsorption since K' for reaction 3 increases with the number of methyl groups in the thiophene. This trend in K' does not entirely parallel K_{rel} values (Table VII), but as noted above, the bulky PPh_3 group sterically weakens the bonding of thiophenes with Me groups in the 2- and 5-positions. Without the bulky PPh_3 group, the trend in K' values for eq 3 would probably be similar to that of K_{rel}. This statement is supported by the rate constants k_1 in Table VII for the dissociation of thiophenes from $Cp(CO)_2Re(\eta^1(S)\text{-Th})$ according to eq 2.[15] Here there is no steric effect, and the 2,5-Me_2T is the slowest to dissociate indicating that it is likely to be the most strongly coordinated, as is observed (K_{rel}) on the catalyst. Thus, the general increase in both K_{rel} and K' (for eq 3) with an increasing number of methyl groups is consistent with $\eta^1(S)$-binding on the catalyst. The observed slight lengthening (0.04 Å) of the C-S bond upon $\eta^1(S)$-coordination of thiophene in $Cp(CO)(PPh_3)Ru(\eta^1(S)\text{-2-MeT})^+$ suggests that this mode of coordination could activate the thiophene to undergo C-S cleavage. Recent evidence[34] for such an activation is the insertion of Rh into a C-S bond in the proposed intermediate $Cp^*(PMe_3)Rh(\eta^1(S)\text{-Th})$. Thus, $\eta^1(S)$-thiophene adsorption and activation on HDS catalysts is a possibility. It is, of course, possible that the mode of coordination and activation depend on the catalyst and even on the reaction conditions.

Table VII. Equilibrium Constants for the Binding of Methyl-Substituted Thiophenes on a Co-Mo/Al_2O_3 Catalyst, in $CpRu(\eta^5\text{-Th})^+$ and $Cp(CO)(PPh_3)Ru(\eta^1(S)\text{-Th})^+$, as well as Rates of Dissociation from $Cp(CO)_2Re(\eta^1(S)\text{-Th})$.

Th	K_{rel}[a]	K'[b]	K'[c]	10^7k_1,[d] s^{-1}
T	1.0	1	1.0	3000
2-MeT	1.6	6	4.1	91
3-MeT	1.7	7	6.3	1200
2,5-Me_2T	2.5	35	2.8	13

a For adsorption on a sulfided Co-Mo/Al_2O_3 catalyst at 350 °C. Reference 2.

b For η^5-Th coordination in $CpRu(\eta^5\text{-Th})^+$ at 50.0 °C in acetone-d_6 according to eq 1. Reference 3.

c For $\eta^1(S)$-Th coordination in $Cp(CO)(PPh_3)(\eta^1(S)\text{-Th})^+$ in CD_2Cl_2 at 25.0° according to eq 3. This work.

d Rate constant (k_1) for the dissociation of Th from $Cp(CO)_2Re(\eta^1(S)\text{-Th})$ in C_6D_6 at 80.0 °C according to eq 2. Reference 15.

Acknowledgment

We are grateful to Dr. Victor G. Young, Jr. of the Iowa State University Molecular Structure Laboratory for determining the structure of **2** and to Johnson Matthey, Inc. for a generous loan of $RuCl_3$.

REFERENCES

(1) Ames Laboratory is operated for the U.S. Department of Energy by Iowa State University under Contract No. W-7405-Eng-82. This research was supported by the Office of Basic Energy Sciences, Chemical Sciences Division.

(2) Zdrazil, M. *Collect. Czech. Chem. Commun.* **1977**, *42*, 1484.

(3) Hachgenei, J. W.; Angelici, R. J. *Organometallics* **1989**, *8*, 14.

(4) (a) Angelici, R. J. *Acc. Chem. Res.* **1988**, *21*, 387.

(b) Sauer, N. N.; Angelici, R. J. *Organometallics* **1987**, *6*, 1146.

(c) Lesch, D. A.; Richardson, J. W.; Jacobson, R. A.; Angelici, R. J. *J. Am. Chem. Soc.* **1984**, *106*, 2901.

(d) Hachgenei, J. W.; Angelici, R. J. *J. Organomet. Chem.* **1988**, *355*, 359.

(e) Rauchfuss, T. B. *Prog. Inorg. Chem.*, in press.

(f) Chen, J.; Daniels, L. M.; Angelici, R. J. *J. Am. Chem. Soc.* **1990**, *112*, 199.

(5) Angelici, R. J. *Coord. Chem. Rev.* **1990**, *105*, 61.

(6) Kuehn, C. G.; Taube, H. *J. Am. Chem. Soc.* **1976**, *98*, 689.

(7) (a) Kuhn, N.; Schumann, H. *J. Organomet. Chem.* **1984**, *276*, 55.

(b) Goodrich, J. D.; Nickias, P. N.; Selegue, J. P. *Inorg. Chem.* **1987**, *26*, 3424.

(8) Catheline, D.; Astruc, D. *J. Organomet. Chem.* **1984**, *272*, 417.

(9) Wasserman, H. J.; Kubas, G. J.; Ryan, R. R. *J. Amer. Chem. Soc.* **1986**, *108*, 2294.

(10) Draganjac, M.; Ruffing, C. J.; Rauchfuss, T. B. *Organometallics* **1985**, *4*, 1909.

(11) (a) Choi, M.-G.; Angelici, R. J. *J. Amer. Chem. Soc.* **1989**, *111*, 8753.

(b) Choi, M.-G.; Angelici, R. J. *Organometallics*, **1991**, *10*, 2436.

(12) (a) Lucas, C. R.; Liu, S.; Newlands, M. J.; Gabe, E. J. *Can. J. Chem.* **1990**, *68*, 1357.

(b) Lucas, C. R.; Liu, S.; Newlands, M. J.; Charland, J.-P.; Gabe, E. J. *Can. J. Chem.* **1989**, *67*, 639.

(c) Liu, S.; Lucas, C. R.; Newlands, M. J.; Charland, J.-P. *Inorg. Chem.* **1990**, *29*, 4380.

(13) Constable, E. C.; Henney, R. P. G.; Tocher, D. A. *J. Chem. Soc., Chem. Commun.* **1989**, 913.

(14) Guerchais, V.; Astruc, D. *J. Organomet. Chem.* **1986**, *316*, 335.

(15) Choi, M.-G.; Angelici, R. J. *Inorg. Chem.* **1991**, *30*, 1417.

(16) Bucknor, S. M.; Draganjac, M.; Rauchfuss, T. B.; Ruffing, C. J.; Fultz, W. C.; Rheingold, A. L. *J. Amer. Chem. Soc.* **1984**, *106*, 5379.

(17) Rao, K. M.; Day, C. L.; Jacobson, R. A.; Angelici, R. J. *Inorg. Chem.*, accepted for publication.

(18) (a) *Experimental Organometallic Chemistry*; Wayda, A. L.; Darensbourg, M. Y. Ed.: ACS Symposium Series 357; American Chemical Society: Washington, D.C., 1987.

(b) Shriver, D. F.; Drezdzon, M. A. *The Manipulation of Air Sensitive Compounds*, 2nd ed.; Wiley: New York, 1986.

(19) Davies, S. G.; Simpson, S. J. *J. Chem. Soc., Dalton Trans.* **1984**, 993.

(20) Spies, G. H.; Angelici, R. J. *Organometallics* **1987**, *6*, 1897.

(21) Janda, M.; Šrogl, J.; Stibor, I.; Němec, M.; Vopatrnǩ, P. *Synthesis* **1972**, 545.

(22) (a) SHELXS-86, G. M. Sheldrick, Institut für Anorganische Chemie der Universität, Göttingen, F. R. G.

(b) Enraf-Nonius Structure Determination Package; Enraf-Nonius: Delft, Holland. Neutral-atom scattering factors and anomalous scattering corrections were taken from *International Tables for X-ray Crystallography*; The Kynoch Press: Birmingham, England, 1974, Vol IV.

(23) T_1 values determined for $Cp(CO)(PPh_3)Ru(Me_4T)^+$ follow: Cp, $T_1 = 5.0 \pm 0.2$ s; Ph, $T_1 = 2.6 \pm 0.2$ s; 3,4 Me's, $1.4 \pm .1$ s; 2,5 Me's, 1.5 ± 0.02.

(24) Kulawiec, R. J.; Faller, J. W.; Crabtree, R. H. *Organometallics* **1990**, *9*, 745.

(25) (a) Choi, M.-G.; Angelici, R. J. *J. Am. Chem. Soc.* **1990**, *112*, 7811.

(b) Burns, C. J.; Andersen, R. A. *J. Am. Chem. Soc.* **1987**, *109*, 915.

(c) Harman, W. D.; Schaefer, W. P.; Taube, H. *J. Am. Chem. Soc.* **1990**, *112*, 2682.

(d) Choi, M.-G.; Angelici, R. J. *J. Am. Chem. Soc.* **1991**, *113*, 5651.

(26) Cordone, R.; Harman, W. D.; Taube, H. *J. Am. Chem. Soc.* **1989**, *111*, 5969.

(27) Sandstrom, J. *Dynamic NMR Spectroscopy*, Academic Press: New York, **1982**, 96.

(28) Choi, M.-G.; Angelici, R. J. *Inorg. Chem.*, in press.

(29) Amarasekera, J.; Rauchfuss, T. B. *Inorg. Chem.* **1989**, *28*, 3875.

(30) (a) Bak, B.; Christensen, D.; Hansen-Nygaard, L.; Rastrup-Andersen, J. R. *J. Mol. Spectrosc.* **1961**, *7*, 58.

(b) Bonham, R. A.; Momany, F. A. *J. Phys. Chem.* **1963**, *67*, 2474.

(c) Harshbarger, W. R.; Bauer, S. H. *Acta Chrystallogr.* **1970**, *B26*, 1010.

(31) It should be noted that the adsorption sites on the catalyst are not necessarily the sites at which thiophene HDS occurs.

(32) Sauer, N. N.; Markel, E. J.; Schrader, G. L.; Angelici, R. J. *J. Catal.* **1989**, *117*, 295.

(33) Chen, J.; Daniels, L. M.; Angelici, R. J. *J. Am. Chem. Soc.* **1991**, *113*, 2544.

(34) Jones, W. D.; Dong, L. *J. Am. Chem. Soc.* **1991**, *113*, 559.

PAPER II. EQUILIBRIUM AND KINETIC STUDIES OF SULFUR-COORDINATED THIOPHENES (Th) IN $Cp(CO)_2Ru(\eta^1(S)\text{-Th})^+$ AND $Cp(CO)(PPh_3)Ru(\eta^1(S)\text{-Th})^+$: MODELS FOR THIOPHENE ADSORPTION ON HYDRODESULFURIZATION CATALYSTS.[1]

ABSTRACT

A series of stable sulfur-bound thiophene complexes, $Cp(CO)_2Ru(\eta^1(S)\text{-}Th)^+$, where Cp = η^5-C_5H_5 and Th = T, 2-MeT, 3-MeT, 2,5-Me_2T, Me_4T, BT and DBT, are synthesized from the reaction of $Cp(CO)_2RuCl$ with Ag^+ and thiophenes. Equilibrium constants, K', for the displacement of thiophene (T) by methyl-substituted thiophenes and benzo[b]thiophene (BT), $Cp(CO)_2Ru(\eta^1(S)\text{-}T)^+ + Th \rightleftharpoons Cp(CO)_2Ru(\eta^1(S)\text{-}Th)^+ + T$, increase with an increasing number of methyl groups in the thiophene: T(1.00) < 2-MeT (3.30) < 3-MeT (4.76) < 2,5-Me_2T (20.7) < BT (47.6) < Me_4T (887). First order rate constants (10^6 k_1, s^{-1}) for phosphine substitution of the thiophenes in $Cp(CO)_2Ru(\eta^1(S)\text{-}Th)^+$, $Cp(CO)_2Ru(\eta^1(S)\text{-}Th)^+ + PR_3 \longrightarrow Cp(CO)_2Ru(PR_3)^+ + Th$, by a dissociative mechanism decrease in the following order: 3-MeT (450) > 2-MeT (410) > BT (100) > 2,5-Me_2T (23). Rate constants for thiophene dissociation in the analogous $Cp(CO)(PPh_3)Ru(\eta^1(S)\text{-}Th)^+$ complexes decrease as follows: T (1400) > 2-MeT (220) > 3-MeT (170) > 2,5-Me_2T (130) > BT (70) > DBT (17) > Me_4T (5.8). In general, methyl groups on the thiophene (Th) increase K' and decrease k_1 which suggests that electron-releasing methyl groups enhance thiophene binding to the metal. No steric effect is detected between α-methyl groups on Th and $Cp(CO)_2Ru(\eta^1(S)\text{-}Th)^+$, as is seen in $Cp(CO)(PPh_3)Ru(\eta^1(S)\text{-}Th)^+$; trends in K' and k_1 follow those of thiophenes adsorbing to HDS catalysts.

INTRODUCTION

Catalytic hydrodesulfurization (HDS) is an important industrial process[2] for the removal of sulfur from petroleum feedstocks. A critical step in the mechanism(s) for the HDS of thiophene is its initial binding to a metal site on the catalyst surface. Organotransition metal complexes of thiophene (T) and its methyl-substituted [2-methylthiophene (2-MeT), 3-methylthiophene (3-MeT), 2,5-dimethylthiophene (2,5-Me_2T) and tetramethylthiophene (Me_4T)] and benzo-substituted [benzo[b]thiophene (BT), dibenzothiophene (DBT)] derivatives provide models for possible modes[3] of thiophene adsorption. Of these modes, the sulfur-bound thiophene ($\eta^1(S)$-T) is one of the least studied since the thiophene S atom is such a weak donor. Thus, in known $\eta^1(S)$-bound thiophene complexes, $Cp(CO)_2Fe(Th)^+$ (Cp = η^5-C_5H_5, Th = T ,[4] 2,5-Me_2T [5]), $(NH_3)_5Ru(T)^{2+}$,[6] $Cp(MeCN)_2Fe(2,5\text{-}Me_2T)^+$,[7] $W(CO)_3(PCy_3)_2(T)$,[8] $Cp'(CO)_2Re(T)$ (Cp' = η^5-C_5H_5 or η^5-C_5Me_5),[9] $Cp(CO)(PPh_3)Ru(Th)^+$,[10] $(C_5H_4CH_2C_4H_3S)Ru(PPh_3)_2^+$ [11] and $[Ru(HL)_2Cl][BF_4]$ (HL = 6-(2-thienyl)-2,2'-bipyridine)[12], the thiophene is easily displaced by other ligands (e.g. MeCN, C_4H_8S and PPh_3).

Two recent studies of organometallic complexes containing the $\eta^1(S)$-bound thiophenes (Th) have examined the effect of methyl substitution on the ability of the thiophene ligand to coordinate to a metal center. Kinetic studies[13] of Th replacement in $Cp(CO)_2Re(\eta^1(S)\text{-Th})$ by PPh_3 (eq 1) show that as the number of Me groups on the

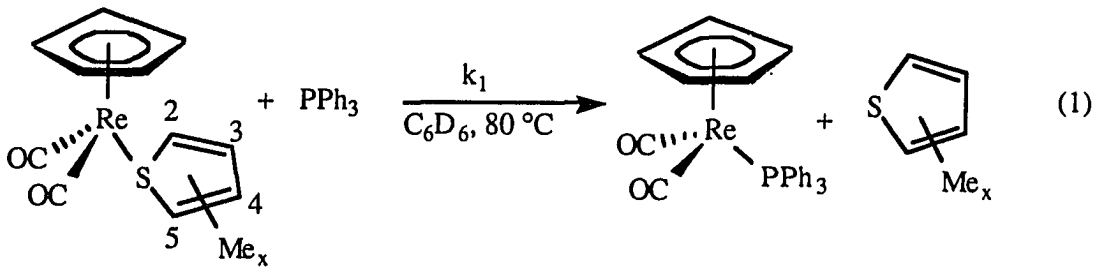

(1)

thiophene increases, the thiophene ligand binds more tightly to the Re. Thus, rate constants (10^7 k_1, s^{-1}), which are determined by rate limiting dissociation of the thiophene, decrease in the order: T (3000) > 3-MeT (1200) > 2-MeT (91) > 2,5-Me_2T (13) > Me_4T (2.7) > DBT (1.6). This order is similar to that for the adsorption of thiophenes on a sulfided Co-Mo/Al_2O_3 heterogeneous catalyst at 350 °C as measured by their relative adsorption coefficients[14], K_{rel}: T (1.0) < 2-MeT (1.6) < 3-MeT (1.7) < 2,5-Me_2T (2.5). In an equilibrium study[10] of η^1(*S*)-Th displacement from Cp(CO)(PPh_3)Ru(η^1(*S*)-Th)$^+$ (eq 2),

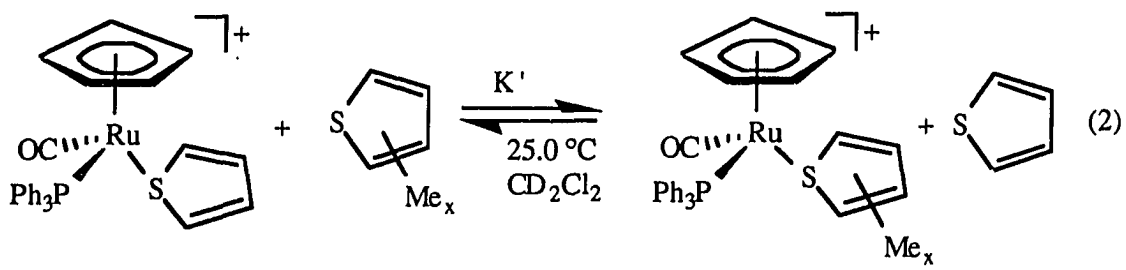

(2)

however, the following trend in K' values is observed: T (1.0) < 2,5-Me_2T (2.8) < 2-MeT (4.1) < 3-MeT (6.3). This order is the same as that for K_{rel} on the sulfided Co-Mo/Al_2O_3 except for the position of 2,5-Me_2T. The lower K' for 2,5-Me_2T in reaction 2 probably results from steric repulsion between an α-methyl group on 2,5-Me_2T and the bulky phosphine phenyl rings.[10]

To further explore this steric effect, a new series of thiophene complexes, Cp($CO)_2$Ru(η^1(*S*)-Th)$^+$, (Th = T (**1**), 2-MeT (**2**), 3-MeT (**3**), 2,5-Me_2T (**4**), Me_4T (**5**), BT (**6**), DBT (**7**)), has been prepared. Here, a CO ligand replaces the bulky PPh_3 in the Ru coordination sphere, thereby greatly reducing steric effects of the 2- and 5-Me groups on Th.

Equilibrium constants for this new series of thiophene complexes are compared with those in the previous study of $Cp(CO)(PPh_3)Ru(\eta^1(S)\text{-}Th)^+$ (eq 2).[10] Also, kinetic studies of thiophene substitution in $Cp(CO)_2Ru(\eta^1(S)\text{-}Th)^+$ and $Cp(CO)(PPh_3)Ru(\eta^1(S)\text{-}Th)^+$ by phosphine ligands, PPh_3, PPh_2Me and $PPhMe_2$, are reported; factors that affect the mechanisms and rates of these reactions are discussed.

EXPERIMENTAL

General Procedures

All reactions were performed under a nitrogen atmosphere using standard Schlenk techniques[15]. Solvents were dried prior to use: methylene chloride, hexanes and heptanes were distilled from CaH_2 and diethyl ether from sodium/benzophenone. Hexanes, heptanes and methylene chloride were stored under nitrogen over molecular sieves. Neutral Al_2O_3, purchased from Aldrich, was deactivated with 5% deionized water after 24 h under vacuum. Deuterated solvents for NMR experiments were purchased from Cambridge and stored over molecular sieves in a desiccator. Thiophene was purified as previously described[16]. Solid thiophenes, DBT and BT, were purchased from Aldrich and sublimed prior to use. Starting materials $Ru_3(CO)_{12}$,[17] Me_4T,[18] $Cp(CO)_2RuCl$,[19] and $Cp(CO)(PPh_3)Ru(\eta^1(S)\text{-Th})^+$ (Th = T, 2-MeT, 3-MeT, 2,5-Me_2T, Me_4T, BT, DBT)[10] were prepared as previously described. Thiophene ligands 2-MeT, 3-MeT and 2,5-Me_2T as well as $AgBF_4$, PPh_3, PPh_2Me and $PPhMe_2$, were purchased from Aldrich and used without further purification.

Infrared spectra of the compounds in CH_2Cl_2 were taken using a Nicolet 710 FT-IR spectrometer. Fast atom bombardment (FAB) mass spectra of compounds in a CH_2Cl_2/3-nitrobenzyl alcohol matrix were obtained using a Kratos MS-50 mass spectrometer. The ^1H and $^{13}C\{^1H\}$ NMR spectra were taken on either a Nicolet NT-300, Bruker WM-200 or Varian VXR-300 spectrometer using CD_2Cl_2 as the solvent and the internal lock. Elemental analyses were performed by Galbraith Laboratories, Inc., Knoxville, TN.

General Procedure for the Preparation of $[Cp(CO)_2Ru(\eta^1(S)\text{-Th})]BF_4$ Complexes (1-7)

To a solution of $Cp(CO)_2RuCl$ (50.2 mg, 0.195 mmol) and 0.97 mmol of a Th in 20 mL of CH_2Cl_2 was added solid $AgBF_4$ (49.1 mg, 0.252 mmol); the solution was stirred at room temperature for 1 h. A white precipitate formed immediately and the solution color lightened. After 1 h, the solution was filtered through Celite, and the volatiles were removed under vacuum (excess BT and DBT were removed with 3 - 5 mL diethyl ether washes). The residue was dissolved in 2 mL of CH_2Cl_2 and precipitated with 10 mL of diethyl ether at -20 °C giving light yellow compounds, **1 - 7**, in 70 - 85% yields.

Characterization of 1-7

$[Cp(CO)_2Ru(T)]BF_4$ (**1**). ^1H NMR: δ 7.67 (m, 2 H) and 7.33 (m, 2 H) T; 5.73 (s, 5 H) Cp. $^{13}C\{^1H\}$ NMR: δ 138.3 (s) and 133.0 (s) T; 192.7 (s), CO; 89.7 (s), Cp. IR: υ(CO) 2080, 2034 cm^{-1}.

$[Cp(CO)_2Ru(2\text{-MeT})]BF_4$ (**2**). ^1H NMR: δ 7.45 (dd, J = 5.4, 0.9 Hz, 1 H), 7.10 (m, 1 H), 6.99 (m, 1 H) and 2.45 (d, J = 1.2 Hz, 3 H), 2-MeT; 5.70 (s, 5 H) Cp. $^{13}C\{^1H\}$ NMR: δ 150.8 (s), 136.1 (s), 132.9 (s), 130.8 (s) and 14.3 (s), 2-MeT; 192.9 (s), CO; 89.8 (s), Cp. IR: υ(CO) 2080, 2033 cm^{-1}. Anal. calcd. for $C_{12}H_{11}BF_4O_2RuS$: C, 35.40; H, 2.72. Found C, 34.90; H, 2.52.

$[Cp(CO)_2Ru(3\text{-MeT})]BF_4$ (**3**). ^1H NMR: δ 7.56 (dd, J = 5.1, 2.7 Hz, 1 H), 7.13 (m, 2 H) and 2.33 (d, J=1.2 Hz, 3 H), 3-MeT; 5.72 (s, 5 H) Cp. $^{13}C\{^1H\}$ NMR: δ 145.0 (s), 138.1 (s), 136.3 (s), 130.9 (s), and 16.4 (s), 3-MeT; 192.9 (s), CO; 89.6 (s), Cp. IR: υ(CO) 2079, 2033 cm^{-1}. Anal. calcd. for $C_{12}H_{11}BF_4O_2RuS$: C, 35.40; H, 2.72. Found C, 35.32; H, 2.69.

$[Cp(CO)_2Ru(2,5\text{-}Me_2T)]BF_4$ (4). ^1H NMR: δ 6.77 (s, 2 H) and 2.38 (s, 6 H), 2,5-Me_2T; 5.61 (s, 5 H) Cp. $^{13}C\{^1H\}$ NMR: δ 148.2 (s), 130.5 (s) and 14.6 (s), 2,5-Me_2T; 193.1 (s), CO; 90.1 (s), Cp. IR: υ(CO) 2080, 2034 cm^{-1}. Anal. calcd. for $C_{13}H_{13}BF_4O_2RuS$: C, 36.88; H, 3.09. Found C, 36.44; H, 2.79.

$[Cp(CO)_2Ru(Me_4T)]BF_4$ (**5**). ^1H NMR: δ 2.26 (s, 6 H) and 2.05 (s, 6 H), Me_4T; 5.63 (s, 5 H) Cp. $^{13}C\{^1H\}$ NMR: δ 141.2 (s), 136.8 (s),13.8 (s) and 12.6 (s), Me_4T; 193.5 (s), CO; 90.0 (s), Cp. IR: υ (CO) 2076, 2030 cm^{-1}. FAB: m/e 363 (M^+); 306 (M^+-2CO); 223 (M^+- Me_4T). Anal. calcd. for $C_{15}H_{17}BF_4O_2RuS$: C, 40.07; H, 3.81. Found C, 39.59; H, 3.44.

$[Cp(CO)_2Ru(BT)]BF_4$ (**6**). ^1H NMR: δ 7.93 (m, 2 H), 7.60 (m, 2 H) and 7.54 (s, 2 H), BT; 5.74 (s, 5 H) Cp. $^{13}C\{^1H\}$ NMR: δ 143.7 (s), 140.1 (s), 133.4 (s), 131.8 (s), 129.6 (s), 128.4 (s), 126.9 (s) and 124.9 (s), BT; 192.9 (s), CO; 89.9 (s), Cp. IR: υ(CO) 2079, 2032 cm^{-1}. FAB: m/e 357 (M^+), 301 (M^+- 2CO), 223 (M^+- BT). Anal. calcd. for $C_{15}H_{11}BF_4O_2RuS$: C, 40.65; H, 2.50. Found C, 40.31; H, 2.41.

$[Cp(CO)_2Ru(DBT)]BF_4$ (**7**). ^1H NMR: δ 8.16 (m, 2 H), 7.93 (m, 2 H), and 7.68 (m, 4 H), DBT; 5.74 (s) Cp. $^{13}C\{^1H\}$ NMR: δ 140.6 (s), 137.1 (s), 130.3 (s), 130.1 (s), 125.8 (s) and 123.7 (s), DBT; 192.9 (s), CO; 90.1 (s), Cp. IR: υ(CO) 2078, 2034 cm^{-1}. Anal. calcd. for $C_{19}H_{13}BF_4O_2RuS$: C, 46.27; H, 2.66. Found C, 45.81; H, 2.52.

Synthesis of $Cp(CO)(PPh_2Me)RuCl$ (8)

This complex was prepared by the method used previously for the synthesis of $Cp(CO)(PPh_3)RuCl$.[20] A solution of 0.136 g of $Ru_3(CO)_{12}$ (0.213 mmol) and 1.0 mL of freshly distilled cyclopentadiene (15.2 mmol) in 60 mL of heptanes was refluxed for 3 h. To the hot solution was added 120 μL of PPh_2Me , and the solution was refluxed for another 30 min. The solvent was removed under vacuum, and the residue was dissolved in 15 mL of

$CHCl_3$ and stirred for 12 h. Following removal of the solvent, the residue was chromatographed on neutral alumina. The complex of interest was collected as the third yellow band using a 1:1 mixture of CH_2Cl_2 and hexanes as the eluting solvent. Following recrystallization from CH_2Cl_2 and hexanes, 0.120 g of $Cp(CO)(PPh_2Me)RuCl$ was recovered as orange crystals in 44 % yield. IR: υ(CO) 1956 cm^{-1}. ^1H NMR: δ 4.90 (s, 5 H, Cp), 7.60 - 7.35 (m, Ph), 2.14 (d, $^2J_{HP}$ = 10 Hz, Me). $^{13}C\{^1H\}$ NMR: δ 200.8 (d, $^1J_{CP}$ = 21.4 Hz, CO); 137.7 (d, $^1J_{CP}$ = 46.1 Hz), 136.4 (d, $^2J_{CP}$ = 51.2 Hz), 132.4 (d, J_{CP} = 10.9 Hz), 131.3 (d, J_{CP} = 10.3 Hz), 130.4 (d, J_{CP} = 2.5 Hz), 130.0 (d, J_{CP} = 2.6 Hz), 128.5 (d, J_{CP} = 10.2 Hz) and 128.3 (d, J_{CP} = 10.2 Hz), PPh; 85.4 (d, $^2J_{CP}$ = 2.1 Hz, Cp); 16.7 (d, $^1J_{CP}$ = 33.9 Hz, PMe). The IR and ^1H NMR spectra are very similar to those of the corresponding PPh_3 complex [20].

Synthesis of $[Cp(CO)(PPh_2Me)Ru(\eta^1(S)\text{-3-MeT})]BF_4$ (9)

To a solution of 50.1 mg of $Cp(CO)(PPh_2Me)RuCl$ (0.117 mmol) and 75 µL (0.59 mmol) of 3-MeT in 20 mL of CH_2Cl_2 was added 38.5 mg (0.198 mmol) of solid $AgBF_4$. The solution was stirred for 1 h at room temperature during which time a precipitate formed and the solution color changed from orange to yellow. The solution was filtered through Celite, and the volatiles were removed under vacuum. The residue was dissolved in 2 mL of CH_2Cl_2 to give a solution to which was added 15 mL of Et_2O; **8** separated as an oil. IR: υ(CO) 1993 cm^{-1}. ^1H NMR: δ 7.04 (dd, J = 5.1, 2.7 Hz, 1 H), 6.96 (dd, J = 5.4, 1.2, 1 H), 6.60 (m, 1 H) and 2.19 (d, J_{HH} = 1.2 Hz, 3 H), 3-MeT; 5.05 (s, 5 H, Cp); 7.65 - 7.40 (m, 10 H) and 2.27 (d, $^2J_{PH}$ = 9.5 Hz, 3 H) PPh_2Me. $^{13}C\{^1H\}$ NMR: δ 143.5 (s), 138.0 (d, $^3J_{CP}$ = 2.1 Hz), 135.1 (s), 131.5 (s) and 16.3 (s), 3-MeT; 200.3 (d, $^2J_{CP}$ = 18.3 Hz, CO); 135.0 (d, $^1J_{CP}$ = 51.8 Hz), 134.2 (d, $^1J_{CP}$ = 51.7 Hz), 132.2 (d, J_{CP} = 11.2 Hz), 131.9 (d, J_{CP} = 2.6 Hz), 131.5 (d, J_{CP} = 10.8 Hz), 131.2 (d, J_{CP} = 2.3 Hz), 129.6 (d, J_{CP}

= 10.6 Hz) and 129.5 (d, J_{CP} = 10.5 Hz), PPh; 87.5 (d, $^2J_{CP}$ = 1.7 Hz, Cp); 19.6 (d, $^1J_{CP}$ = 34.9 Hz, PMe). These spectral features are very similar to those of $Cp(CO)(PPh_3)Ru(\eta^1(S)\text{-3-MeT})^+$.[10]

Equilibrium Studies

Equilibrium constants, K, were determined for the thiophene substitution reactions in equation 3 by ^1H NMR spectrometry. Approximately 0.020 mmol (8.2 - 9.4 mg) of a

$$Cp(CO)_2Ru(\eta^1(S)\text{-Th})^+ + Th' \underset{25.0\ °C}{\overset{K}{\rightleftharpoons}} Cp(CO)_2Ru(\eta^1(S)\text{-Th}')^+ + Th \quad (3)$$

$[Cp(CO)_2Ru(\eta^1(S)\text{-Th})]BF_4$ complex was placed in a 5 mm NMR tube, dissolved in 0.50 mL of CD_2Cl_2 under nitrogen and mixed with an equimolar amount of another thiophene (Th'). The tube was placed in liquid nitrogen and flame sealed under vacuum. The solution was allowed to thaw, and the tube was placed in a 25.0 ± 0.1 °C temperature bath. The ^1H NMR spectrum of the sample was recorded on a Varian VXR-300 spectrometer with the probe thermostated at 25.0 ± 0.1 °C using CD_2Cl_2 as the solvent, internal lock and reference (δ 5.32 ppm). Equilibrium constants, K, for eq 3 were calculated from integrations of the proton signals of each species in the ^1H NMR spectrum using eq 4, where I_{Cp} and $I_{Cp'}$ are

$$K = \frac{[Cp(CO)_2Ru(Th')^+]\,[Th]}{[Cp(CO)_2Ru(Th)^+]\,[Th']} = \frac{\left(\frac{I_{Cp'}}{5}\right)\left(\frac{I_{Th}}{x}\right)}{\left(\frac{I_{Cp}}{5}\right)\left(\frac{I_{Th'}}{y}\right)} \quad (4)$$

the integrals of the Cp peaks of each complex, I_{Th} and $I_{Th'}$ are integrals of the free thiophenes and x and y are the number of protons for the particular thiophene peak being integrated. The Me peaks were integrated on 2-MeT, 3-MeT and Me_4T. The signal for H3 and H4 on 2,5-Me_2T and T and the H2 peak on BT were integrated. For example, if Th = 2-MeT and Th' = T, then x = 3 and y = 2. A long delay time of 38 s between scans was used so that all the protons were fully relaxed. The reactions were followed by NMR to make sure that they reached equilibrium. This occurred within 24 h for most reactions. The reaction of $Cp(CO)_2Ru(\eta^1(S)\text{-}Me_4T)^+$ with BT (reaction G, Table I) took 52 h to reach equilibrium. Each equilibrium constant is the average of at least three different spectra taken during a 2 to 49 day period. Solutions containing complexes of 2-MeT, 3-MeT and T showed some signs of decomposition; the solution color turned from yellow to orange, and new Cp peaks appeared in the NMR spectra at δ 5.58 (most intense), 5.55 and 5.51 ppm. Over a period of three weeks, however, this decomposition was less than 5% of the Ru complex; the equilibrium constants were not affected by this decomposition because they are based on integrals of all reactants and products in eq 3. The K values resulting from these studies are shown in Table I.

Kinetic Studies

Reaction solutions of $Cp(CO)_2Ru(\eta^1(S)\text{-Th})[BF_4]$ (Th = 2-MeT, 3-MeT, BT and 2,5-Me_2T), $Cp(CO)(PPh_3)Ru(\eta^1(S)\text{-Th})[BF_4]$ (Th = T, 2-MeT, 3-MeT, 2,5-Me_2T and BT) and $Cp(CO)(PPh_2Me)Ru(\eta^1(S)\text{-3-MeT})[BF_4]$, whose reaction (eq 5) half lives were less than 7 h, were prepared as follows. A 0.0050 mmol sample of the complex was placed in an NMR tube with an excess, weighed amount of PPh_3. The tube was evacuated, flushed with nitrogen and capped with a septum. A 0.50 mL aliquot of CD_2Cl_2 was added, and the tube was shaken to dissolve the reactants. The tube was immediately placed in the probe of a

Table I. Equilibrium Constants, K, for Reactions (Eq 3) of $Cp(CO)_2Ru(\eta^1(S)\text{-Th})^+$ with Th' at 25.0 °C in CD_2Cl_2

Reaction	Th	Th'	K
A	2-MeT	T	0.303(1)
B	2-MeT	3-MeT	1.52(5)
C	2-MeT	2,5-Me_2T	6.26
D	BT	2,5-Me_2T	0.435(11)
E	3-MeT	T	0.210(12)
F	3-MeT	2-MeT	0.660
G	Me_4T	BT	0.0526
H	BT	Me_4T	19.2
I	2,5-Me_2T	Me_4T	40.7

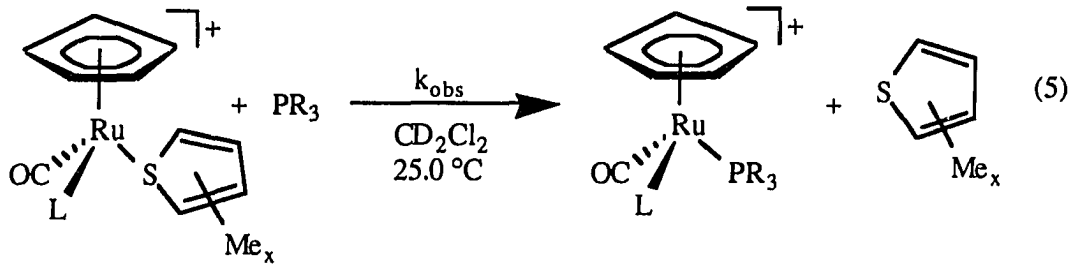

(5)

L = CO; PPh_3; PPh_2Me

Varian VXR-300 NMR spectrometer thermostated at 25.0 ± 0.1 °C. The spectrometer was preprogrammed to take spectra at specific time intervals; the acquisition time for each spectrum was 60 s (16 scans at 3.744 s/scan). Rate constants, k_{obs}, were obtained from the least squares slopes of plots of ln(1+F) (where F = [Product]/[Reactant]) vs. time; reactant and product concentrations were determined by integrating Cp peaks. Correlation coefficients of these plots were always greater than 0.995. Three samples were run at each concentration; the results (Tables II and III) are the average of the three runs at each concentration with the average deviation in the last digit given in parentheses. The products formed in these kinetic studies were $Cp(CO)_2(PPh_3)Ru^+$ or $Cp(CO)(PPh_3)_2Ru^+$, and the free thiophenes; they were identified by their NMR spectra which were the same as those previously reported in the literature.[20-22] The product $Cp(CO)(PPh_3)Ru(PPh_2Me)^+$, (δ 5.02 ppm, Cp) was identified from its ^1H NMR spectrum, which closely corresponded to that of $Cp(CO)(PPh_3)_2Ru^+$.[20, 21] Preparations of samples of $Cp(CO)(PPh_3)Ru(\eta^1(S)$-Th)$[BF_4]$ (Th = Me_4T and DBT), whose reaction half lives were greater than 12 h, were slightly different. A sample (0.0050 mmol) of $Cp(CO)(PPh_3)Ru(\eta^1(S)$-Th)$^+$ was placed in an NMR tube with an excess, weighed amount of PPh_3. The tube was evacuated and flushed with nitrogen. A 0.50 mL aliquot of CD_2Cl_2 was added, and the tube was immediately immersed in liquid nitrogen. The tube was then flame sealed under vacuum. After the solution thawed, the tube was placed in a constant temperature bath thermostated to 25.0 ± 0.1 °C. Periodically the tube was removed from the bath, placed in the probe and a spectrum was recorded on a Nicolet NT-300 spectrometer at room temperature using CD_2Cl_2 as the internal lock and standard (δ 5.32). The tube was then returned to the bath within a 15 min period. The peaks of interest were integrated using a curve fitting routine on NMRi[23] software. Rate constants were calculated as described above. Three samples were

Table II. Rate Constants, k_{obs} (s^{-1}), for Reactions of 0.010M $Cp(CO)(PPh_3)Ru(\eta^1(S)\text{-Th})^+$ with PR_3 at 25.0 °C in CD_2Cl_2 According to Eq 5

Th	PR_3	10^4 k_{obs}, s^{-1} 0.10M PR_3	10^4 k_{obs}, s^{-1} 0.20M PR_3	10^4 k_{obs}, s^{-1} 0.40M PR_3
T	PPh_3	11.1(5)	15.0(3)	17.1(6)
2-MeT	PPh_3	2.3(1)	2.1(1)	2.2(1)
3-MeT	PPh_3	1.7(1)	1.7(1)	1.8(1)
2,5-Me_2T	PPh_3	1.2(1)	1.3(1)	1.3(1)
BT	PPh_3	0.64(3)	0.70(1)	0.76(1)
	$PPhMe_2$	0.66(2)	0.71(2)	0.75(2)
DBT	PPh_3	0.16(1)	0.16(2)	0.18(3)
Me_4T	PPh_3	0.055(1)	0.056(1)	0.063(1)

run at each phosphine concentration; the k_{obs} values given in Table III are the average of the three runs with the average deviation in the last digit given in parentheses.

For kinetic studies of reactions using the liquid phosphines, PPh_2Me and $PPhMe_2$, 0.0050 mmol of $Cp(CO)_2Ru(\eta^1(S)\text{-2,5-}Me_2T)[BF_4]$ or $Cp(CO)(PPh_3)Ru(\eta^1(S)\text{-BT})[BF_4]$ were placed in an NMR tube. The tube was evacuated and flushed with nitrogen. Under a flow of nitrogen, 0.50 mL of CD_2Cl_2 was added, and the tube was capped with a septum. The phosphine was injected into the solution through the septum using a microsyringe, and the tube was immediately placed in the probe of a Varian VXR-300 spectrometer thermostated at 25.0 ± 0.1 °C. The spectrometer was programmed to

Table III. Rate Constants, k_{obs} (s^{-1}), for Reactions of 0.010M $Cp(CO)_2Ru(\eta^1(S)\text{-Th})^+$ with PR_3 at 25.0 °C in CD_2Cl_2 According to Eq 5

Th	PR_3	$[PR_3]$	$10^4\ k_{obs}$, s^{-1}
2-MeT	PPh_3	0.10	4.1(2)
		0.20	4.1(1)
		0.40	4.1(1)
3-MeT	PPh_3	0.10	4.5(1)
		0.20	4.4(2)
		0.40	4.7(1)
BT	PPh_3	0.10	0.99(2)
		0.20	0.99(2)
		0.40	1.1(1)
2,5-Me_2T	PPh_3	0.10	0.27(1)
		0.20	0.30(3)
		0.30	0.35(1)
		0.40	0.37(1)
	PPh_2Me	0.10	0.45(1)
		0.15	0.53(7)
		0.20	0.64(3)
		0.30	0.86(9)
	$PPhMe_2$	0.10	3.7(1)

acquire spectra at specific time intervals, and the data were worked up as described above. The products of these kinetic reactions were identified from their ^1H NMR spectra, which were similar to those of $Cp(CO)_2(PPh_3)Ru^+$ [20, 21] or $Cp(CO)(PPh_3)_2Ru^+$ [22] reported in the literature: $Cp(CO)(PPh_3)Ru(PPhMe_2)^+$ (δ 5.02 ppm, Cp), $Cp(CO)_2Ru(PPh_2Me)^+$ (δ 5.63 ppm, Cp) and $Cp(CO)_2Ru(PPhMe_2)^+$ (δ 5.59 ppm, Cp).

RESULTS

Synthesis of $Cp(CO)_2Ru(\eta^1(S)\text{-Th})^+$ (1-7)

The thiophene containing complexes $Cp(CO)_2Ru(\eta^1(S)\text{-Th})^+$ (**1-7**) were synthesized in a manner identical to that of the $Cp(CO)(PPh_3)Ru(\eta^1(S)\text{-Th})^+$ complexes[10] using $AgBF_4$ to abstract the Cl^- from $Cp(CO)_2RuCl$ in the presence of excess thiophene (eq 6). The structures of BT and DBT are shown below. These complexes are thermally less

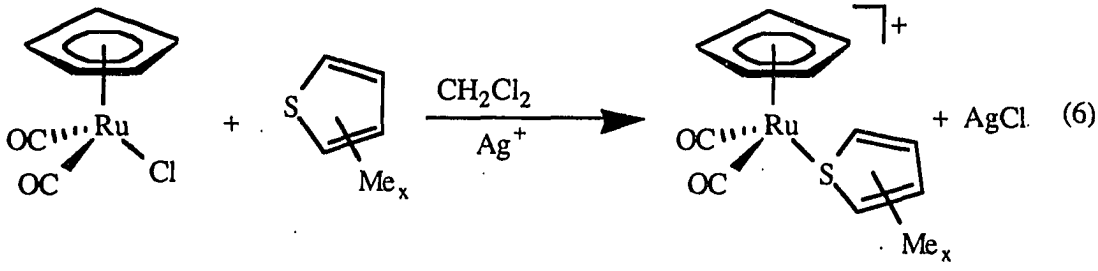

(6)

1, Th=T **2**, Th=2-MeT
3, Th=3-MeT **4**, Th=2,5-Me_2T
5, Th=Me_4T **6**, Th=BT
7, Th=DBT

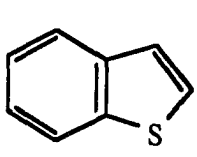

BT

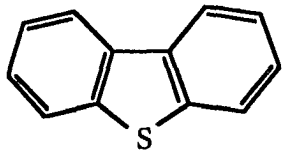

DBT

stable and are more air-sensitive than the corresponding $Cp(CO)(PPh_3)Ru(\eta^1(S)\text{-Th})^+$ complexes. The alkyl and aryl iodide complexes of $Cp(CO)(PPh_3)Ru(I\text{-}R)^+$ (R=alkyl,

aryl)[24] were also more stable than their $Cp(CO)_2Ru(I\text{-}R)^+$ analogs. The thiophene complex (**1**) was not isolated as an analytically pure compound but was identified by its ^1H and ^{13}C NMR and IR spectra. Solid samples of the T (**1**), 2-MeT (**2**) and 3-MeT (**3**) complexes show noticeable decomposition at room temperature in air and under nitrogen after 24 h but may be kept under N_2 at -20 °C for over one month. In CD_2Cl_2 solution, complexes **1, 2** and **3** also show decomposition within 24 h, producing the free thiophenes and a number of species containing the Cp ligand (in all cases, the major product has a Cp peak at δ 5.58 ppm in the ^1H NMR) as seen in the ^1H NMR spectra. None of these products were identified. There was also no evidence for $CpRu(\eta^5\text{-}T)^+$, which exhibits a singlet at δ 5.40 ppm (Cp) and a pair of multiplets at δ 6.32 and 6.16 ppm (T).[25] The η^5-T complex was previously identified as a product of the decomposition of $Cp(PPh_3)_2Ru(\eta^1(S)\text{-}T)^+$ in CD_2Cl_2 [11]. On the other hand, the $Cp(CO)(PPh_3)Ru(\eta^1(S)\text{-}T)^+$ complex, which is stable at room temperature in solution, decomposes in refluxing CH_2Cl_2 to give the Cl bridging dimer $[Cp(CO)(PPh_3)Ru]_2Cl^+$ (IR: υ(CO) 1973 cm^{-1}. ^1H NMR: δ 4.82 (s, Cp), 7.54 (m), 7.45 (m) and 7.25 (m, PPh_3). FAB: m/e 948.8 (M+)). Similar halide bridging dimers[26], e.g. $[Cp(CO)_2M]_2X^+$ (M = Fe, Ru; X = Cl, Br, I) are known. Complexes **4-7** are stable as solids and in solution at room temperature under N_2.

The DBT complex (**7**) is only slightly soluble in CH_2Cl_2. Due to its low solubility, **7** was not used in either the kinetic or equilibrium experiments.

Reactions of $Cp(CO)_2Ru(\eta^1(S)\text{-}Th)^+$ and $Cp(CO)(PPh_3)Ru(\eta^1(S)\text{-}Th)^+$ with PPh_3 produce the substituted products, $Cp(CO)_2(PPh_3)Ru^+$, [20, 21] and $Cp(CO)(PPh_3)_2Ru^+$,[22] respectively, and the free thiophenes (see Kinetic Studies in Experimental Section). Likewise, reaction of $Cp(CO)_2Ru(\eta^1(S)\text{-}BT)^+$ and $Cp(CO)(PPh_3)Ru(\eta^1(S)\text{-}T)^+$ with $[(n\text{-}Bu)_4N]Br$ give $Cp(CO)_2RuBr$[19] and $Cp(CO)(PPh_3)RuBr$[27] and free Th; $Cp(CO)(PPh_3)Ru(\eta^1(S)\text{-}BT)^+$ reacts with MeCN to give $Cp(CO)(PPh_3)Ru(NCMe)^+$ [10, 24]

and BT. These reaction products were identified by the ^1H NMR spectra based on data reported in the literature.

Compounds **1-7** were characterized by IR and ^1H and $^{13}C\{^1H\}$ NMR, FAB mass spectroscopy and elemental analysis (see Experimental Section). The υ(CO) absorptions in their IR spectra are 24 to 30 cm^{-1} higher than those of the neutral starting material, $Cp(CO)_2RuCl$ (υ(CO)=2056, 2004 cm^{-1}). The Cp protons in their ^1H NMR spectra are slightly deshielded (0.15 - 0.29 ppm) as compared with $Cp(CO)_2RuCl$ (δ 5.45 ppm). The thiophene ring protons in **1-4** are downfield (0.11 - 0.27 ppm) from those of the free thiophene, as was found in the $Cp(CO)_2Fe(\eta^1(S)\text{-T})^+$ [4a] complex. These resonances are also slightly downfield of those in the $Cp(CO)_2Re(\eta^1(S)\text{-Th})$[9] and $Cp(CO)(PPh_3)Ru(\eta^1(S)\text{-Th})^+$,[10] complexes with more electron-rich metal centers. If the thiophene ligands were bound to the metal in an η^2 -fashion through one of the C-C double bonds, the thiophene ring protons would be expected to shift significantly upfield, as reported for complexes of η^2-thiophene,[28] η^2- selenophenes,[29] η^2–benzo[b]thiophene[3c] and olefins.[30] In the ^{13}C NMR spectra of complexes **1-7**, the thiophene carbons are slightly downfield (5.8 - 11.0 ppm) of those in the free thiophene, as was also observed for $Cp(CO)_2Fe(\eta^1(S)\text{-Th})^+$,[4a] $Cp(CO)(PPh_3)Ru(\eta^1(S)\text{-Th})^+$,[10] and $Cp(CO)_2Re(\eta^1(S)\text{-Th})$[9]. Again, an upfield shift in the ^{13}C resonances would have been expected[3c, 29] for η^2-carbons if the thiophenes were η^2-bound through two carbons. Thus, the NMR spectra establish that the thiophenes are $\eta^1(S)$-bound. This type of coordination is confirmed by X-ray diffraction studies of $Cp(CO)_2Re(\eta^1(S)\text{-T})$[9] and $Cp(CO)(PPh_3)Ru(\eta^1(S)\text{-2-MeT})^+$.[10]

Only one CO resonance is observed in ^{13}C NMR spectra of complexes **2, 3** and **6** at room temperature in CD_2Cl_2. If the unsymmetric thiophenes in these complexes were non-fluxional, one would expect the diastereotopic CO groups to give two signals. Thus there is a dynamic process which makes the two carbonyls equivalent on the NMR time scale. At

temperatures below 198 K, the ^{13}C NMR spectrum of $Cp(CO)_2Ru(\eta^1(S)\text{-BT})^+$ in CD_2Cl_2 shows two peaks (δ 192.9 and 192.5 ppm) for the CO groups. At the coalescence temperature (205 K), the free energy of activation, $\Delta G^{\neq}$, is calculated[31] to be 43 kJ/mol. The fluxional process involved is likely to be inversion of the thiophene sulfur, as has been observed in other systems.[4a, 10, 32] Previously, $\Delta G^{\neq}$ values of 39 kJ/mol at 190 K[4a] for $Cp(CO)_2Fe(\eta^1(S)\text{-BT})^+$ and 40 kJ/mol at 213 K[10] for $Cp(CO)(PPh_3)Ru(\eta^1(S)\text{-Th})^+$ (Th=2,5-Me_2T and Me_4T) were obtained. Since $Cp(CO)_2Ru(\eta^1(S)\text{-BT})^+$ has a higher inversion barrier at higher temperature than $Cp(CO)_2Fe(\eta^1(S)\text{-BT})^+$, the inversion is slower in the Ru complex.

Equilibrium Studies

Results of the equilibrium studies of reaction 3 are shown in Table I. Numbers in parentheses are average deviations for at least 3 runs of the same reaction. Reactions B and F along with G and H approach equilibrium from opposite directions. The K value for reaction B (1.52) is identical to that of the inverse of F (1/0.660 = 1.52); likewise, the K value for H (19.2) is within experimental error of that of the inverse of G (1/0.0526 = 19.0). Similarly, adding reactions A and F together gives reaction E. Multiplying the experimental K values for A (0.303) and F (0.660) gives a calculated K value for reaction E of 0.200, which is within 5% of the experimental K value for reaction E (0.210). All other comparisons done in this manner result in calculated values that are within 6% of the directly measured value, ensuring the validity of the experimental K values.

Kinetic Studies

Results of kinetic studies of thiophene replacement in $Cp(CO)(PPh_3)Ru(\eta^1(S)\text{-Th})^+$, $Cp(CO)_2Ru(\eta^1(S)\text{-Th})^+$, and $Cp(CO)(PPh_2Me)Ru(\eta^1(S)\text{-3-MeT})^+$ with PR_3 (PR_3 = PPh_3,

PPh_2Me, $PPhMe_2$) according to equation 5 are shown in Tables II and III. The studies were done under pseudo first-order conditions, always with a greater than 10-fold excess of phosphine. Except for the reactions of $Cp(CO)(PPh_3)Ru(\eta^1(S)\text{-BT})^+$ and $Cp(CO)_2Ru(\eta^1(S)\text{-2,5-}Me_2T)^+$ (**4**), the k_{obs} values are independent of phosphine concentration within experimental error (Tables II and III) and follow the rate law in eq 7,

$$\frac{d\,[Cp(CO)LRu(\,\eta^1(S)\text{-Th})^{+}]}{dt} = k_{obs}\,[Cp(CO)LRu(\,\eta^1(S)\text{-Th})^{+}] \qquad (7)$$

where $k_{obs} = k_1$. This rate law indicates that the slow step in these reactions is the dissociation of Th from the Ru; this is followed by fast reaction of the 16 e^- intermediate with PR_3 to form the product.

For the reaction of $Cp(CO)(PPh_3)Ru(\eta^1(S)\text{-BT})^+$ with PPh_3, the rate constants (Table II) appear to increase with increasing phosphine concentration; however, when the more basic, less sterically crowded phosphine, PMe_2Ph, is used as the incoming nucleophile, the reaction rate constants are the same within experimental error. So these reactions of this complex also follow the first order rate law (eq 7), but the errors are larger than in the other reactions.

Rate constants (k_{obs}) for the reactions of complex **4** increase slightly with increasing PPh_3 concentration. It is evident (Table III and Figure 1) that there is a phosphine dependence in this case, and the rate law contains both first- and second- order terms (eq 8).

$$k_{obs} = k_1 + k_2\,[PR_3] \qquad (8)$$

Linear correlations (Figure 1) are obtained when the k_{obs} values (Table III) for the reactions of **4** with PPh_3 and PPh_2Me are plotted against phosphine concentration. The lines fit eq 9 (PPh_3) and eq 10 (PPh_2Me) as determined by linear least squares regression analysis

$$k_{obs} = 0.235 \times 10^{-4} + 0.350 \times 10^{-4} [PPh_3] \quad (9)$$

$$k_{obs} = 0.230 \times 10^{-4} + 2.08 \times 10^{-4} [PPh_2Me] \quad (10)$$

(the correlation coefficients, r = 0.988 and 0.998, respectively). The y-intercepts of both lines give the same value for k_1 within experimental error. The slope of the PPh_2Me line gives a second-order rate constant (k_2= 2.08 x 10^{-4} M^{-1} s^{-1}) that is larger than that of the PPh_3 line (k_2=0.350 x 10^{-4} M^{-1} s^{-1}), which is consistant with PPh_2Me being the better nucleophile.

Reactions of $Cp(CO)(PPh_3)Ru(\eta^1(S)\text{-T})^+$ and $Cp(CO)_2Ru(\eta^1(S)\text{-BT})^+$ with Br^- to give $Cp(CO)(PPh_3)RuBr$[27] and $Cp(CO)_2RuBr$[19] are very rapid compared to those with phosphines. In an NMR tube, reactions of 0.020 moles of both Ru complexes with 0.080 moles of $[(n\text{-}Bu)_4N]Br$ in 0.50 mL of CD_2Cl_2 were complete before the first spectrum was taken (less than 5 min). Under the same conditions, the reaction of $Cp(CO)(PPh_3)Ru(\eta^1(S)\text{-T})^+$ with PPh_3, requires 35 min to reach 95% completion. Thus, unlike PPh_3 reactions, those of Br^- must involve nucleophilic attack on the complex.

The k_{obs} values (Table III) for the reaction with **4** with PPh_2Me show greater errors than for all of the other reactions. These errors may be due, in part, to a light catalysis of the reaction. This was demonstrated by observing that the reaction was only 10% complete after 12 min when the NMR reaction tube was wrapped in aluminum foil prior to placing it in the spectrometer probe and taking the first spectrum. The same reaction, when allowed to stand

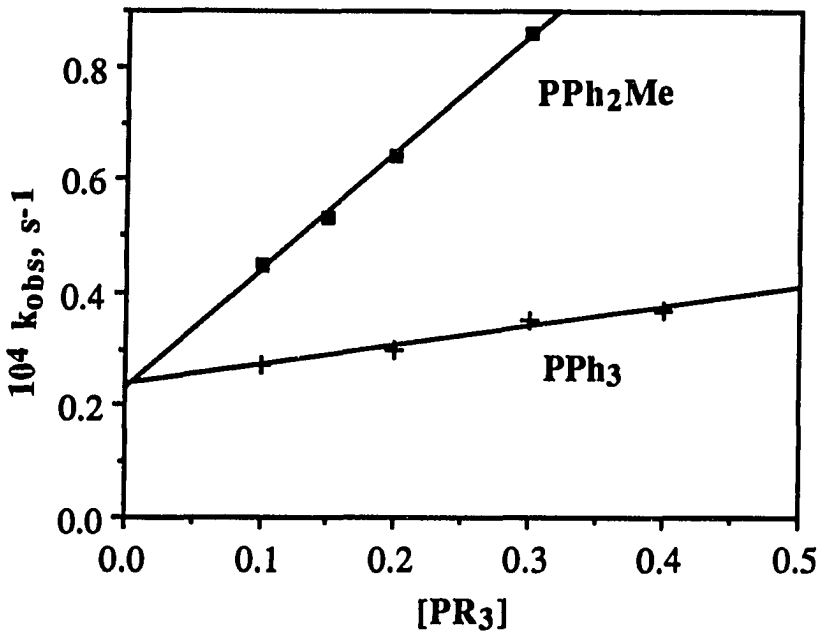

Figure 1. Plot of k_{obs} vs. phosphine concentration for the reactions of $Cp(CO)_2Ru(\eta^1(S)$-2,5-$Me_2T)^+$ (4) with PPh_2Me and PPh_3 according to eq 5 at 25 °C.

in the light for the same amount of time, was more than 75% complete. Since tubes in the NMR probe are not completely shielded from light, this exposure probably affects the reproducibility of the reactions with PPh_2Me. The reaction of **5** with PPh_3 was so light-sensitive that it was impossible to obtain reproducible rate constants.

DISCUSSION

Equilibrium Studies of Thiophene Substitution in $Cp(CO)_2Ru(\eta^1(S)\text{-Th})^+$

Relative equilibrium constants, K', for the displacement of thiophene by methyl-substituted thiophenes and benzo[b]thiophene (eq 11) were calculated from the

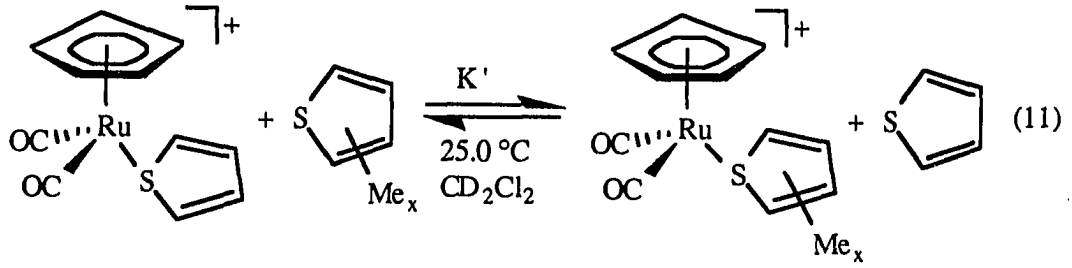

(1) (2 - 6)

experimental K values in Table I. These values together with K' values for the analogous equilibrium (eq 2)[10] involving $Cp(CO)(PPh_3)Ru(\eta^1(S)\text{-Th})^+$ are given in Table IV.

The K' values for reaction (11) increase in the following order: T (1.00) < 2-MeT (3.30) < 3-MeT (4.76) < 2,5-Me_2T (20.7) < BT (47.6) < Me_4T (887). Thiophene itself is the most weakly coordinating ligand studied. Adding a methyl group to thiophene in the 2-position increases K' to 3.30. Moving the methyl group to the 3-position increases the value slightly to 4.76. This increase in binding ability is most likely due to the electron donating ability of the Me group, which makes the S atom a better donor to the Ru. With two methyl groups in the α-positions, as in 2,5-Me_2T, the K' value (20.7) increases by more than a factor of 6 as compared with 2-MeT. Finally, adding two more Me groups in the 3- and 4-positions on the thiophene ring makes Me_4T by far the most strongly coordinating thiophene. This trend of increasing K' values with increased Me substitution is slightly different than

Table IV: Relative Equilibrium Constants, K', for Reactions (Eq 11 and 2) of $Cp(CO)(L)Ru(\eta^1(S)\text{-Th})^+$ with Th' at 25.0 °C

Th	$Cp(CO)_2Ru(Th)^+$	$Cp(CO)(PPh_3)Ru(Th)^+$,[a]
T	1.00	1.00
2-MeT	3.30	4.11
3-MeT	4.76	6.30
$2,5\text{-Me}_2T$	20.7	2.76
BT	47.6	29.9
Me_4T	887	57.4
DBT		74.1

[a] Ref.10

that (Table IV) determined in equilibrium studies of thiophene displacement from $Cp(CO)(PPh_3)Ru(\eta^1(S)\text{-Th})^+$,[10] (eq 2); in this latter case, $2,5\text{-Me}_2T$ was found to be a weaker binding ligand than either 2-MeT or 3-MeT. Based on an X-ray determined structure and computer modeling studies, we argued[10] that steric hindrance between an α-methyl group on thiophene and the phenyl groups on PPh_3 in $Cp(CO)(PPh_3)Ru(\eta^1(S)\text{-}2,5\text{-Me}_2T)^+$ significantly reduced the K' value for $2,5\text{-Me}_2T$ as compared with the other thiophenes. This argument is reinforced in the present equilibrium study, since replacement of the PPh_3 in $Cp(CO)(PPh_3)Ru(\eta^1(S)\text{-Th})^+$ with the less sterically crowding CO ligand dramatically increases the relative K' values for $2,5\text{-Me}_2T$ and Me_4T. Also, an X-ray structure

determination of the structurally similar $Cp^*(CO)_2Re(\eta^1(S)\text{-T})$[9] shows no indication of steric hindrance between the T and the two carbonyls. Thus, in $Cp(CO)_2Ru(\eta^1(S)\text{-Th})^+$, the trend of increasing K' values with the number of methyl groups is due to the electron donating ability of the methyl groups.

There may also be some steric reduction of $\eta^1(S)$-BT binding in $Cp(CO)(PPh_3)Ru(\eta^1(S)\text{-BT})^+$, since its K' value (29.9), relative to the uncrowded thiophene complex, is significantly less than that (47.6) in $Cp(CO)_2Ru(\eta^1(S)\text{-Th})^+$.

Kinetic Studies of Thiophene Dissociation from $Cp(CO)LRu(\eta^1(S)\text{-Th})^+$

First-order rate constants (k_1) for thiophene substitution by PR_3 in $Cp(CO)_2Ru(\eta^1(S)\text{-Th})^+$ and $Cp(CO)(PPh_3)Ru(\eta^1(S)\text{-Th})^+$ (eq 6) are listed in Table V. Since these constants are for a rate law which is independent of PR_3 concentration, they correspond to a mechanism (eq 12) which involves rate-determining dissociation of the

$$Cp(CO)LRu(\eta^1(S)\text{-Th})^+ \xrightarrow[-Th]{k_1} Cp(CO)LRu^+ \xrightarrow[PR_3]{fast} Cp(CO)LRu(PR_3)^+ \qquad (12)$$

thiophene followed by rapid reaction of the unsaturated ruthenium residue with PR_3 to give the final product. For the $Cp(CO)_2Ru(\eta^1(S)\text{-Th})^+$ complexes, the k_1 values decrease with the thiophene in the following order: 3-MeT ≥ 2-MeT > BT > 2,5-Me_2T. The dissociation rates of 3-MeT ($10^6\,k_1 = 450\ s^{-1}$) and 2-MeT ($10^6\,k_1 = 410\ s^{-1}$) are almost identical. Adding a second Me group to the thiophene to give 2,5-Me_2T decreases the rate of dissociation by a factor of 20 compared to 3-MeT and 18 compared to 2-MeT. The trend is similar to that of thiophene dissociation from $Cp(CO)_2Re(\eta^1(S)\text{-Th})$ (eq 2): 3-MeT ($10^6\,k_1$=120 s^{-1}) > 2-MeT ($10^6\,k_1$=9.1 s^{-1}) > 2,5-Me_2T ($10^6\,k_1$=1.3 s^{-1}) in C_6D_6 at 80 °C. These trends suggest that Me groups on the thiophene strengthen the Ru-S bond by making the sulfur

Table V. First Order Rate Constants, k_1 (s^{-1}), for the Dissociation of Th from $Cp(CO)_2Ru(\eta^1(S)\text{-Th})^+$ and $Cp(CO)(PPh_3)Ru(\eta^1(S)\text{-Th})^+$ in CD_2Cl_2 at 25.0 °C According to Eq 5

Th	$Cp(CO)(PPh_3)Ru(Th)^+$ $10^6 k_1, s^{-1}$	$Cp(CO)_2Ru(Th)^+$ $10^6 k_1, s^{-1}$
T	1400	
2-MeT	220	410
3-MeT	170	450
2,5-Me_2T	130	23[a]
BT	70	100
DBT	17	
Me_4T	5.8	

[a]Second-order rate constants for reactions of $Cp(CO)_2Ru(\eta^1(S)\text{-2,5-}Me_2T)^+$ with PR_3: k_2 = 35 x 10^{-6} $s^{-1}M^{-1}$ (PPh_3); k_2 = 208 x 10^{-6} $s^{-1}M^{-1}$ (PPh_2Me).

a stronger donor. Methyl groups affect the equilibrium constants (eq 11, Table IV) for thiophene exchange in the same way, as discussed in the previous section.

For the $Cp(CO)(PPh_3)Ru(\eta^1(S)\text{-Th})^+$ complexes, the 10^6 k_1 values (s^{-1}) decrease as follows: T (1400) > 2-MeT (220) > 3-MeT (170) > 2,5-Me_2T (130) > BT (70) > DBT (17) > Me_4T (5.8) . As in the $Cp(CO)_2Ru(\eta^1(S)\text{-Th})^+$ system, the rate of thiophene dissociation decreases as the number of Me groups in the thiophene increases. However, there is

evidence that methyl groups in the 2- and 5-positions sterically accelerate the dissociation by interacting with the bulky PPh_3. For example, 2-MeT dissociates more rapidly than 3-MeT, but the reverse was true in the $Cp(CO)_2Ru(\eta^1(S)\text{-Th})^+$ and $Cp(CO)_2Re(\eta^1(S)\text{-Th})$ (eq 1). Also, the rate of 2,5-Me_2T dissociation in $Cp(CO)(PPh_3)Ru(\eta^1(S)\text{-Th})^+$ is just slightly slower (less than a factor of 2) than 2-MeT. In the less sterically hindered systems, $Cp(CO)_2Ru(\eta^1(S)\text{-Th})^+$ and $Cp(CO)_2Re(\eta^1(S)\text{-Th})$, where 2,5-$Me_2$T dissociation is not enhanced by crowding, 2,5-Me_2T dissociates much more slowly than 2-MeT. This steric interaction is supported by trends in equilibrium constants, K', for Th binding in $Cp(CO)(PPh_3)Ru(\eta^1(S)\text{-Th})^+$ (eq 2) that showed 2,5-Me_2T to be less strongly bound than the 2-MeT, but in the less crowded $Cp(CO)_2Ru(\eta^1(S)\text{-Th})^+$ (eq 4), 2,5-Me_2T binds more strongly than 2-MeT.

Rates of BT ($10^6\ k_1$=70 s^{-1}) and DBT ($10^6\ k_1$=17 s^{-1}) dissociation from $Cp(CO)(PPh_3)Ru(\eta^1(S)\text{-Th})^+$ are substantially slower than those of T. Relative equilibrium constants, K', for these thiophenes (Table IV) also in the $Cp(CO)(PPh_3)Ru(\eta^1(S)\text{-Th})^+$ system, follow the same trend: T (1.00) < BT (29.9) < DBT (74.1).

The interaction between the thiophenes and the metal may be described as a donation of sulfur electron density to the metal center. This bonding picture suggests that an increase in electron density at the metal center should weaken the Ru-S bond. To test this effect, we compared the rates of dissociation of the sterically small 3-MeT from $Cp(CO)(PPh_3)Ru(\eta^1(S)\text{-3-MeT})^+$ and $Cp(CO)(PPh_2Me)Ru(\eta^1(S)\text{-3-MeT})^+$. Reactions of $[Cp(CO)(PPh_2Me)Ru(\eta^1(S)\text{-3-MeT})]BF_4$ (**9**) with PPh_3 to give $[Cp(CO)(PPh_2Me)Ru(PPh_3)]BF_4$ follow a first-order rate law (eq 7) giving the following k_1 values: 4.2(1) x 10^{-4} s^{-1} (0.10M PPh_3), 4.1(2) x 10^{-4} s^{-1} (0.20M PPh_3) and 4.7(1) x 10^{-4} s^{-1} (0.40M PPh_3). As expected, k_1 for this dissociation is faster for $Cp(CO)(PPh_2Me)Ru(\eta^1(S)\text{-3-MeT})^+$ (k_1= 4.3 x 10^{-4} s^{-1}) than for $Cp(CO)(PPh_3)Ru(\eta^1(S)$-

3-MeT)$^+$ (k_1= 1.7 x 10^{-4} s^{-1}). This observation is consistent with the effect of the Cp' ligand on the rate of 3-MeT dissociation from Cp'$(CO)_2$Re(η^1(*S*)-3-MeT) (Cp' = Cp, Cp*) complexes;[13] here the rate of 3-MeT dissociation from the more basic Re complex containing Cp* (Cp* = η^5-C_5Me_5) is 3.5 times faster than that from the analogous Cp complex.

The reaction of $Cp(CO)_2Ru(\eta^1(S)$-2,5-$Me_2T)^+$ (**4**) with phosphines show a significant contribution from a second order (k_2) pathway that is not observed with any of the other $Cp(CO)_2Ru(\eta^1(S)$-Th)$^+$ complexes. Complex **4** is also the slowest to undergo Th dissociation; it is perhaps this slow 2,5-Me_2T dissociation that allows the rate of nucleophilic attack of the PR_3 to become competetive with the dissociation. That nucleophilic attack is possible on these complexes is suggested by the fast reaction of Br^- with $Cp(CO)_2Ru(\eta^1(S)$-BT)$^+$ (**6**) (see Results).

Relevance to Thiophene Adsorption on HDS Catalysts

Relative adsorption coefficients (K_{rel}) for thiophenes (Table VI) on a sulfided Co-Mo/Al_2O_3 HDS catalyst at 350 °C increase[33] with the number of methyl groups in the thiophene: T (1.0) < 2-MeT (1.6) < 3-MeT (1.7) < 2,5-Me_2T (2.5).[14] The absence of a steric effect that reduces adsorption by thiophenes with 2- and 5-methyl groups was interpreted to mean that $\eta^1(S)$-coordination to a metal site on the catalyst was unlikely; therefore, η^5 was suggested as the most probable mode of thiophene adsorption. This conclusion was supported by equilibrium studies[34] (eq 13) that showed that K' also increases

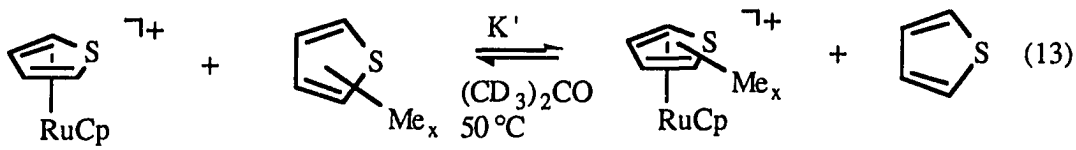

(13)

Table VI. Equilibrium Constants for Binding of Methyl-Substituted Thiophenes on a Co-Mo/Al_2O_3 Catalyst, in $CpRu(\eta^5\text{-Th})^+$, $Cp(CO)_2Ru(\eta^1(S)\text{-Th})^+$ and $Cp(CO)(PPh_3)Ru(\eta^1(S)\text{-Th})^+$; Also, Rates of Th Dissociation from $Cp(CO)_2Re(\eta^1(S)\text{-Th})$, $Cp(CO)_2Ru(\eta^1(S)\text{-Th})^+$ and $Cp(CO)(PPh_3)Ru(\eta^1(S)\text{-Th})^+$

Th	K_{rel}[a]	K'[b]	K'[c]	K'[d]	10^7k_1[e]	10^6k_1[f]	10^6k_1[g]
T	1.0	1	1.0	1.0	3000		1400
2-MeT	1.6	6	4.1	3.3	91	410	220
3-MeT	1.7	7	6.3	4.8	1200	450	170
2,5-Me_2T	2.5	35	2.8	20	13	23	130
Me_4T		1300	74	887	2.7		5.8

[a] For adsorption on a sulfided Co-Mo/Al_2O_3 catalyst at 350 °C; ref 14.

[b] For η^5-Th coordination in $CpRu(\eta^5\text{-Th})^+$ at 50.0 °C in acetone-d_6, according to eq 13; ref 34.

[c] For $\eta^1(S)$-Th coordination in $Cp(CO)(PPh_3)Ru(\eta^1(S)\text{-Th})^+$ at 25.0 °C in CD_2Cl_2 according to eq 2; ref 10.

[d] For $\eta^1(S)$-Th coordination in $Cp(CO)_2Ru(\eta^1(S)\text{-Th})^+$ at 25.0 °C in CD_2Cl_2 according to eq 11; this work.

[e] Rate constants (k_1) for the dissociation of Th from $Cp(CO)_2Re(\eta^1(S)\text{-Th})$ at 80.0 °C in C_6D_6 according to eq 1; ref 13.

[f] Rate constants (k_1) for the dissociation of Th from $Cp(CO)_2Ru(\eta^1(S)\text{-Th})^+$ at 25.0 °C in CD_2Cl_2 according to eq 5; this work.

[g] Rate constants (k_1) for the dissociation of Th from $Cp(CO)(PPh_3)Ru(\eta^1(S)\text{-Th})^+$ at 25.0 °C in CD_2Cl_2 according to eq 5; this work.

with the number of methyl groups on the thiophene: T (1) < 2-MeT (6) ≤ 3-MeT (7) < 2,5-Me_2T (35). Moreover, there is much evidence to indicate that η^5-coordination[25, 35] in organometallic complexes activates the thiophene to undergo a variety of reactions, some of which have been used as the basis of proposed thiophene HDS mechanisms.[36]

While η^5-coordination logically accounts for the trend in methyl thiophene adsorption on the Co-Mo/Al_2O_3 catalyst, $\eta^1(S)$-binding also accounts for this trend. Thus, equilibrium constants, K', for $\eta^1(S)$-binding of thiophenes in $Cp(CO)_2Ru(\eta^1(S)\text{-Th})^+$ increase in the same order: T (1.0) < 2-MeT (3.30) < 3-MeT (4.76) < 2,5-Me_2T (20.7). In these studies, there appears to be no steric effect caused by methyl groups in the 2- and 5-positions. Steric effects do become significant in the related $Cp(CO)(PPh_3)Ru(\eta^1(S)\text{-Th})^+$ (Table IV, VI) which contains a bulky PPh_3 ligand. However, such bulky ligands are normally not present on the surface of an HDS catalyst. Thus, the $\eta^1(S)$-coordination mode also accounts for the trend in thiophene adsorption on the Co-Mo/Al_2O_3 catalyst. There is also recent evidence to suggest that $\eta^1(S)$-coordination can activate the thiophene by inserting into a C-S bond.[18, 37] This could occur as the metal migates between the sulfur ($\eta^1(S)$-) and olefin (η^2-) coordination (eq 14).[37] This migration has been established in the selenophene (Sel)

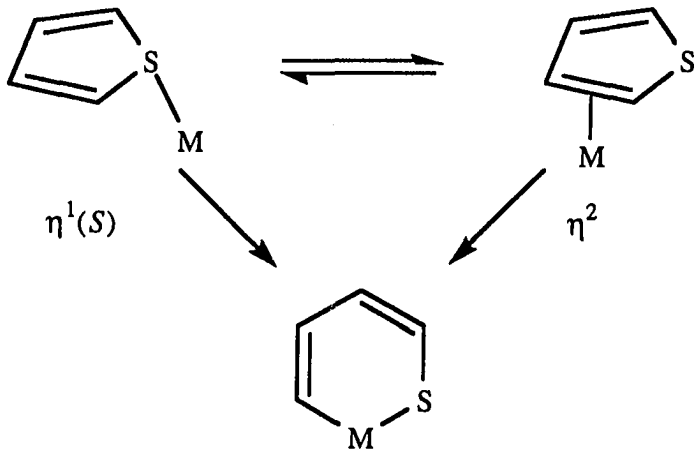

(14)

complexes $Cp(CO)_2Re(SeI)$[29] and in $Cp(CO)_2Re(BT)$[3c]. The C,S-ring-opened structure has been observed in $Cp^*Ir(C,S\text{-}C_4R_4S)$[38] and $Cp^*(PR_3)M(C,S\text{-}C_4R_4S)$[18, 37, 38c]. Thus, it is possible that thiophene could adsorb in the $\eta^1(S)$-form and be activated to undergo HDS by a pathway that begins with the insertion in equation 14.

A comparison of the $\eta^1(S)$-coordinating abilities of thiophene and the benzothiophenes (Tables IV, V) show that they increase in the order T < BT < DBT. If these thiophenes coordinate in the same way at a metal site on a catalyst surface, one would expect to find the same trend in their adsorption on the catalyst. However, at this time there are no data on the relative binding abilities of these thiophenes on HDS catalysts that would allow this comparison to be made.

Acknowledgment

We are grateful to Johnson Matthey, Inc. for a generous loan of $RuCl_3$.

REFERENCES

(1) Ames Laboratory is operated for the U. S. Department of Energy by Iowa State University under Contract No. W-7405-Eng-82. This research was supported by the Office of Basic Energy Sciences, Chemical Sciences Division.

(2) (a) *Geochemistry of Sulfur in Fossil Fuels*; Orr, W. L., White, C. M., Eds.; ACS Symposium Series 429; American Chemical society; Washington D.C. **1990.**

(b) Prins, R.; deBeer, V. H. J.; Somorjai, G. A. *Catal. Rev.-Sci. Eng.* **1989**, *31*, 1.

(c) McCulloch, D. C. In *Applied Industrial Catalysis*; Leach, B. E., Ed.; Academic: New York, **1983**; Vol. 1, p. 69.

(d) Gates, B. C.; Katzer, J. R.; Schuit, G. C. A. *Chemistry of Catalytic Processes*; McGraw-Hill: New York, **1979**, Chapter 5.

(e) Satterfield, C. N. *Heterogeneous Catalysis in Industrial Practice*; McGraw-Hill: New York, **1991**, 378.

(3) (a) Angelici, R. J. *Coord. Chem. Rev.* **1990**, *105*, 61.

(b) Rauchfuss, T. B. *Prog. Inorg. Chem.* **1991**, *39*, 259.

(c) Choi, M.-G.; Robertson, M. J.; Angelici, R. J. *J. Am. Chem. Soc.* **1991**, *113*, 4005.

(d) Choi, M.-G.; Angelici, R. J. *Organometallics*, submitted.

(e) Rao, K. M.; Day, C. L.; Jacobson, R. A.; Angelici, R. J. *Inorg. Chem.*. **1991**, *30*, 5046.

(f) Chen, J.; Su, Y.; Jacobson, R. A. ; Angelici, R. J. *J. Organomet. Chem.* **1992**, *428*, 415.

(g) Huckett, S. C.; Miller, L. L.; Jacobson, R. A.; Angelici, R. J. *Organometallics* **1988**, *7*, 686.

(h) Huckett, S. C.; Angelici, R. J. *Organometallics* **1988**, *7*, 1491.

(i) Wang, C.-M. J.; Angelici, R. J. *Organometallics* **1990**, *9*, 1770.

(4) (a) Goodrich, J. D.; Nickias, P. N.; Selegue, J. P. *Inorg. Chem.* **1987**, *26*, 3424.

(b) Kuhn, N.; Schumann, H. *J. Organomet. Chem.* **1984**, *276*, 55.

(5) Guerchais, V.; Astruc, D. *J. Organomet. Chem.* **1986**, *316*, 335.

(6) Kuehn, C. G.; Taube, H. *J. Am. Chem. Soc.* **1976**, *98*, 689.

(7) Catheline, D.; Astruc, D. *J. Organomet. Chem.* **1984**, *272*, 417.

(8) Wasserman, H. J.; Kubas, G. J.; Ryan, R. R. *J. Am. Chem. Soc.* **1986**, *108*, 2294.

(9) (a) Choi, M.-G.; Angelici, R. J. *J Am. Chem. Soc.* **1989**, *111*, 8753.

(b) Choi, M.-G.; Angelici, R. J. *Organometallics* **1991**, *10*, 2436.

(10) Benson, J. W.; Angelici, R. J. *Organometallics* **1992**, *11*, 922.

(11) Draganjac, M.; Ruffing, C. J.; Rauchfuss, T. B. *Organometallics* **1985**, *4*, 1909.

(12) Constable, E. C.; Henney, R. P.G.; Tocher, D. A. *J. Chem. Soc., Dalton Trans.* **1991**, 2335.

(13) Choi, M.-G.; Angelici, R. J. *Inorg. Chem.* **1991**, *30*, 1417.

(14) Zdrazil, M. *Collect. Czech. Chem. Commun.* **1977**, *42*, 1484.

(15) (a) *Experimental Organometallic Chemistry*; Wayda, A.L.; Darensbourg, M. Y. Eds.; ACS Symposium Series 357 American Chemical Society: Washington D.C. 1987.

(b) Shriver, D. F.; Drezdzon, M. A. *The Manipulation of Air Sensitive Compounds*, 2nd ed.; Wiley: New York, 1986.

(16) Spies, G. H.; Angelici, R. J. *Organometallics* **1987**, *6*, 1897.

(17) Jensen, C. M.; Jones, N. L. *Inorg. Synth* **1990**, *28*, 216.

(18) Dong, L.; Duckett, S. B.; Ohman, K. F.; Jones, W. D. *J. Am. Chem. Soc.* **1992**, *114*, 151.

(19) Eisenstadt, A.; Tannenbaum, R.; Efraty, A. *J. Organomet. Chem.* **1981**, *221*, 317.

(20) Humphries, A. P.; Knox, A. R. *J. Chem. Soc., Dalton Trans.* **1975**, 1710.

(21) Davies, S.G.; Simpson, S. J. *J. Chem. Soc., Dalton Trans.* **1984**, 993.

(22) Blackmore, T.; Bruce, M. I.; Stone, F. G. A. *J. Chem. Soc., A* **1971**, 2376.

(23) New Methods Research, Inc. (NMRi), Syracuse, New York.

(24) Kulawiec, R. J.; Faller, J. W.; Crabtree, R. H. *Organometallics* **1990**, *9*, 745.

(25) (a) Spies, G. H.; Angelici, R. J. *J. Am. Chem. Soc.* **1985**, *107*, 5569.
(b) Sauer, N. N.; Angelici, R. J. *Organometallics* **1987**, *6*, 1146.

(26) (a) Haines, R. J.; duPreez, A. L. *J. Chem. Soc., A* **1970**, 2341.
(b) Haines, R. J.; duPreez, A. L. *J. Chem. Soc., Dalton Trans.* **1972**, 944.

(27) Brown, D. A.; Lyons, H. J.; Shane, R. T. *Inorg. Chim. Acta.* **1970**, *4*, 621.

(28) Cordone, R.; Harman, W. D.; Taube, H. *J. Am. Chem. Soc.* **1989**, *111*, 5969.

(29) (a) Choi, M.-G.; Angelici, R. J. *J Am. Chem. Soc.* **1990**, *112*, 7811.
(b) Choi, M.-G.; Angelici, R. J. *J Am. Chem. Soc.* **1991**, *113*, 5651.

(30) (a) Burns, C. J.; Anderson, R. A. *J. Am. Chem. Soc.* **1987**, *109*, 915.
(b) Harman, W. D.; Schafer, W. P.; Taube, H. *J. Am. Chem. Soc.* **1990**, *112*, 2682.

(31) Sandstrom, J. *Dynamic NMR Spectroscopy*, Academic Press: New York **1982**, p. 96.

(32) Abel, E. W.; Orrell, K. G.; Bhargava, S. K. *Prog. Inorg. Chem.* **1984**, *32*, 1.

(33) It should be noted that the adsorption sites on the catalyst are not necessatily the sites at which thiophene HDS occurs.

(34) Hachgenei, J. W.; Angelici, R. J. *Organometallics* **1989**, *8*, 14.

(35) (a) Lesch, D. A.; Richardson, J. W.; Jacobson, R. A.; Angelici, R. J. *J. Am. Chem. Soc.* **1984**, *106*, 2901.

(b) Hachgenei, J. W.; Angelici, R. J. *J. Organomet. Chem.* **1988**, *355*, 359.

(36) (a) Chen, J.; Daniels, L. M.; Angelici, R. J. *J. Am. Chem. Soc.* **1991**, *113*, 2544.

(b) Angelici, R. J. *Acc. Chem. Res.* **1988**, *22*, 387.

(37) Jones, W. D.; Dong, L. *J. Am. Chem. Soc.* **1991**, *113*, 559.

(38) (a) Chen, J.; Angelici, R.A. *Organometallics* **1992**, *11*, 992.

(b) Chen, J.; Angelici, R.A. *Organometallics* **1990**, *9*, 849.

(c) Chen, J.; Daniels, L. M.; Angelici, R. J. *Polyhedron* **1990**, *9*, 1883.

PAPER III. REACTIONS OF 2-BENZO[b]THIENYL (2-BTyl) COMPLEXES WITH ACID TO GIVE $Cp(PMe_3)_2Ru(\eta^1(S)\text{-}BT)^+$ AND $Cp(CO)(PPh_3)Ru(\eta^1(S)\text{-}BT)^+$: A MODEL FOR BENZO[b]THIOPHENE (BT) DEUTERIUM EXCHANGE ON HYDRODESULFURIZATION CATALYSTS.[1]

ABSTRACT

The 2-benzothienyl complexes, $Cp(PMe_3)_2Ru(2\text{-}BTyl)$ (**1**) and $Cp(CO)(PPh_3)Ru(2\text{-}BTyl)$ (**2**) are prepared from reactions of 2-benzothienyllithium with $Cp(PMe_3)_2RuX$ (X = Cl, CF_3SO_3) and $Cp(CO)(PPh_3)RuCl$. Protonation of **2** with CF_3SO_3H gives the η^1(S)-benzo[b]thiophene(BT) complex $Cp(CO)(PPh_3)Ru(\eta^1(S)\text{-}BT)^+$ (**4**). The analogous protonation of **1** appears to initially add H^+ to the S atom in the BTyl ligand; this intermediate subsequently rearranges to the η^1(S)-BT complex, $Cp(PMe_3)_2Ru(\eta^1(S)\text{-}BT)^+$ (**3**). These reactions suggest a possible pathway for deuterium exchange in the 2-position of benzothiophene over hydrodesulfurization catalysts.

INTRODUCTION

Hydrodesulfurization[2] (HDS) of benzo[b]thiophene (BT) over Co-Mo/Al_2O_3 catalysts to give ethylbenzene and H_2S is proposed to occur by two mechanistic pathways[3]: either by initial hydrogenation to give 2,3-dihydrobenzothiophene followed by desulfurization to form the final products, or by initial desulfurization to give vinyl benzene followed by hydrogenation to ethyl benzene. Regardless of the pathway, the reaction involves only the thiophenic part of BT as the benzene ring is not hydrogenated. Also, deuterium exchange of BT, when passed with D_2 over HDS catalysts, occurs predominantly in the 2- and 3-positions[4,5] of the thiophene rather than in the benzene ring. A mechanism which accounts for this deuterium exchange has been proposed by Cowley[4] (Figure 1). He postulates that BT binds to a metal atom on the catalyst surface through either C2 or C3 forming 2-benzothienyl (2-BTyl) or 3-benzothienyl (3-BTyl) intermediates; these intermediates then incorporate deuterium from the surface to give deuterated BT. Only the mechanism for deuteration at C2 is shown in Fig. 1.

Recent investigations of BT binding in organometallic complexes have indicated some possible modes for its binding to the catalyst surface. Benzothiophene binds stronger

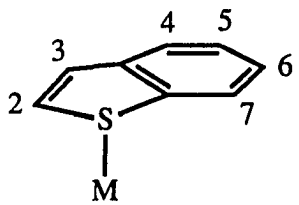

(η^1(S)-BT)

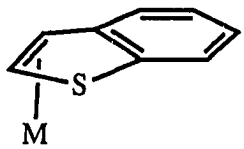

(2,3-η^2-BT)

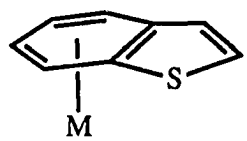

(η^6-BT)

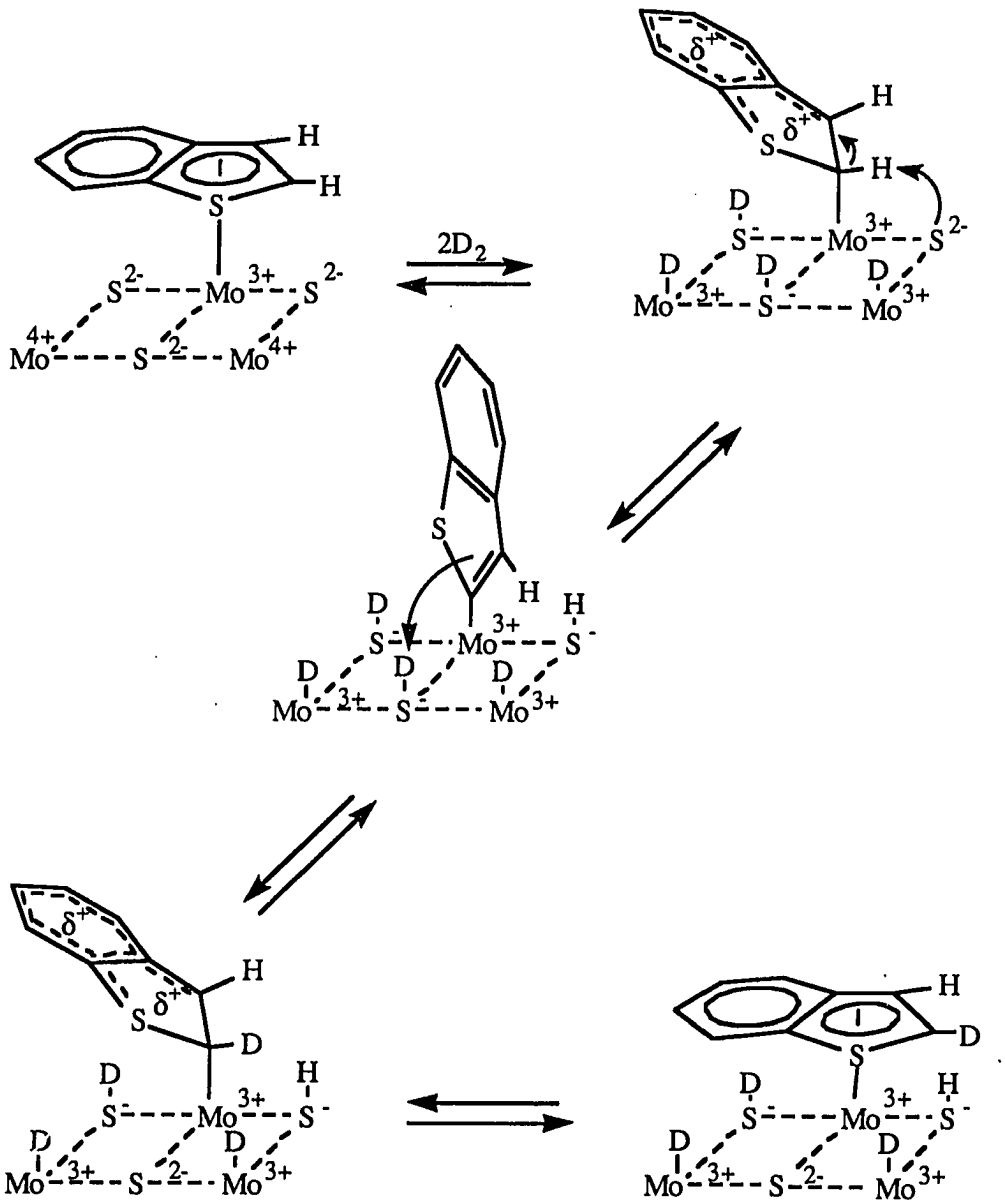

Figure 1. Cowley's proposed mechanism[4] for deuterium exchange of H at the 2-position.

through the S atom than thiophene, yet weaker than dibenzothiophene as determined by equilibrium and kinetic studies[6] of these and other η^1(S)-thiophenes (Th) in $Cp(CO)_2Ru(\eta^1(S)\text{-}Th)^+$ and $Cp(CO)(PPh_3)Ru(\eta^1(S)\text{-}Th)^+$. Of the other known η^1(S)-BT complexes, $Cp(CO)_2Fe(\eta^1(S)\text{-}BT)^+$,[7] and $Cp'(CO)_2Re(\eta^1(S)\text{-}BT)$[8] ($Cp'=\eta^5\text{-}C_5H_5$, $\eta^5\text{-}C_5Me_5$), $Cp'(CO)_2Re(\eta^1(S)\text{-}BT)$ is in equilibrium with its 2,3-η^2-bound isomer. At present, there is no evidence that η^1(S)-coordination promotes deuterium exchange in these complexes; so, this adsorption mode does not account for deuterium exchange of the 2- and 3- hydrogens in BT on HDS catalysts.[4,5] Deuterium exchange of 2,3-η^2-bound BT by *cis*-dideuteration followed by H_2 elimination would lead to equal deuteration in the 2- and 3-positions. However, results of Cowley[4] and our group[5] show that exchange occurs faster in the 2- than the 3-position, which suggests that 2,3-η^2 adsorption of BT is not involved in deuterium exchange on the catalysts. The third known mode of coordination, η^6, is observed in $CpM(\eta^6\text{-}BT)^{2+}$ (M=Rh, Ir),[9] $CpRu(\eta^6\text{-}BT)^+$,[9,10] and $(CO)_3Cr(\eta^6\text{-}BT)$.[11] However, since base catalyzed deuterium exchange[5] in $Cp(Ru)(\eta^6\text{-}BT)^+$ occurs primarily at the 2- and 7- rather than the 2- and 3-positions, η^6-coordination of BT does not account for the observed 2- and 3-exchange observed on HDS catalysts.

In order to probe the possibility that σ-coordination of benzothienyl (BTyl) to a metal accounts for preferential deuterium exchange at the 2- and 3-positions as proposed by Cowley (Figure 1),[4] we describe herein the synthesis of 2-BTyl complexes of Ru and examine their reactions with CF_3SO_3H.

EXPERIMENTAL

General Procedures

The IR spectra were taken in CH_2Cl_2 on a Nicolet 710 FT-IR spectrometer. The ^1H NMR spectra were recorded on either a Nicolet NT-300 or Varian VXR-300 spectrometer using deuterated solvents as the internal lock. The $^{13}C\{^1H\}$ NMR spectra were taken on either Bruker WM-200 or Varian VXR-300 spectrometers using deuterated solvents as the internal lock and reference ($CDCl_3$, δ 77.0 ppm; CD_2Cl_2, δ 53.8 ppm CD_3NO_2, δ 62.8 ppm). Fast atom bombardment (FAB) mass spectra were obtained in a CH_2Cl_2/3-nitrobenzyl alcohol matrix with a Kratos MS-50 mass spectrometer. Elemental analyses were performed by Galbraith Laboratories, Inc., Knoxville, TN and Desert Analytics, Tucson, AZ.

Reactions were performed under nitrogen atmosphere using standard Schlenk techniques.[12] Solvents were dried under N_2 prior to use; hexanes and CH_2Cl_2 were distilled from CaH_2, and THF and diethyl ether were distilled from Na/benzophenone. Methanol was distilled from magnesium alkoxide, which was generated from magnesium turnings and iodine in absolute MeOH.[13] Starting materials $Cp(PMe_3)_2RuCl$,[14] $Cp(PMe_3)_2RuI$[14] and $Cp(CO)(PPh_3)RuCl$[15] were prepared by literature methods. The synthesis of $[Cp(CO)(PPh_3)Ru(\eta^1(S)\text{-BT})]BF_4$ was described previously.[6a] Benzo[b]thiophene (BT) was purchased from Aldrich and sublimed under vacuum at room temperature prior to use. A 2.1 M solution of n-BuLi in n-hexane was purchased from Johnson Matthey. Triflic acid, CF_3SO_3H, (3M Co) was distilled at ambient pressure under N_2. Silver triflate ($AgCF_3SO_3$), $NH_4(PF_6)$ and $Me_3O(BF_4)$ were used as purchased from Aldrich. Neutral alumina, Brockman I (~150 mesh), was purchased from Aldrich and deactivated with 5% (w/w) deionized H_2O after 24 h under vacuum. The CF_3SO_3D was prepared by stirring D_2O (99.8 atom %) (0.72 g, 0.036 mol) and $(CF_3SO_2)_2O$ (10.0 g, 0.0354 mol) for 3 h and then

distilling the deutero acid at ambient pressure at 162 °C. Subsequent reactions of **1** and **2** (see Results & Discussion Section) with CF_3SO_3D indicated the presence of 40% CF_3SO_3H. This may be due to exchange of CF_3SO_3D with small amounts of water in the solvent or adsorbed on the glassware.

Synthesis of $Cp(PMe_3)_2Ru(2\text{-}BTyl)$ (1)

Method A. A solution of 1.138 g (8.480 mmol) of BT in 30 mL of THF was cooled at 0 °C. To this solution was added 4.0 mL (8.4 mmol) of a 2.1 M solution of n-BuLi in n-hexane. After allowing the solution to warm to room temperature with stirring for 30 min, it was refluxed for an additional 30 min, cooled to room temperature and then to 0 °C in an ice bath. To this solution was added 0.500 g (1.41 mmol) of $Cp(PMe_3)_2RuCl$ in 30 mL of THF. The resulting solution was refluxed for 2 h. Complex **1** was isolated as the first yellow band eluting from a neutral alumina column (2 cm x 20 cm) with a 1:5 mixture of CH_2Cl_2 and hexanes. Removal of solvent gave 0.1675 g of **1** as a yellow powder (26.3% yield). ^1H NMR (CD_2Cl_2): δ 7.48 (d, J = 7.7 Hz, 1H), 7.33 (d, J = 7.8 Hz, 1H), 7.00 (td, J = 6.9, 1.1 Hz, 1H), 6.82 (td, J = 7.5, 1.1 Hz, 1H) and 6.76 (s, 1H) BTyl; 4.70 (s, 5H) Cp; 1.45 (pst, 18H) PMe_3. $^{13}C\{^1H\}$ NMR (CD_2Cl_2): δ 164.5 (t, $^2J_{CP}$ = 17.5 Hz), 146.6(s), 144.1(s), 130.2 (t, $^3J_{CP}$ = 4.2 Hz), 122.3(s), 119.3(s), 118.7(s) and 118.1(s) BTyl; 82.3 (t, J_{CP} = 2.1 Hz) Cp; 23.5 (t, J = 14.3 Hz) PMe_3. Anal. calcd for $C_{19}H_{28}P_2RuS$: C, 50.54; H, 6.25. Found: C, 50.87; H, 6.16.

Method B. A solution of 0.1630 g (1.215 mmol) of BT in 20 mL of THF was cooled in an ice bath. To this solution was added 0.60 mL (1.3 mmol) of a 2.1 M n-BuLi solution in n-hexane. The resulting solution was allowed to warm to room temperature while stirring for 30 min. The solution was then refluxed for 30 min, cooled to room temperature and cooled again in the ice bath. In a separate flask, 0.1050 g (0.2358 mmol) of $Cp(PMe_3)_2RuI$

was dissolved in 20 mL of THF. Solid $AgCF_3SO_3$ (65.1 mg, 0.253 mmol) was added, and the resulting solution was stirred for 10 min. A precipitate formed immediately. The cloudy, orange solution was filtered and added to the LiBTyl solution. The resulting dark red solution was allowed to warm to room temperature while being stirred for 1 h. Solvent was removed under vacuum, and the residue was chromatographed on neutral alumina. Product **1** was isolated as above as a yellow powder (45.1 mg, 42% yield).

Synthesis of $Cp(CO)(PPh_3)Ru(2\text{-}BTyl)$ (2)

A solution of 0.1899 g (1.415 mmol) of BT in 30 mL of THF was cooled to 0 °C. To this solution was added 0.70 mL (1.5 mmol) of a 2.1 M n-BuLi solution in n-hexane. The flask was removed from the ice bath, and the mixture was stirred for 30 min at room temperature. The solution was then refluxed for 30 min, cooled to room temperature and cooled again in the ice bath. To this solution was added 0.1065 g (0.2165 mmol) of $Cp(CO)(PPh_3)RuCl$ in 20 mL of THF. The resulting solution was stirred for 1 h, and the solvent was removed under vacuum. The residue was chromatographed on a neutral alumina column (2 cm x 20 cm). Complex **2** was isolated as the second yellow band, eluting with a 1:3 mixture of CH_2Cl_2 and hexanes. Solvent was removed under vacuum and 48.1 mg of **2** was recovered as a yellow powder in 38.0% yield. IR: ν(CO) 1940 cm^{-1}. ^1H NMR ($CDCl_3$): δ 7.55 (d, J = 7.8 Hz, 1H), 7.04 (t, J = 8.1 Hz, 1H), 6.90 (t, J = 7.0 Hz, 1H) and 6.48 (s, 1H) BTyl; 5.06 (s, 5H) Cp; 7.29 (m, 16H) PPh_3 + 1BTyl H. $^{13}C\{^1H\}$ NMR ($CDCl_3$) δ 147.1 (d, $^2J_{CP}$ = 16 Hz), 146.0(s), 142.7(s), 135.8(s), 122.2(s), 119.5(s), 119.3(s) and 119.0(s) BTyl; 87.7(s) Cp; 205.1 (d, $^2J_{CP}$ = 21 Hz) CO; 133.8 (d, $^1J_{CP}$ = 109 Hz), 133.4 (d, J_{CP} = 11.4 Hz), 129.9(s) and 127.9 (d, J_{CP} = 10.4 Hz) PPh_3. Anal. calcd. for $C_{35}H_{25}OPRuS$: C, 65.18; H, 4.27. Found: C, 65.08; H, 4.44.

Synthesis of $[Cp(PMe_3)_2Ru(\eta^1(S)\text{-}BT)]PF_6$ (3)

A solution of 0.1010 g (0.2855 mmol) of $Cp(PMe_3)_2RuCl$ and 0.0882 g (0.657 mmol) of BT in 20 mL of MeOH was refluxed for 1.5 h. Solid $NH_4(PF_6)$ (0.2304 g, 1.414 mmol) was added, and the solution was cooled to room temperature. Solvent was removed under vacuum, 10 mL of CH_2Cl_2 was added to the residue and the solution was filtered. The solution volume was reduced under vacuum, and complex **3** was precipitated (0.1211 g, 71.0% yield) by addition of 15 mL of Et_2O. ^1H NMR (CD_2Cl_2): δ 7.87 (m, 1H), 7.74 (m, 1H), 7.53 (m, 2H), 7.46 (d, J = 5.6 Hz, 1H) and 7.20 (d, J = 5.6 Hz, 1H) BT; 4.47(s) Cp; 1.68(pst, 18H) PMe_3. $^{13}C\{^1H\}$ NMR (CD_3NO_2): δ 150.3(s), 141.3(s), 136.9(s), 129.6(s), 128.7(s), 127.6(s), 127.1(s) and 124.3(s), BT; 83.4(s) Cp; 22.9 (t, J_{CP} = 16.5 Hz) PMe_3. FAB m/e 453.0 (M^+), 319.0 (M^+-BT) and 243.0 (M^+-BT-PMe_3). Anal. calcd for $C_{19}H_{29}F_6P_3RuS \cdot 0.5\ CH_2Cl_2$: C, 36.59; H, 4.72. Found: C, 36.86; H, 4.91. The solvating CH_2Cl_2 was identified in the ^1H NMR spectrum of **3** in CD_2Cl_2 solvent.

Reaction of 1 with CF_3SO_3H to give 3

In a 5mm NMR tube, 5.1 mg (0.011 mmol) of $Cp(PMe_3)_2Ru$(2-BTyl) was dissolved in 0.50 mL of CD_2Cl_2 under N_2, and the tube was capped with a septum. Using a microsyringe, 1.0 μL (0.011 mmol) of CF_3SO_3H was injected through the septum into the solution. The color changed immediately from yellow to orange. The ^1H NMR spectrum showed two Cp peaks at δ 5.28 and 4.47 ppm. The peak at δ 5.28 decreased in intensity as the peak at 4.47 increased; the peak at δ 4.47 was due to complex **3**, which was identified by its complete ^1H NMR spectrum; **3** was formed quantitatively after 1.5 h.

Reaction of 2 with CF_3SO_3H to give 4

A solution of 6.8 mg (0.012 mmol) of **2** in 0.50 mL of CD_2Cl_2 was prepared under nitrogen in a 5 mm NMR tube. The tube was capped with a septum. Using a microsyringe, 1.0 μL (0.011 mmol) of CF_3SO_3H was injected into the solution. The solution color immediately turned from yellow to orange. Complex **4**, identified by its ^1H NMR spectrum,[5a] was formed quantitatively.

RESULTS AND DISCUSSION

Lithiation of BT with n-BuLi to give 2-benzothienyllithium (LiBTyl) occurs exclusively at C2.[16] This LiBTyl reacts *in situ* with $Cp(PMe_3)_2RuX$ (X=Cl, O_3SCF_3) or $Cp(CO)(PPh_3)RuCl$ to give the 2-benzothienyl complexes, $Cp(PMe_3)_2Ru(2\text{-}BTyl)$ (**1**) and $Cp(CO)(PPh_3)Ru(2\text{-}BTyl)$ (**2**) (eq 1). A better leaving group ($CF_3SO_3^-$) on the metal

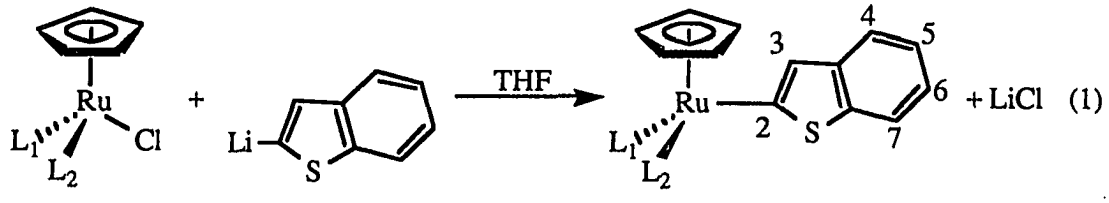

(1)

$L_1L_2 = (PMe_3)_2$ (**1**); $(CO)(PPh_3)$ (**2**)

expedites the reaction; thus, milder conditions are required and a higher yield is obtained when $AgCF_3SO_3$ is used to abstract I^- from $Cp(PMe_3)_2RuI$ (method B) prior to reaction with LiBTyl (eq 2). No reaction is observed when $Cp(PMe_3)_2RuI$ is refluxed with LiBTyl for

$$Cp(PMe_3)_2RuI \xrightarrow[-AgI]{AgCF_3SO_3} \xrightarrow[-CF_3SO_3Li]{LiBTyl} \mathbf{1} \qquad (2)$$

10 h.

The 2-benzothienyl complexes, **1** and **2**, are characterized by ^1H and $^{13}C\{^1H\}$ NMR and elemental analyses (see Experimental Section). In their ^1H NMR spectra, the five BTyl protons are well resolved and exhibit a singlet (H3), 2 doublets (H4, H7) and 2 triplets (H5, H6) for both complexes (one of the doublets in **2** is obscured by Ph peaks). The ^{13}C NMR spectra of **1** and **2** show coupling of C2 to the phosphorus of the PR_3 ligands. In complex

2, the two-bond coupling constant ($^2J_{CP}$ = 16 Hz) is similar to that of the CO (δ 205.1, $^2J_{CP}$ = 21 Hz) in this same complex. In **1**, C2 occurs as a triplet (δ 164.5 ppm, $^2J_{CP}$ = 17.5 Hz) as a result of coupling to the P atoms in the two PMe_3 ligands. Here, C3 in BTyl is also split by phosphorus (δ 130.2, $^3J_{CP}$ = 4.2 Hz). Thus, the NMR spectra of **1** and **2** are consistent with bonding of Ru to the C2 carbon of the benzothienyl ligand.

Protonation of **2** in CD_2Cl_2 with CF_3SO_3H gives the η^1(S)-BT complex, **4** (eq 3)

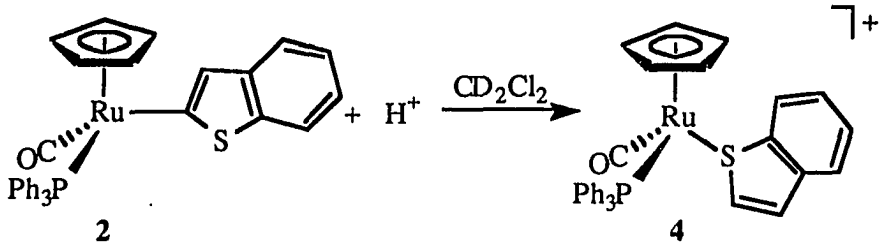

2 **4** (3)

immediately and quantitatively as seen in the ^1H NMR spectrum of the reaction mixture at room temperature. Complex **4** was identified by its ^1H NMR spectrum.[5a] Likewise, addition of one equivalent of CF_3SO_3H to a CH_2Cl_2 solution of **1** at room temperature gives **3** (eq 4). Complex **3** is also prepared by a second method[17] in which $Cp(PMe_3)_2RuCl$ is

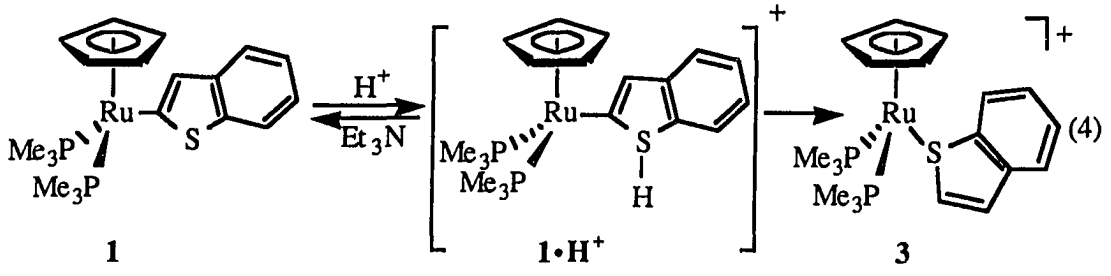

1 **1•H+** **3** (4)

refluxed in MeOH with excess BT. Prepared by this route, **3** was characterized by ^1H and ^{13}C NMR, and FAB mass spectroscopy and elemental analysis. The ^1H and $^{13}C\{^1H\}$ NMR spectra of **3** are similar to those of other η^1(S)-BT complexes.[6,7] In an NMR tube reaction

of **1** with CF_3SO_3H in CD_2Cl_2, an intermediate (**1**•H^+) was detected (eq 4); it exhibits a singlet at δ 5.28 ppm for Cp, a pseudotriplet at δ 1.54 ppm for PMe_3 and two complex multiplets at δ 7.5 and 7.3 ppm for the BTyl ligand (the BTyl peaks are partially obscured by the η^1(S)-BT peaks of **3**). At room temperature, these peaks rapidly disappear ($t_{1/2}$ ~11 min) as **3** is formed.

As it is rapidly isomerizing to **3**, the structure of the intermediate, **1**•H^+, in reaction (4) is difficult to establish from its ^1H NMR spectrum. Complex **1** contains three likely sites for H^+ addition: at Ru, at C3 or S. An ^1H NMR spectrum of **1**•H^+ in CD_2Cl_2 shows no evidence of a metal hydride peak at high field (up to δ -25 ppm), which rules out H^+ addition at Ru. Addition of H^+ at C3 on BTyl (eq 5), in a reaction similar to protonation of a vinyl

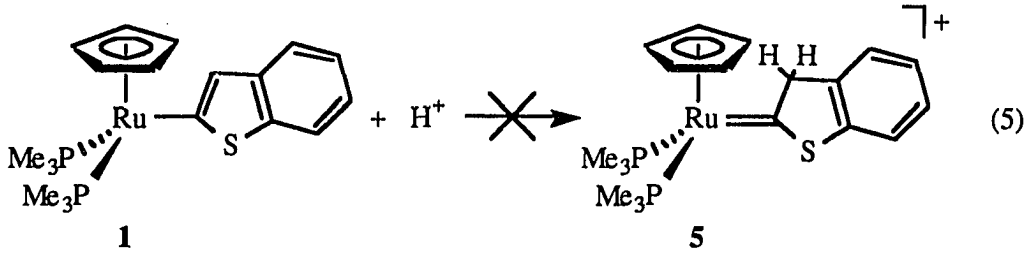

1 **5** (5)

group,[18] would likely give the carbene complex **5**. That **5** is unlikely to be the structure of **1**•$H^+$is supported by the following experiments. When one equivalent of CF_3SO_3D reacts with **1** and **2** in CD_2Cl_2, D is found exclusively in the 2-position of the η^1(S)-BT in the final products **3** and **4**. This was established by integrating the individual BT peaks in **3**. Since the PPh_3 peaks obscure the BT peaks in **4**, the CD_2Cl_2 solution of **4** resulting from CF_3SO_3D addition to **2** was treated with a 10-fold excess of MeCN to displace BT. After 12 h, the solution was passed through a small plug of Al_2O_3. The resulting solution contained only free BT and MeCN; after reducing the solution volume, the free BT in acetone-d_6 was analyzed by ^1H NMR spectroscopy. In the BT ligand of both **3** and **4**, the integral of the H2

doublet was 40% of the H3 doublet, which integrated 1:1 with the H4 and H7 multiplets and 1:2 with the H5 and H6 multiplet; this establishes that deuterium is only in the H2 position and not in H3; some deuterium would be expected at H3 if **1H**$^+$ had the carbene structure **5**. Also supporting the conclusion that **5** is not the **1H**$^+$ intermediate is the result of an experiment in which one equivalent of Et_3N was added immediately to **1•D**$^+$, which was formed by the addition of CF_3SO_3D to a CD_2Cl_2 solution of **1**. The Et_3N regenerates **1** which does not contain deuterium in the 3-position or in any other position of the BTyl ligand. If the **1•D**$^+$ intermediate had structure **5**, deuterium would have had to be found in the 3-position of the regenerated **1**. Since the proton in **1•H**$^+$ is not on the Ru or C3, it is most likely to be bound to the S atom in the benzothienyl ligand. This is supported by the reaction of BT with $Me_3O(PF_6)$ in CH_2Cl_2 which gives the S-methylated BT•CH_3^+.[19] In reaction (4), the S-protonated intermediate **1•H**$^+$ apparently rearranges to **3** by proton migration to C2, which results in Ru-C bond cleavage. This rearrangement occurs more rapidly in the reaction of **2** than **1**, since a protonated intermediate is not detected in reaction (3).

Complexes **3** and **4** were not deprotonated to give **1** and **2** (the reverse of eqs 3 and 4) as shown by reactions of **3** or **4** in CD_2Cl_2 with one equivalent of NEt_3 at room temperature over a 12 h period; only a small amount of free BT was observed in the ^1H NMR spectrum.

Relevance to Deuterium Exchange of Benzo[b]thiophene on HDS Catalysts

The reactions (eqs 3 and 4) of the 2-benzothienyl complexes **1** and **2** with CF_3SO_3D result in deuteration of the 2-position of the benzothiophene in the BT products **3** and **4**. This is a reaction that is very similar to that (Figure 1) proposed by Cowley[4] for deuterium exchange of BT with D_2 on an HDS catalyst surface. His mechanism involves a 2-BTyl

intermediate which reacts with a D^+ on a surface sulfide to give the 2-deuterobenzothiophene. To account for the lesser amount of deuterium incorporated into the 3-position of BT, he suggests the formation of a 3-BTyl surface group which reacts with D^+ to give deuterium at the 3-position. The studies presented in this paper are consistent with the idea that both 2- and 3-benzothienyl intermediates are necessary to account for the observed deuteration of BT at the 2- and 3-positions when BT exchanges with D_2 over HDS catalysts. Cowley's mechanism can be elaborated based on results presented in this paper and on other recent studies of BT complexes as shown in Figure 2. In step (1), BT adsorbs as an equilibrium mixture of the η^1(S)- and η^2- forms, based on the analogous equilibrium known[8] to exist in $Cp'(CO)_2Re(BT)$. The η^2 intermediate could convert to either the 2-BTyl (path *a*) or 3-BTyl (path *b*) surface species. Deuterium transfer from the surface to the 2-BTyl group would give 2-deutero-BT (step (2)) and to the 3-BTyl would give 3-deutero-BT (step (3)). Path *a* would be faster than path *b* since more deuteration occurs[4,5] in the 2- than in the 3-position. In fact, the 2-BTyl surface species may be thermodynamically favored over the 3-BTyl species. This is supported by the reported[20] rearrangment of the 3-thienyl complex $(C_5Me_5)(PMe_3)Rh$(3-thienyl)(H) to the more stable 2-thienyl analog (eq 6); this isomerization is proposed to occur via

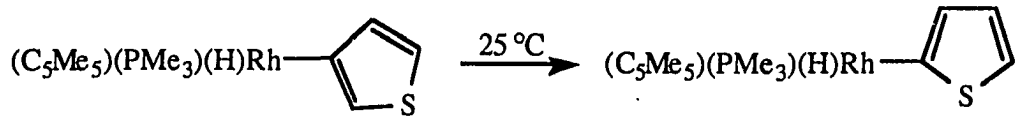

(6)

reductive elimination of H and the 3-thienyl group to give a coordinated thiophene, which undergoes oxidative-addition across the 2-position C-H bond to give the 2-thienyl product.

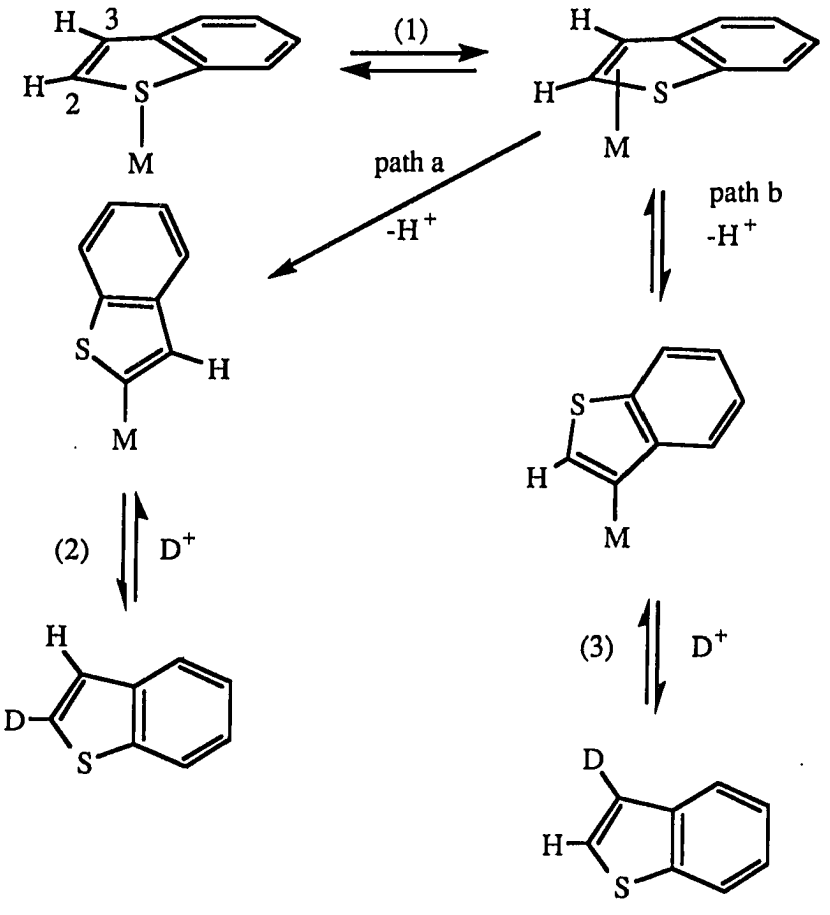

Figure 2. Mechanism for deuterium exchange on BT which accounts for incorporation of D into the 2- and 3-postions.

In summary, the mechanism shown in Figure 2, which is a modification of Cowley's original proposal (Figure 1), reasonably accounts for preferential deuteration of BT at the 2-position based on reactions of organometallic benzothienyl and thienyl complexes.

Acknowledgment

We thank Johnson Matthey for a loan of $RuCl_3$.

REFERENCES

(1) Ames Laboratory is operated for the U.S. Department of Energy by Iowa State University under Contract No. W-7405-Eng-82. This research was supported by the Office of Basic Energy Sciences, Chemical Sciences Division.

(2) (a) *Geochemistry of Sulfur in Fossil Fuels*; Orr, W. L., White, C. M., Eds.; ACS Symposium Series 429; American Chemical Society: Washington, D.C. 1990.

(b) Prins, R.; deBeer, V. H. J.; Somorjai, G. A. *Catal. Rev.-Sci. Eng.* **1989**, *31*, 1.

(c) McCulloch, D. C. In *Applied Industrial Catalysis*; Leach, B. E., Ed.; Academic; New York, 1983; Vol. 1, p. 69.

(d) Gates, B. C.; Katzer, J. R.; Schuit, G. C. A. *Chemistry of Catalytic Processes*; McGraw-Hill: New York, 1979, Chapter 5.

(3) (a) López, R.; Peter, R.; Zdrazil, M. *J. Catal.* **1982**, *73*, 406.

(b) Obedunmi, E. O.; Ollis, D. F. *J. Catal.* **1983**, *80*, 65.

(c) Pokorny, P.; Zdrazil, M. *Coll. Czech. Chem. Commun.* **1981**, *46*, 2185.

(d) Bartsch, R.; Tanielian, C. *J. Catal.* **1974**, *35*, 353.

(e) deBeer, V. H. J.; Dahlmans, J. G. J.; Smeets, J. G. M. *J. Catal.* **1976**, *42*, 467.

(f) Furinsky, E.; Amberg, C. H. *Can. J. Chem.* **1976**, *54*, 1507.

(g) Bartsch, R.; Tanielian, C. *J. Catal.* **1977**, *50*, 35.

(h) Givens, E. N.; Venuto, P. B. *Am. Chem. Soc., Div. Fuel Chem., Prepr.* **1970**, *14(pt. 2)*, 135.

(i) Geneste, P.; Amblard, P.; Bonnet, M.; Graffin, P. *J. Catal.* **1980**, *61*, 115.

(j) Daly, F. P. *J. Catal.* **1978**, *51*, 221.

(k) Girgis, M. J.; Gates, B. C. *Ind. Eng. Chem. Res.* **1991**, *30*, 2021.

(l) Levaché, D.; Guida, A.; Geneste, P. *Bull. Soc. Chim. Belg.* **1981**, *90*, 1285.

(m) Sánchez-Delgado, R. A.; Gonález, E. *Polyhedron* **1989**, *8*, 1431.

(4) Cowley, S. W. *Ph.D. Thesis* Southern Illinois University, 1975.

(5) Huckett, S. C.; Angelici, R. J.; Ekman, M. E.; Schrader, G. L. *J. Catal.* **1988**, *113*, 36.

(6) (a) Benson, J. W.; Angelici, R. J. *Organometallics* **1992**, *11*, 922.

(b) Benson, J. W.; Angelici, R. J. *Organometallics*, submitted.

(7) Goodrich, J. D.; Nickias, P. N.; Selegue, J. P. *Inorg. Chem.* **1987**, *26*, 3424.

(8) (a) Choi, M.-G.; Robertson, M. J.; Angelici, R. J. *J. Am. Chem. Soc.* **1991**, *113*, 4005.

(b) Choi, M.-G.; Angelici, R. J. *Organometallics*, in press.

(9) Huckett, S. C.; Miller, L. L.; Jacobson, R. A.; Angelici, R. J. *Organometallics* **1988**, *7*, 686.

(10) Chaudret, B.; Jalón, F.; Pérez-Manrique, M.; Lahoz, F.; Plou, F. J.; Sanchez-Delgado, R. *New. J. Chem.* **1990**, *14*, 331.

(11) Fischer, E. O.; Goodwin, H. A.; Kreiter, C. G.; Simmons, H. D., Jr.; Sonogashira, K.; Wild, S. B. *J. Organomet. Chem.* **1968**, *14*, 359.

(12) (a) *Experimental Organometallic Chemistry*; Wayda, A. L.; Darensbourg, M. Y., Eds.; ACS Symposium Series 357; American Chemical Society: Washington, D.C.

(b) Shriver, D. F.; Drezdon, M. A. *The Manipulation of Air Sensitive Compounds*, 2nd ed.; Wiley: New York, 1986.

(13) Perrin, D. D.; Armarego, W. L. F.; Perrin, D. R. *Purification of Laboratory Chemicals*, 2nd ed.; Pergamon Press: New York, 1987, p. 249.

(14) Treichel, P. M.; Komar, D. A. *Synth. React. Inorg. Met.-Org. Chem.* **1980**, *10*, 205.

(15) Davies, S. G.; Simpson, S. J. *J. Chem. Soc., Dalton Trans.* **1984**, 993.

(16) (a) Gschwend, H. W.; Rodriguez, H. R. *Organic Reactions* **1979**, *26*, 1.

(b) Kellogg, R. M. *Comprehensive Heterocyclic Chemistry* **1984**, *4*, 771.

(17) (a) Haines, R. J.; DuPreez, A. L. *J. Organomet. Chem.* **1975**, *84*, 357.

(b) Treichel, P. M.; Komar, D. A.; Vincenti, P. J. *Inorg. Chim. Acta.* **1984**, *88*, 151.

(c) Treichel, P. M.; Vincenti, P. J. *Inorg. Chem.* **1985**, *24*, 228.

(18) (a) Bodner, T.; Cutler, A. R. *J. Organomet. Chem.* **1981**, *213*, C31.

(b) Brookhart, M.; Tucker, J. R.; Husk, G. R. *J. Am. Chem. Soc.* **1983**, *105*, 258.

(19) Acheson, R. M.; Harrison, D. R. *J. Chem. Soc. C* **1970**, 1764.

(20) Dong, L.; Duckett, S. B.; Ohman, K. F.; Jones, W. D. *J. Am. Chem. Soc.* **1992**, *114*, 151.

PAPER IV. STUDIES OF THE MECHANISM OF THIOPHENE HYDRODESULFURIZATION: ^{2}H NMR AND MASS SPECTRAL ANALYSIS OF 1,3-BUTADIENE PRODUCED IN THE DEUTERODESULFURIZATION (DDS) OF THIOPHENE OVER $PbMo_{6.2}S_8$ CATALYST

ABSTRACT

The deuterodesulfurization (DDS) of thiophene was investigated over $PbMo_{6.2}S_8$ at 400 °C using a flow-microreactor. Evidence indicates that 1,3-butadiene (BDE) is the first desulfurized product; its deuterium content was established by ^2H NMR and mass spectrometries. At different levels of thiophene conversion (0.86-10.2%), the amount of deuterium incorporated into BDE remains constant at 3.47 D atoms per BDE molecule. Unconverted thiophene incorporates 0.42 D atoms at 10.2% thiophene conversion but only 0.05 D atoms at 0.86% conversion. Reaction of 2,5-dihydrothiophene (2,5-DHT) with D_2 at 400 °C over $PbMo_{6.2}S_8$ liberates BDE as the only hydrocarbon product. This BDE incorporates no deuterium. Thiophene, H_2S and 2,5-DHT effectively poison the catalyst, inhibiting both BDE hydrogenation and deuterium exchange. The results indicate that during the DDS process, a total of 3.2 deuterium atoms are incorporated into the BDE; 0.83 D are in the D_A-position while 1.2 D are in each of the D_B-and D_C-positions. Several HDS mechanisms proposed in the literature are consistent with these results; two are not.

INTRODUCTION

Catalytic hydrodesulfurization (HDS) is a large-scale industrial process for the removal of sulfur from petroleum feedstocks.[1] Because it is one of the most difficult organosulfur compounds to desulfurize in these feedstocks, thiophene has been studied extensively. The reaction of thiophene with H_2 over supported HDS catalysts, Co-Mo/Al_2O_3, Ni-Mo/Al_2O_3 and Ni-W/Al_2O_3, produces H_2S and a mixture of four-carbon hydrocarbons:[2, 3] 1,3-butadiene, 1-butene, *cis*- and *trans*-2-butene and butane (eq 1). Of the C_4 products, 1,3-

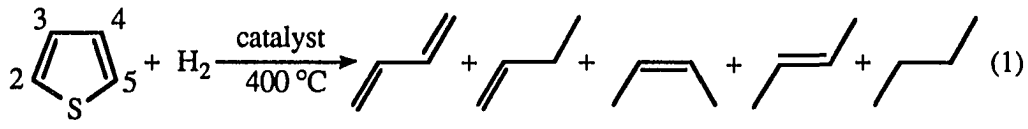

(1)

butadiene has been suggested as the most likely product formed directly following C-S bond cleavage because it is detected[2 - 4] under reduced hydrogen pressure where its hydrogenation to butenes and butane is less favorable. Other evidence supports this proposal. First, the relative amount of 1,3-butadiene produced in the HDS of thiophene over MoS_2[3a] and Chevrel-phase catalysts[4] increases with decreasing thiophene conversion. Second, 1-butene is produced in these reactions in greater than equilibrium amounts (20% 1-butene, 31% *cis*-2-butene, 49% *trans*-2-butene at 400 °C),[5] supporting a sequential hydrogenation path from 1,3-butadiene to 1-butene. Direct hydrogenation of 1,3-butadiene over MoS_2 at 320 °C also produces excess 1-butene.[3a] Studies of 1-butene hydrogenation over several Chevrel-phase catalysts (including $PbMo_{6.2}S_8$)[6] show no evidence of 1,3-butadiene at 400 °C in a flow reactor. Thus, it is unlikely that 1,3-butadiene is produced from 1-butene dehydrogenation.

Based on evidence that 1,3-butadiene is likely to be the first HDS product, mechanisms proposed for thiophene HDS often involve pathways leading to its formation. Our approach

to testing these mechanisms is to compare the deuterium content and location in 1,3-butadiene produced during the deuterodesulfurization (DDS, using D_2 instead of H_2) of thiophene over $PbMo_{6.2}S_8$ at 400 °C with that predicted by each mechanism. In order to do the deuterium studies it was necessary to choose a catalyst that produced reasonable amounts of 1,3-butadiene. Since the Chevrel-phase catalyst, $PbMo_{6.2}S_8$, is a relatively poor olefin hydrogenation catalyst,[4, 6a] it does indeed yield 1,3-butadiene (6.5% of the C_4 hydrocarbon products). An additional benefit of this catalyst is its low activity toward catalyzing the exchange of hydrogens in thiophene with deuterium;[4] substantial deuterium incorporation into thiophene before the HDS reaction would further complicate interpretation of the deuterium composition of the 1,3-butadiene product. The total amount of deuterium incorporation was determined experimentally by mass spectrometry, and the relative amounts of deuterium incorporated into each of the three distinguishable positions of 1,3-butadiene (D_A, D_B, D_C; Figure 1) were determined by integration of their peaks in the ^2H NMR spectrum. Prior to considering the experimental results, it is useful to examine the deuterium content of 1,3-butadiene that would be predicted from mechanisms that have been proposed in the literature. For the remainder of this paper, 1,3-butadiene will be abbreviated BDE.

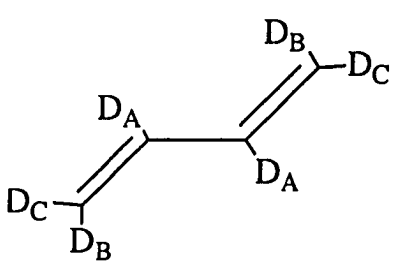

Figure 1. Structure of 1,3-butadiene showing the positions of deuterium incorporation as detected by ^2H NMR.

This analysis of thiophene HDS mechanisms will be limited to those mechanisms that are given in sufficient detail to allow one to predict from them the number and locations of deuterium in the BDE product. One such mechanism (Figure 2),[7] proposed in these laboratories and based on a series of organometallic and reactor studies, involves partial thiophene hydrogenation. The thiophene adsorbs to a metal site through all five atoms (η^5); this adsorption activates the thiophene to react with a surface hydride at the 2-position (step *a*) to give an allyl sulfide intermediate. A strongly acidic H^+, perhaps from an -SH group, adds in step *b* to the 3-position forming adsorbed 2,3-dihydrothiophene (2,3-DHT). Isomerization of 2,3-DHT to 2,5-dihydrothiophene (2,5-DHT) (step *c*) is followed by cleavage of both C-S bonds (step *d*) to give BDE and an adsorbed S atom. One equivalent of H_2 removes S as H_2S to regenerate the active site (step *e*). Under DDS conditions, where the amount of D_2 is much greater than that of thiophene, this mechanism predicts the addition of one D atom in each step *a* and *b*. During the isomerization (step *c*), a third D atom is added to the 5-position, while either D or H is lost from the 3-position. The 2,3-DHT formed in step *b* could be bound through both the olefin and the sulfur as shown, or through just the S atom; only sulfur-coordination is observed in its transition metal complexes.[8] In this latter case, either H or D could be lost from the 3-position since either side of the ring can contact the surface as a result of rapid inversion at the sulfur and flipping of the ring. This type of inversion is known to occur in S-coordinated 2,3-DHT complexes.[8] Because the deuterium isotope effect[9] will cause the C(3)-D bond to be stronger than C(3)-H in 2,3-DHT, the 3-position of 2,5-DHT will probably contain more D than H. Based on a k_H/k_D isotope effect of 3.33,[9] 2,5-DHT will have 0.77 D atoms at C(3) and 2.8 D atoms in the whole molecule. In the desulfurization step (*d*), no deuterium is incorporated and the resulting BDE should contain 2.8 D, and these deuterium atoms should be distributed (Figure 1) as follows: 0.77 D at D_A, 1.0 D at D_B, and 1.0 at D_C. (It is not possible to predict whether the deuterium

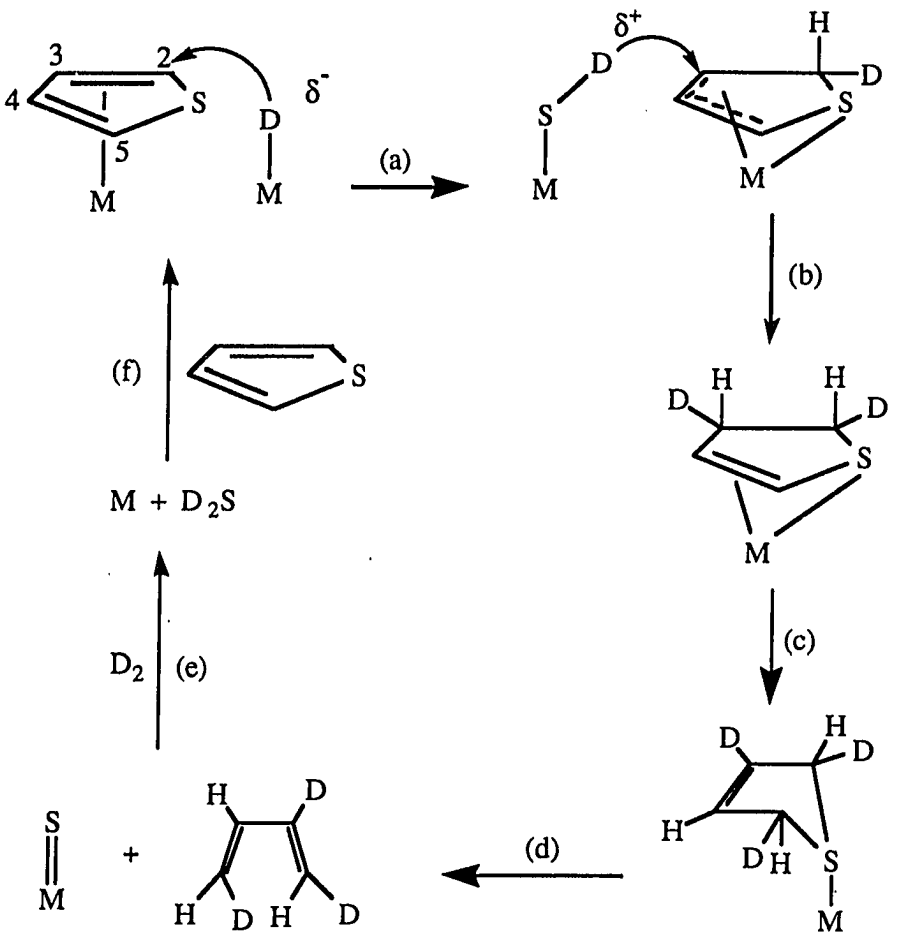

Figure 2. Hydrogenation mechanism proposed by Sauer, Markel, Schrader and Angelici[7] indicating sites of deuterium incorporation.

content at D_B and D_C will be equal or unequal.)

A second mechanism involving partial hydrogenation of thiophene was proposed by Kwart, Schuit and Gates (Figure 3).[10] The first step of this mechanism (step *a*) is η^2-coordination of thiophene through one of its double bonds to a surface metal atom. As the thiophene S atom interacts with a nearby surface S atom, one H atom adds to C2 (step *b*). Next, either another H atom adds to give a 2,3-DHT intermediate bound through only the S atom (step *c*) followed by β-elimination and C2-S bond cleavage (step *d*) to give an adsorbed butadiene thiolate, or the butadiene thiolate is formed directly (step e) without addition of the second proton. The authors are unclear as to which path (steps *c* and *d*, or step *e*) would be favored or whether both occur simultaneously. Repetition of these steps (steps *f*, *g* and *h* or steps *f* and *i*) at the other double bond cleaves the second C-S bond and gives adsorbed BDE as the final product.

Under DDS conditions, formation of the 2,3-DHT intermediate (steps *b* and *c*) requires addition of two D atoms. Again, as in Figure 2, H would transfer more rapidly to the surface than deuterium during the β-elimination step *d*. On the other hand, step *e* requires addition of only one D atom. Repetition of these steps at the second C-C double bond gives BDE with either 0.0 D atoms at the D_A-positions by paths *e* and *i* or 1.54 D, based on the 3.33 k_H/k_D isotope effect,[9] at the D_A-position by paths *c*, *d*, *g* and *h*. Both pathways introduce a total of two D atoms at the D_B- and D_C-positions for a total of 2.0-3.5 D in the product BDE.

A third hydrogenation mechanism (Figure 4) was proposed by Delmon and Dallons.[11] In this mechanism, thiophene is initially η^4-bound through the π-system to a coordinatively unsaturated surface metal atom while the thiophene S atom acts as a Lewis acid toward the S atoms of neighboring surface -SH groups (step *a*). Such an intermediate seems unlikely since the sulfur in known η^4-coordinated thiophene complexes is a strong Lewis base,[12] rather than a Lewis acid. Two H atoms add in step *b* to saturate C3 and C4 as C2 and C5

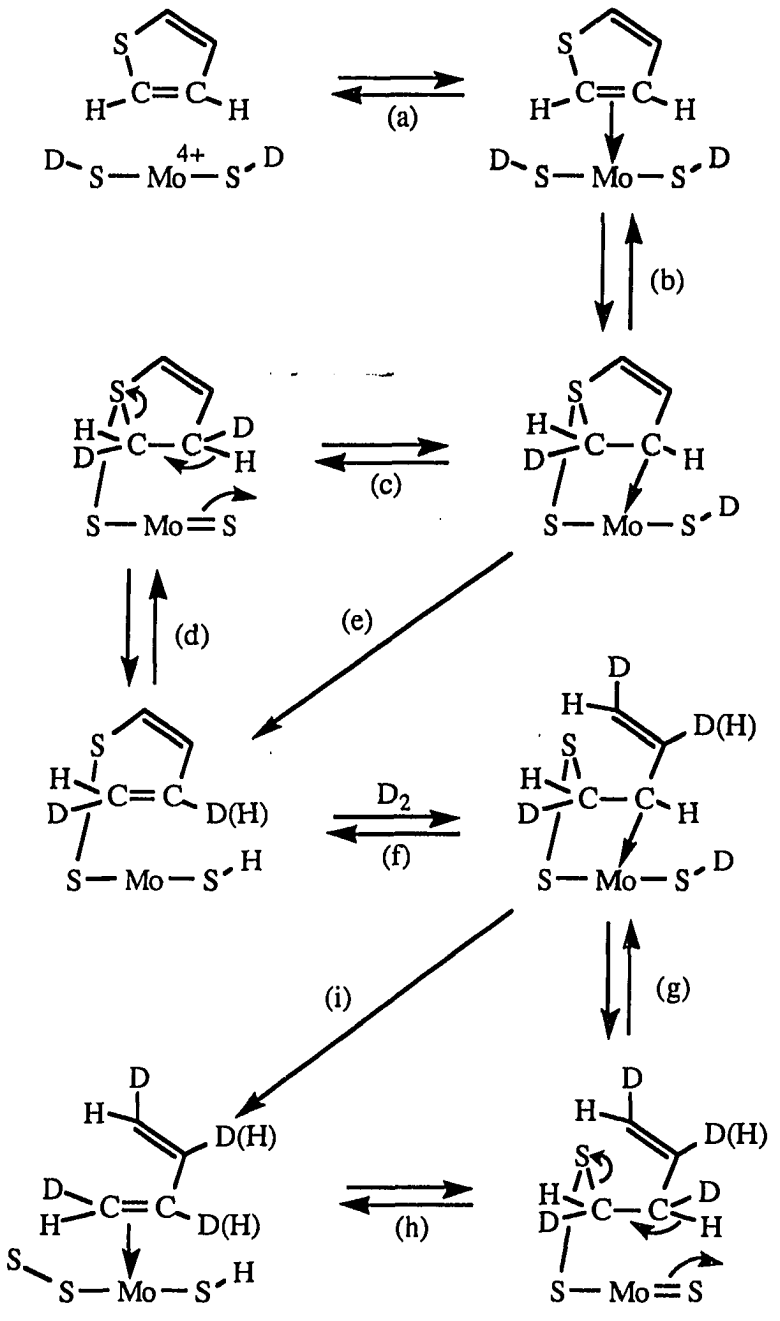

Figure 3. Multipoint mechanism proposed by Kwart, Schuit and Gates[10] indicating sites of deuterium incorporation.

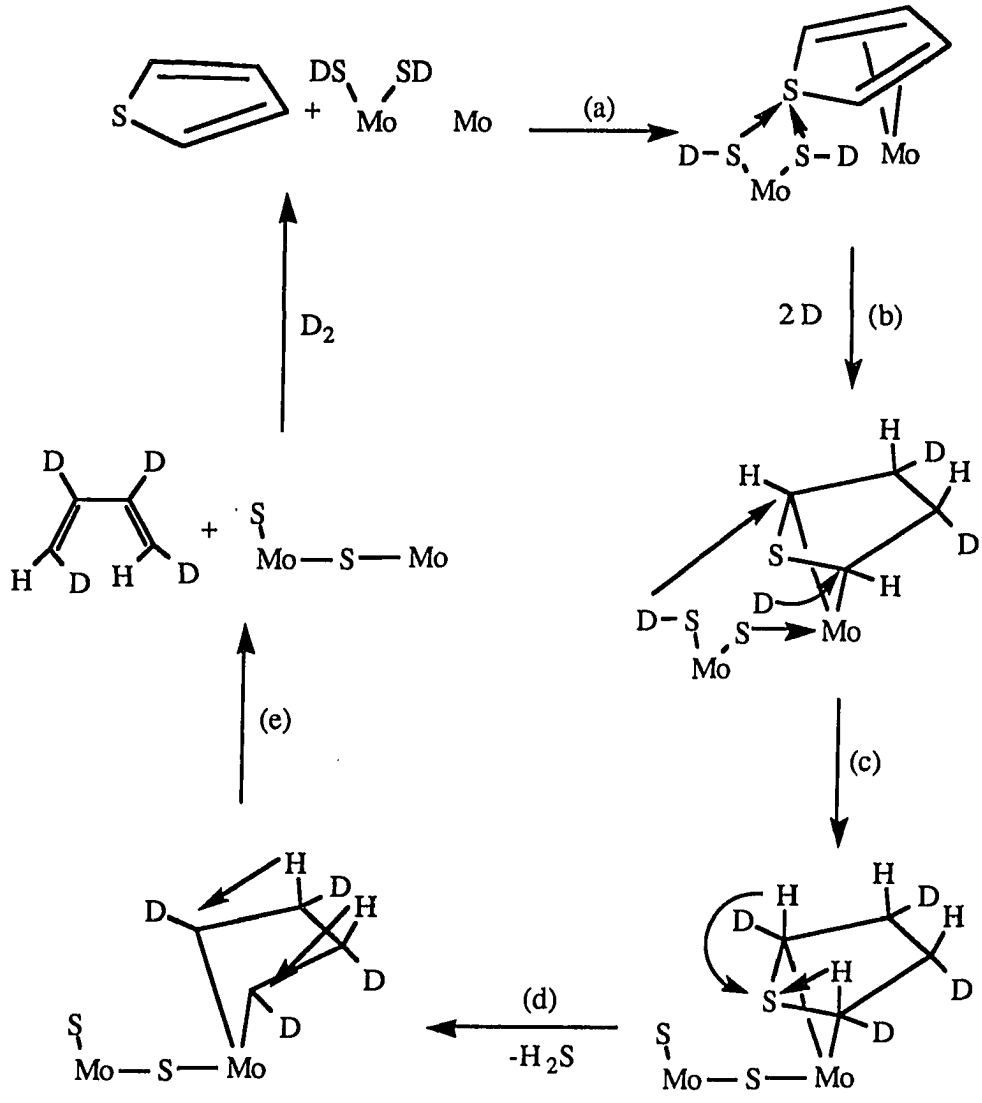

Figure 4. HDS mechanism proposed by Delmon and Dallons[11] indicating sites of deuterium incorporation.

form σ-bonds with the metal atom. Transfer of H atoms from the surface -SH groups to C2 and C5 creates two hypervalent carbons in a transition state (step *c*) which lose the two original thiophene protons to the thiophene S atom to give H_2S (step *d*). Under low H_2 pressure, hydrogens from C3 and C4 migrate to C2 and C5 (step *e*) and BDE is desorbed from the surface. Under DDS conditions, this mechanism adds two D atoms to C3 and C4 in step *b*. Step *c* adds two more deuterium atoms from the surface to C2 and C5 as H_2S is lost in step *d*. Migration of hydrogens from C3 and C4 to C2 and C5, desorbs BDE with four D atoms. According to the isotope effect,[9] 1.54 D atoms will remain at the D_A-position of BDE (Figure 1), and 2.5 D atoms will occupy the D_B- and D_C-positions. The total number of D atoms in the BDE product would be 4.0.

Kolboe[13] proposed dehydrosulfurization as the initial step (Figure 5) in his

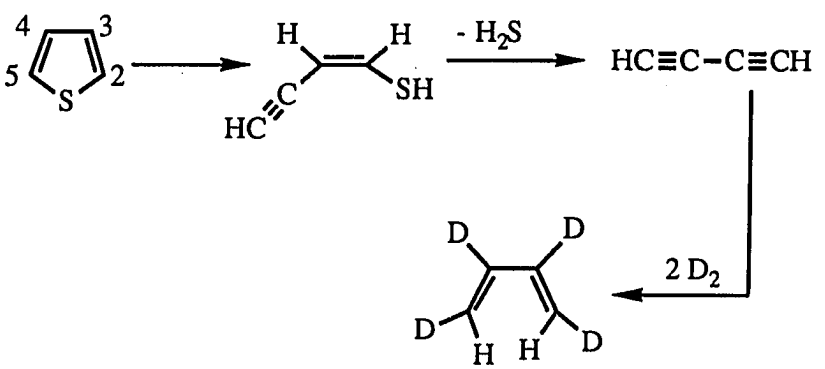

Figure 5. Dehydrosulfurization mechanism proposed by Kolboe.[13]

mechanism. It involves stepwise elimination of H3 and H4 which promotes C-S bond cleavage to give H_2S and 1,3-butadiyne. Two equivalents of H_2 hydrogenate 1,3-butadiyne to give BDE. Two equivalents of D_2 during DDS would produce 1,3-butadiene-d_4. Two D atoms would be in the D_A-positions of BDE and two would be in the D_B- and D_C-positions (Figure 1). Again, it is not possible to ascertain from the mechanism whether the two D atoms in the D_B and D_C sites would be equally or unequally distributed between these positions.

Reactions of the transition metal complex, Cp*Ir(η^4-2,5-dimethylthiophene) (Cp*=η^5-C_5Me_5) provide the basis for an HDS mechanism (Figure 6)[14] proposed by Chen and

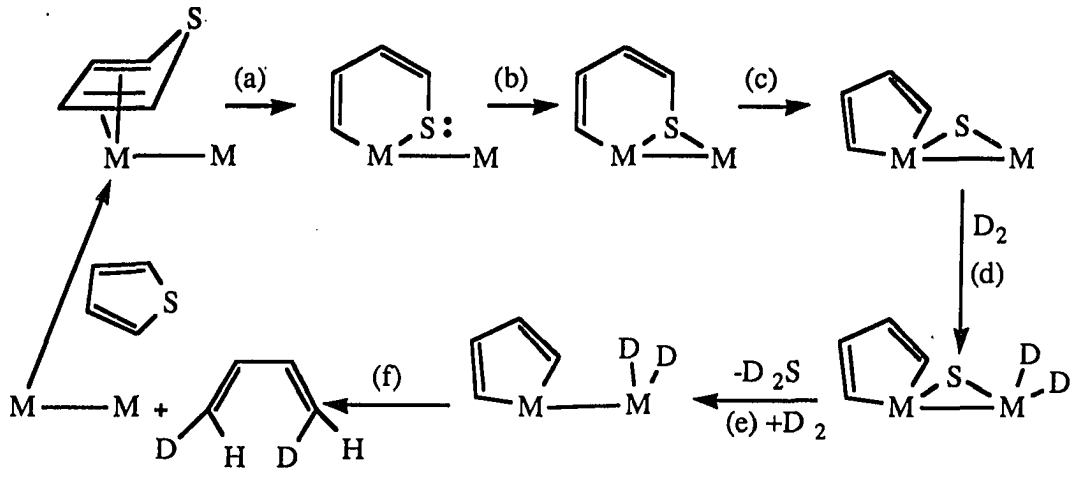

Figure 6. C-S cleavage mechanism proposed by Chen and Angelici[14] indicating deuterium incorporation into 1,3-butadiene.

Angelici. In this mechanism, thiophene is activated by π-coordination of just the diene fragment of thiophene (η^4) to undergo base-catalyzed (basic Al_2O_3) C-S bond cleavage (step *a*), forming a six-membered ring. Coordination of an adjacent surface metal atom to the sulfur (step *b*) cleaves the second C-S bond (step *c*) forming a metallacyclopentadiene. Addition of one equivalent of H_2 eliminates H_2S (step *e*); a second equivalent of H_2 cleaves the M-C bonds and desorbs BDE (step *f*). Deuterium incorporation into BDE during DDS would occur only during step *f*, giving 1,3-butadiene-d_2. This mechanism predicts that deuterium would occupy only the D_B- and D_C-positions (Figure 1) with no deuterium incorporation at the D_A-position.

Other mechanisms for thiophene HDS, which lead to butadiene-d_2 with the deuterium in only the D_B- and D_C-positions and involve C-S bond hydrogenolysis prior to hydrogenation of the unsaturated hydrocarbon part of thiophene have also been proposed. Differing in the initial coordination mode and subsequent reactions, mechanisms by Desikan and Amberg,[15] Lipsch and Schuit,[16] Curtis[17] and Cowley[18] all add two equivalents of H_2 to cleave the C-S bond to produce BDE and H_2S. During DDS of thiophene by these mechanisms, only the D_B- and D_C-positions of 1,3-butadiene-d_2 would have D atoms, and there would be a total of only two D atoms in those positions.

Table 1 summarizes the number of deuterium atoms (deuterium number, D.N.) and their locations (D_A, D_B, or D_C, Figure1) predicted for each of the mechanisms discussed above. Deuterium numbers range from 2 to 4; a total of at least two D atoms are in the D_B- and D_C-positions for all mechanisms (the mechanisms are unclear as to whether D_B or D_C would be favored). On the other hand, the number of D atoms in the D_A-position varies from 0 to 2. Thus, the amount of deuterium atoms in the D_A-positions as well as the total

Table 1. Deuterium Numbers (D.N.) and Deuteration Sites Predicted by Various Mechanisms for Deuterodesulfurization.

Mechanism Figure #	D.N.	D_A	D_B and D_C	ref.
2	2.8	0.77	2.0	7
3	2.0-3.5	0.0-1.5	2.0	10
4	4.0	1.5	2.5	11
5	4.0	2.0	2.0	13
6	2.0	0	2.0	14

number of deuterium atoms (D.N.) distinguish several of the mechanisms from each other, and experimental measurements of D.N. and deuterium location in the BDE should allow us to narrow the number of mechanisms that are possible during HDS under the conditions of our studies.

In our present study, we examine the deuterium content and location in BDE produced during thiophene DDS over the Chevrel-phase catalyst $PbMo_{6.2}S_8$ at 400 °C.[4] The deuterium (D.N.) of the BDE produced in this reaction as determined by mass spectrometry gives the average number of D atoms per molecule of BDE. The relative amounts of deuterium at each position (D_A, D_B, or D_C) of the 1,3-butadiene were determined by integrating the peaks in the ^2H NMR spectrum. The results are used to evaluate the viability of each of the mechanisms discussed above. In the course of these studies, it became necessary to also investigate reactions of D_2 with BDE, 2,5-DHT and H_2S under the same conditions as the thiophene HDS studies; all of these results are reported herein.

The focus here is on deuterium content and location in the BDE product. The more saturated 1- and 2-butene products of thiophene DDS over $PbMo_{6.2}S_8$ contain[4] much higher levels of deuterium (D.N. = 5.36 to 5.54), presumably because they form as a result of deuteration of the initially formed 1,3-butadiene. Since these butenes were formed in subsequent reactions of BDE, their deuterium content was not of direct relevance to the HDS mechanism and therefore was not investigated in this study.

EXPERIMENTAL

Catalyst Preparation

The Chevrel catalyst, $PbMo_{6.2}S_8$, was prepared as previously described;[6b] characterization by X-ray diffraction was carried out to determine the bulk purity of the catalyst on a Siemens D500 diffractometer using CuKα radiation. Raman spectroscopy was performed on a Spex 1403 double monochromator spectrometer which confirmed the absence of MoS_2 (bands at 383 and 409 cm^{-1}) using the 514.5 nm line of a Spectra Physics argon laser operating at 200 mW (measured at the source). The catalyst was crushed and sieved to produce 40-100 mesh particles for all reactions. Surface area measurements were made on the same catalyst particle size, using the BET method on a Micromeritics 2100E Accusorb instrument at liquid nitrogen temperature using Kr as the adsorbing gas. The average surface area was found to be 0.80 ± 0.09 m^2/g.

Reactants

Thiophene (99+%) was purchased from Aldrich and purified as previously described.[19] Deuterium gas (Research grade, 99.99%), hydrogen gas (zero grade, 99.997%) and helium gas (zero grade, 99.997%) were purchased from Air Products. C.P. grade (99.0%) 1,3-butadiene and C.P. grade (99.5%) hydrogen sulfide were purchased from Matheson. The 2,5-dihydrothiophene (2,5-DHT) was prepared by a literature method[20] and found to be greater than 97% pure by ^1H NMR.

Reactor System

Deuterodesulfurization of thiophene and 2,5-dihydrothiophene were performed on a fixed-bed, continuous-flow microreactor similar to that previously described.[6] The reactor

bed was constructed from a 1.5 in x 0.25 in (o.d.) stainless steel tube. The catalyst (0.10-0.40 g) was held in place between two pads of quartz wool. The gases, H_2, D_2 and He, were purified by passing through an oxy-trap (Alltech), 5Å molecular sieves (Alltech), activated charcoal (Alltech) and a 5 μm filter (Alltech). Reactant gases, 1,3-butadiene and H_2S were passed through 5Å molecular sieves and a 5 μm filter. The flow rate through the reactor was 31 mL/min; operating pressure was near atmospheric. A Sage 341B syringe pump was used to inject thiophene and 2,5-DHT from a 2.50 mL gas-tight syringe into a heated saturator (6 in x 1/2 in stainless steel tubing packed with 5 mm glass beads) to completely volatilize the thiophenes. A series of two 6-port and one 4-port switching valves allowed for pulse- and continuous-flows of reactants over the catalyst as well as reaction stream sampling for G.C. analysis.

Gas chromatography was used for determinations of percent conversion of thiophene and C_4 product distribution. The G.C., a Varian 3400 equipped with an FID detector, was hooked up on-line to a 6-port valve on the reactor; 1.0 mL gas samples were injected directly from a 1.0 mL sample loop. The separated products were quantified on a Varian 4270 integrator. A 4-port valve and a 10-port valve on the G.C. allowed for the operation of two separate G.C. columns and for the reversal of column flow. Percent conversion of thiophene was determined on a 12 in x 1/8 in (o.d.) stainless steel column packed with Porapak Q (Alltech); the flow through the column was 20 mL/min at 110 °C. The C_4 hydrocarbons were separated on a 6 ft x 1/8 in (o.d.) column packed with 0.19% picric acid on Graphpac G.C.; the He flow through the column was 40 mL/min. The column temperature was held at 40 °C for 5 min followed by a 35°/min ramp to 65 °C. After a 2 min hold, a final ramp (35°/min) to 110 °C was used as the column flow was reversed to separate thiophene or to remove thiophene and 2,5-DHT (thiophene and 2,5-DHT did not separate on this column).

Experiment A. Deuterodesulfurization of Thiophene

Liquid thiophene was syringed into the reactor system at a rate of 0.12 mL/h (2.5×10^{-5} mol/min); D_2 flow was 31 mL/min (1.3×10^{-3} mol/min). The $PbMo_{6.2}S_8$ (0.1-0.4 g) was heated to 400 ± 1 °C in a stream of He (20 mL/min). The saturator, feed lines and valves were heated to 120 ± 2 °C to ensure that thiophene (b.pt. = 84 °C) was vaporized. The empty reactor showed no hydrodesulfurization activity. The reactor temperatures were allowed to stabilize for 1 h before the feed stream was brought on-line. Percent conversion and C_4 product distribution were monitored throughout the reaction by G.C. Trapping of the reaction products at the vent in a liquid-nitrogen-cooled pyrex tube containing 5 mm glass beads commenced 15 min after the reactants were brought on-line, and continued for 12 h, the duration of the experiment. These products were analyzed by mass and ^2H NMR spectrometries.

Experiment B. Deuterodesulfurization of 2,5-DHT

The 2,5-DHT reaction with D_2 over $PbMo_{6.2}S_8$ (0.200 g) was conducted in a manner similar to that of thiophene (*vide ante*). Liquid 2,5-DHT was syringed at a rate of 0.12 mL/h (2.5×10^{-5} mol/min); D_2 flow was 31 mL/min (1.3×10^{-3} mol/min). The $PbMo_{6.2}S_8$ catalyst was heated to 400 ± 1 °C in a stream of He (20 mL/min). The saturator, feedlines and valves were heated to 160 ± 2 °C to ensure that 2,5-DHT (b.pt. = 122 °C) was vaporized. Conversion of 2,5-DHT in the empty reactor was negligible (< 0.5%). Reactor temperatures stabilized for 1 h before the reactor feed was brought on-line. Percent conversion of 2,5-DHT and the C_4 product distribution were monitored throughout the reaction. The products were trapped for mass and ^2H NMR spectral analyses over a period of 6 h.

Experiment C. Reaction of Thiophene, D_2 and 2,5-DHT

A mixture of 2.5 mL (0.031 mol) of 2,5-DHT and 4.9 mL (0.062 mol) of thiophene was prepared; a 2.5 mL sample of it was loaded into the gas-tight syringe. The flow rate of this mixture was 0.12 mL/h; the D_2 flow was 31 mL/min (1.3×10^{-3} mol/min). The reactor was set up as for the reaction of 2,5-DHT with D_2 (*vide ante*). The products were monitored by G.C. Trapping of the products at the vent was carried out for 6 h.

Experiment D. Reaction of 1,3-Butadiene, D_2 and H_2S

The flow of butadiene was set at 0.048 mL/min (2.0×10^{-6} mol/min) as calibrated by G.C.; H_2S flow was set at either 0.043 mL/min (1.8×10^{-6} mol/min) or 0.74 mL/min (3.1×10^{-5} mol/min) using a bubble meter. The catalyst (0.200 g) was heated to 400 ± 1 °C in a He stream (20 mL/min), and the reactor system was allowed to stabilize for 1 h. The reactants were brought on-line in D_2 (31 mL/min, 1.3×10^{-3} mol/min), and the products were trapped at the vent. At the higher H_2S flow rate (0.74 mL/min, 3.1×10^{-5} mol/min), the reaction was run for 6 h; at the lower flow rate (0.043 mL/min, 1.8×10^{-6} mol/min), the reaction was run for 12 h. The C_4 product distributions were monitored throughout the reaction, and the products were trapped for analysis at the vent.

Experiment E. Reaction of Thiophene, D_2 and 1,3-Butadiene

The reactor was set up as above with the same flow rates of thiophene (0.12 mL/h, 2.5×10^{-5} mol/min) and D_2 (31 mL/min, 1.3×10^{-3} mol/min). The catalyst (0.500 g) was loaded to achieve 5% conversion of T; 1,3-butadiene was mixed with the reactant stream (0.18 mL/h, 7.5×10^{-6} mol/min). The C_4 product distribution was monitored throughout the reaction; the products were trapped at the vent for 12 h.

Deuterium Analysis of 1,3-Butadiene, Thiophene and 2,5-DHT

For each reaction, the trapped products were vacuum transferred into a 5 mm NMR tube containing 0.50 mL $CHCl_3$ (distilled from CaH_2 under N_2) for analysis by ^2H NMR and mass spectrometries. The ^2H NMR spectra were obtained on a Varian VXR-300 spectrometer using $CHCl_3$ as the internal ^1H lock and standard (δ 7.24 ppm). Mass spectral data for each component were obtained using a Finnigan 4000 GC-MS data system. The products were separated on a 30 m GS-alumina megabore (0.53 mm (i.d.), J & W Scientific) column. Low ionization energy (13-16 eV) was used in the mass spectrometer in order to reduce the fragmentation of the parent ion. The M-1 peak (loss of H) was always less than 9%. All deuterium exchange data were corrected[21] by comparing to similar data for authentic, unreacted samples; this allowed for correction of naturally occurring ^2H, ^{13}C and ^{34}S and of the parent ion fragmentation. The resulting data were expressed as a deuterium distribution, $d_0, d_1 \ldots, d_n$, where d_i is the fraction of the component containing i D atoms. This distribution can be represented as an average number of deuterium atoms per molecule, or deuterium number (D.N.) calculated using equation 2, where n is the total number of

$$D.N. = \sum_{i}^{n} i d_i \qquad (2)$$

H atoms in the molecule. The total numbers of D atoms in each position on 1,3-butadiene (D_A, D_B, D_C, Figure 1) were calculated using equation 3 where i is the D_A, D_B, or D_C

$$D_i = \left(\frac{I_i}{\Sigma I_i} \right) D.N. \qquad (3)$$

position, and I_i is the integral of the corresponding peaks in the ^2H NMR spectrum.

EXPERIMENTAL RESULTS

Deuterodesulfurization of Thiophene. Experiment A (eq 4)

Product distributions for reactions of thiophene under steady state conditions with deuterium gas (eq 4) at six different catalyst loadings of $PbMo_{6.2}S_8$ at 400 ± 1 °C are shown

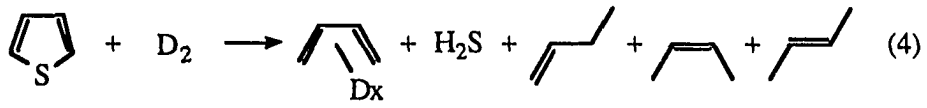

(4)

in Table 2. No hydrogenated thiophenes (2,3-DHT, 2,5-DHT or THT), butanethiol or butane were detected under these conditions. The catalyst loading was varied to produce different levels of thiophene conversion to C_4 products. The relative amounts of *cis*- and *trans*-2-butenes decrease as thiophene conversion decreases, with only trace amounts (< 0.5%) detected at the lowest conversion (0.86%). On the other hand, the relative amounts of 1-butene and BDE increase as conversion decreases; the increase in BDE is consistent with it being the initial product of HDS. The amount of 1-butene is always in excess of the equilibrium distribution at 400 °C (equilibrium at 400 °C: 20% 1-butene, 49% *trans*-2-butene; 31% *cis*-2-butene),[5] which is consistent with it being formed as the initial product of BDE hydrogenation. It is unlikely that 1-butene is the initial product which dehydrogenates to butadiene under the D_2 atmosphere. This is supported by the observation that 1-butene, when passed over $PbMo_{6.2}S_8$ at 400 °C, produces no BDE.[6]

Deuterium distributions in the unreacted thiophene and BDE products at different catalyst loadings are shown in Table 3. The reaction run numbers in Table 3 correspond to those in Table 2. Thiophene deuterium numbers (D.N.) decrease (0.42-0.05) with decreasing thiophene conversion (10.2-0.86%). A plot (Figure 7) of thiophene D.N. against thiophene conversion is nearly linear, as would be expected from the decreased residence

Table 2. Percent Conversion and Product Distribution from Thiophene Deuterodesulfurization over $PbMo_{6.2}S_8$ at 400 °C (Experiment A).[a]

	Reaction Number					
	1	2	3	4	5	6
g catalyst	0.403	0.265	0.327	0.195	0.126	0.110
% Thiophene	89.8	91.8	91.9	93.2	97.4	99.1
% C_4's	10.2	8.20	8.09	6.81	2.63	0.86
% 1-Butene[b]	47.7	49.8	52.0	53.3	67.7	70.8
% *cis*-2 Butene[b]	22.0	20.9	19.4	19.2	10.7	trace
% *trans*-2-Butene[b]	26.7	24.5	23.9	21.9	11.5	trace
% 1,3-Butadiene[b]	3.50	4.51	4.67	5.65	10.1	29.2

[a] Thiophene flow rate is 0.12 mL/h (2.5×10^{-5} mol/min); D_2 flow rate is 31 mL/min (1.3×10^{-3} mol/min).

[b] Percent of the C_4 hydrocarbons formed.

time in the catalyst bed. Thus, the amount of deuterium exchange on thiophene is dependent on the amount of conversion.

The sites (Figure 1) of deuterium exchange in thiophene and BDE can be determined by integrating peaks in the ^2H NMR spectrum. A typical ^2H NMR spectrum of the olefinic region is shown in Figure 8. The peaks are slightly broadened as compared to an ^1H NMR spectrum due to quadrupolar relaxation of the nuclei; however, the chemical shifts (in ppm) are essentially the same in the ^1H and ^2H NMR spectra of butadiene and butadiene-d_6.[22, 23]

Table 3. Deuterium Distribution and Deuteration Sites in 1,3-Butadiene and Thiophene Produced during Thiophene Deuterodesulfurization over $PbMo_{6.2}S_8$ at 400 °C (Experiment A).[a]

	Reaction Numbers					
	1	2	3	4	5	6
d_0	0.0077	0.0105	0.0100	0.0110	0.0177	0.0255
d_1	0.0573	0.0575	0.0586	0.0616	0.0255	0.0491
d_2	0.172	0.168	0.159	0.147	0.121	0.176
d_3	0.297	0.259	0.298	0.300	0.254	0.301
d_4	0.252	0.281	0.264	0.261	0.278	0.275
d_5	0.158	0.166	0.157	0.165	0.227	0.145
d_6	0.0553	0.0576	0.0545	0.542	0.0775	0.0290
BDE D.N.	3.42	3.47	3.44	3.45	3.74	3.30
D_A	0.79	0.81	0.78	0.86	0.91	0.85
D_B	1.41	1.38	1.36	1.36	1.40	1.19
D_C	1.23	1.28	1.31	1.23	1.44	1.26
D_A:D_B:D_C	1:1.8:1.6	1:1.7:1.6	1:1.8:1.7	1:1.6:1.4	1:1.5:1.6	1:1.4:1.5
Thiophene D.N.	0.42	0.32	0.29	0.23	0.08	0.05

[a] See footnote a in Table 2 for reactant amounts and conditions.

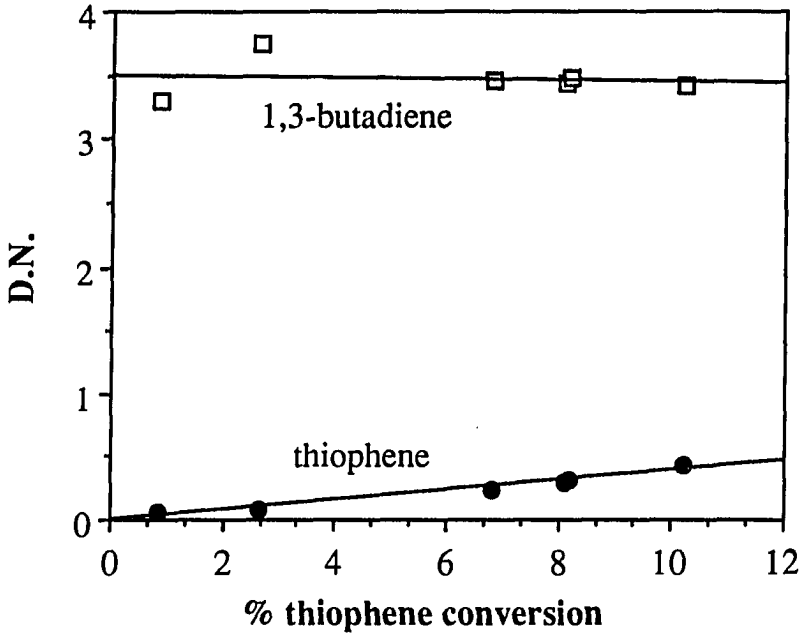

Figure 7. Change in thiophene D.N. and 1,3-butadiene D.N. with % thiophene conversion (Experiment A, eq 4).

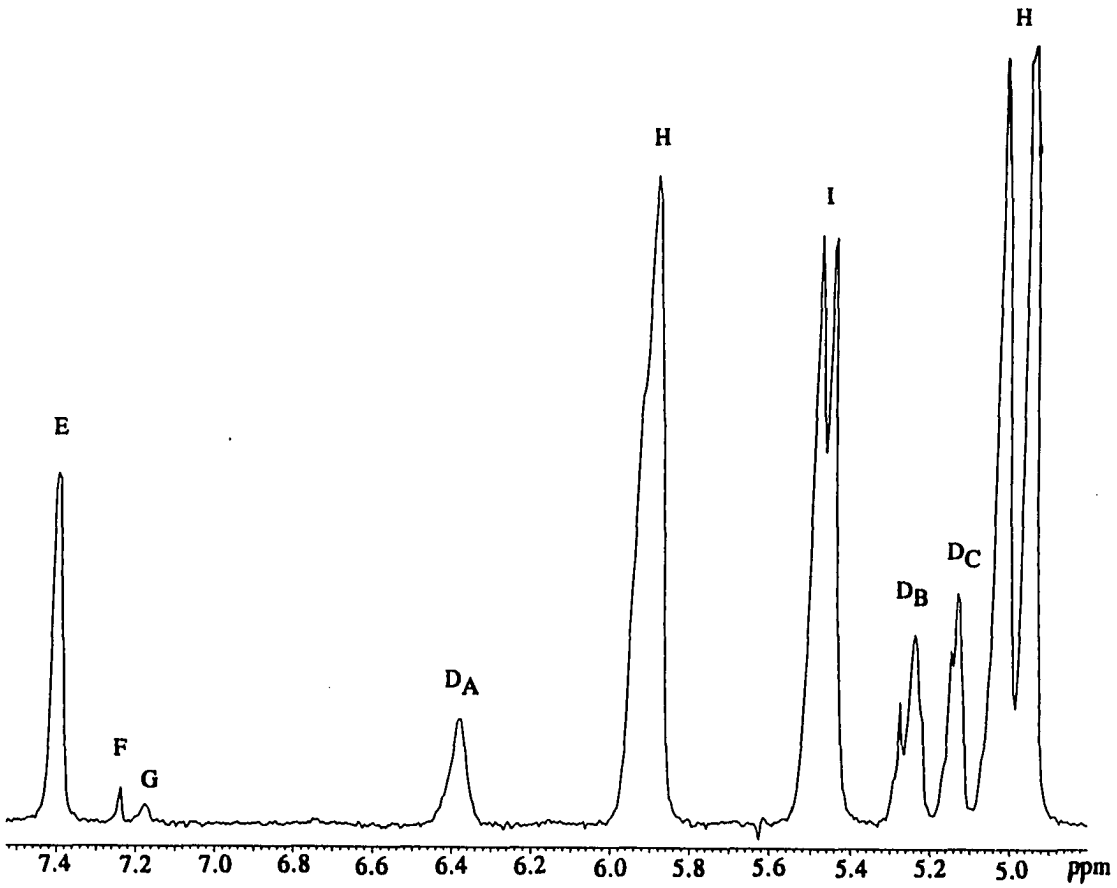

Figure 8. Olefinic region of an ^2H NMR spectrum of DDS reaction products. Labled peaks are as follows: D_A, D_B, and D_C of 1,3-butadiene with labeled positions corresponding to those in Figure 1; E is the 2,5-positions on thiophene; F is $CDCl_3$ in $CHCl_3$ solvent; G is the 3,4-positions on thiophene; H is 1-butene; I is 2-butenes.

Coupling constants between two ^2H atoms is usually only 2.3% of the corresponding coupling between two ^1H atoms; coupling between ^1H and ^2H is about 15% of the corresponding ^1H, ^1H coupling. Thus, ^1H, ^2H coupling most likely accounts for the observed splittings in the ^2H NMR spectrum (Figure 8). The peaks for thiophene (E, δ 7.40 ppm (s) and G, δ 7.19 ppm (s) in Figure 8) indicate that most of the deuterium exchange (95%) occurs in the 2- and 5-positions rather than the 3,4-positions; predominant exchange in the 2,5-positions has also been observed over MoS_2 and Co-Mo/Al_2O_3.[24, 25]

Deuterium numbers calculated from the mass spectral data (eq 2) for BDE remain constant (average D.N. = 3.47) despite the decrease in thiophene conversion (Table 3, Figure 7) from 10.2% to 0.86%. It is evident from the mass spectrometric data (Table 3), however, that there is considerable scrambling of hydrogen and deuterium in the BDE product since the BDE deuterium content ranges from d_0 to d_6; butadiene-d_3 and butadiene-d_4 are the major BDE products.

The amount of deuterium in each position (D_A, D_B, D_C; Table 3) was calculated from the D.N. and integrals of the individual peaks in the ^2H NMR spectra (eq 3). Peaks for butadiene (D_A, δ 6.38 ppm (s); D_B, δ 5.25 ppm (m); D_C, δ 5.14 ppm (m); Figure 8) in the ^2H NMR spectra are easily distinguished from those of 1-butene (H, δ 5.90 (s) and 4.99 ppm (d)) and the 2-butenes (I, δ 5.47 ppm (d)) which allows the D_A, D_B and D_C butadiene peaks to be integrated. The amount of deuterium in the D_A position (0.78-0.91) (Table 3) is always less than that in either the D_B (1.19-1.41) or D_C (1.23-1.44) positions.

DDS of 2,5-DHT. Experiments B and C (eq 5)

Product distributions the reaction of for 2,5-DHT with D_2 (Experiment B) (eq 5) and

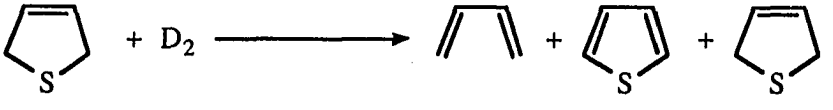

(5)

for the mixture of thiophene and 2,5-DHT with D_2 (Experiment C) are shown in Table 4. The reaction of 2,5-DHT with D_2 produces 27.7% BDE as the only desulfurized product; butenes are present in trace amounts (< 1%). The dehydrogenated product, thiophene is also detected. Thiophene was also detected from 2,5-DHT HDS over 5% Re/Al_2O_3 at 400 °C.[7c] Although the amount of thiophene decreases from 52% at the beginning of the run to 15% after 6 h and the amount of unreacted 2,5-DHT increases from 25% to 61% during the same time, the amount of BDE remains constant. The 1,3-butadiene also incorporates virtually no deuterium (99% is d_0 and d_1, D.N. = 0.04) as does thiophene (D.N. = 0.04) for samples collected over the 6 h duration of the run (Table 5); 2,5-DHT is all d_0. Although the amounts of thiophene and 2,5-DHT change during the run, there is no effect of this change on the incorporation of deuterium into butadiene or 2,5-DHT.

When thiophene is added to 2,5-DHT (Experiment C) in a 2:1 mole ratio, the conversion to C_4 products drops to 20.5% (Table 4), 91% of which is 1,3-butadiene. Thus, thiophene inhibits the decomposition of 2,5-DHT to BDE. Small amounts of 1-butene (4.7%), *cis*-2-butene (1.9%) and *trans*-2-butene (2.2%) are also detected; again 1-butene is in excess of the equilibrium distribution of butenes. At the beginning of the reaction, all of the 2,5-DHT is converted to either C_4 products or thiophenes; however, after 3 h, 2,5-DHT is detected and its concentration steadily increases to 8% after 6 h. Virtually no deuterium (Table 5) is incorporated into either 2,5-DHT (D.N. = 0.0) or thiophene (D.N. = 0.02), but the amount of deuterium in BDE (D.N. = 0.33) is greater than it was in the reaction (Experiment B) of just 2,5-DHT with D_2. The deuterium in the BDE obtained from the 2,5-DHT, thiophene, D_2 reaction may come at least in part from the BDE produced from thiophene DDS. The ratio of deuterium in the D_A, D_B and D_C positions in BDE is the same as that obtained from thiophene DDS (Table 3).

Table 4. Product Distributions from Reactions of D_2 with 2,5-DHT (Experiment B), 2,5-DHT and Thiophene (Experiment C), and H_2S and 1,3-Butadiene (Experiment D) over $PbMo_{6.2}S_8$ at 400 °C.[a]

	Experiments			
	B[b]	C[c]	D[d]	D[e]
g catalyst	0.210	0.210	0.200	0.200
% C_4's	27.7	20.5	100	100
% T	52[f]-15[g]	73[f]-79[g]	-	-
% 2,5-DHT	25[f]-61[g]	0[f]-8.3[g]	-	-
% 1-Butene	< 1%	4.7	30.71	6.70
% *cis*-2-Butene	trace	1.9	22.66	5.23
% *trans*-2-Butene	trace	2.2	24.39	5.71
% Butadiene	~99	~91	32.24	82.36

[a]D_2 flow is 31 mL/min (1.3×10^{-3} mol/min) for all reactions.

[b]2,5-DHT flow rate was 0.12 mL/h (2.5×10^{-5} mol/min).

[c]2:1 mole ratio of thiophene (0.08 mL/h, 1.7×10^{-5} mol/min) and 2,5-DHT (0.04 mL/h, 8.3×10^{-6} mol/min) in feed.

[d]Low H_2S flow of 0.043 mL/min (1.8×10^{-6} mol/min) and BDE flow of 0.048 mL/min (2.0×10^{-6} mol/min).

[e]High H_2S flow of 0.74 mL/min (3.1×10^{-5} mol/min) and BDE flow of 0.048 mL/min (2.0×10^{-6} mol/min).

[f]Start of reaction.

[g]After 6 h of continuous reaction.

Table 5. Deuterium Distribution in 1,3-Butadiene and Thiophene Produced in Reactions of D_2 with 2,5-DHT (Experiment B), 2,5-DHT and Thiophene (Experiment C), H_2S and 1,3-Butadiene (Experiments D), and Thiophene and 1,3-Butadiene (Experiment E).[a]

	Experiments				
	B[b]	C[c]	D[d]	D[e]	E[f]
d_0	0.974	0.792	0.124	0.992	0.187
d_1	0.019	0.130	0.157	0.008	0.270
d_2	0.004	0.044	0.221	-	0.285
d_3	0.002	0.024	0.229	-	0.146
d_4	-	0.009	0.165	-	0.078
d_5	-	0.001	0.082	-	0.029
d_6	-	-	0.022	-	0.005
BDE D.N.	0.04	0.33	2.49	0.01	1.58
D_A	0.01	0.09	0.53	-[g]	0.29
D_B	0.02	0.13	1.04	-	0.64
D_C	0.04	0.12	0.91	-	0.65
Thiophene D.N.	0.04	0.02	-	-	0.08
2,5-DHT D.N.	0.0	0.0	-	-	-

Table 5. (continued)

[a]D_2 flow for all reactions was 31 mL/min (1.3 x 10^{-3} mol/min) over $PbMo_{6.2}S_8$ at 400 °C.

[b]2,5-DHT flow rate was 0.12 mL/h (2.5 x 10^{-5} mol/min).

[c]2:1 mole ratio of thiophene (0.08 mL/h, 1.7 x 10^{-5} mol/min) and 2,5-DHT (0.04 mL/h, 8.3 x 10^{-6} mol/min) in feed.

[d]Low H_2S flow 0.043 mL/min (1.8 x 10^{-6} mol/min) and BDE flow of 0.048 mL/min (2.0 x 10^{-6} mol/min).

[e]High H_2S flow 0.74 mL/min (3.1 x 10^{-5} mol/min) and BDE flow of 0.048 mL/min (2.0 x 10^{-6} mol/min).

[f]Thiophene flow of 0.12 mL/min (2.5 x 10^{-5} mol/min) and BDE flow of 0.18 mL/min (7.5 x 10^{-6} mol/min).

[g]No BDE is detected in ^2H NMR.

Reaction of 1,3-Butadiene, H_2S and D_2. Experiment D (eq 6)

The BDE flow rate (eq 6) was set (0.048 mL/min, 2.0 x 10^{-6} mol/min) at a level

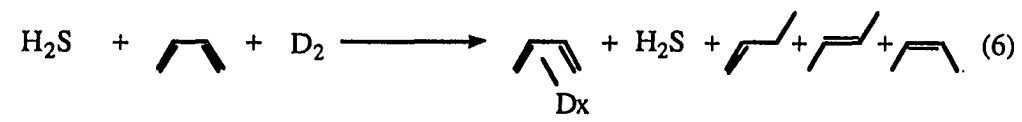

(6)

corresponding to the amount of C_4 products observed at 10% thiophene conversion (Experiment A). In separate reactions, the flow of H_2S was set at a level corresponding to the equivalent amount of thiophene (0.74 mL/min, 3.1 x 10^{-5} mol/min) and at the amount corresponding to the H_2S produced during thiophene HDS (0.043 mL/min, 1.8 x 10^{-6} mol/min). The H_2S and BDE were passed over the catalyst together with D_2 gas at a flow rate of 31 mL/min (1.3 x 10^{-3} mol/min). The C_4 product distributions are shown in Table 4. At both H_2S flow rates, the C_4 product distribution remained constant for the entire reaction (6 h and 12 h) indicating steady state conditions were achieved. The effect of catalyst poisoning by H_2S is seen in the product distributions; at the lower H_2S flow rate, 78% of the BDE is hydrogenated compared to only 18% at the higher H_2S flow rate. In both cases, 1-butene is in excess of the equilibrium values for butenes at 400 °C.[5]

The deuterium content in BDE from the reactions of H_2S, BDE and D_2 (Table 5), also show the effect of catalyst poisoning. At the lower H_2S flow (0.043 mL/min, 1.8 x 10^{-6} mol/min), the D.N. is 2.49 (90% d_0-d_4), indicating that butadiene undergoes significant exchange over the HDS catalyst. However, at the higher H_2S flow (0.74 mL/min, 3.1 x 10^{-5} mol /min) where the number of moles of H_2S feed is similar to that of thiophene in thiophene DDS (Experiment A) (2.5 x 10^{-5} mol/min of thiophene), 99% of the butadiene does not undergo deuterium exchange (D.N. = 0.01). Since the amount of H_2S produced in the DDS of thiophene is similar to that in the lower H_2S experiment, it seems likely that the formed

D_2S (or H_2S) in the DDS of T will not completely inhibit deuterium exchange with the butadiene that is formed. However, the large excess of thiophene may be sufficient to essentially prevent this exchange as suggested by other experiments.

Reaction of Thiophene, BDE and D_2. Reaction E (eq 7)

The flow rate of BDE (0.18 mL/min, 7.6 x 10^{-6} mol/min) was set at approximately six

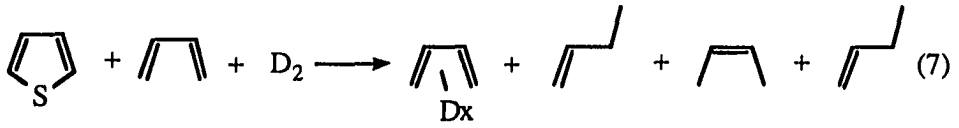

(7)

times the amount of C_4 products produced during thiophene DDS (Experiment A, eq 4) at 5% thiophene conversion. Thus, the majority of BDE trapped and analyzed should be from the added BDE and not a product of thiophene DDS. Without thiophene in the feed stream, but otherwise using the same conditions, BDE is completely hydrogenated to 1-butene and *cis*- and *trans*-2-butenes at 400 °C over $PbMo_{6.2}S_8$. No butane is detected. A small amount of cracking (5%) to C_3 and C_2 products is also observed. Thus, thiophene in the reactant feed inhibits BDE hydrogenation. This reaction (eq 7), however, does not achieve steady state conditions. Figure 9 shows a dramatic change in C_4 product distribution during the 12 h reaction. The relative amount of 1-butene stays constant; BDE increases while *cis*- and *trans*-2-butene decrease. There is always an excess of 1-butene over the equilibrium value for the 1- and 2-butenes at 400 °C.[5] The D.N. of BDE is significantly less (1.58) (Table 5) than that of BDE from thiophene DDS. Only 0.29 D atoms (eq 3) are in the D_A-position, indicating

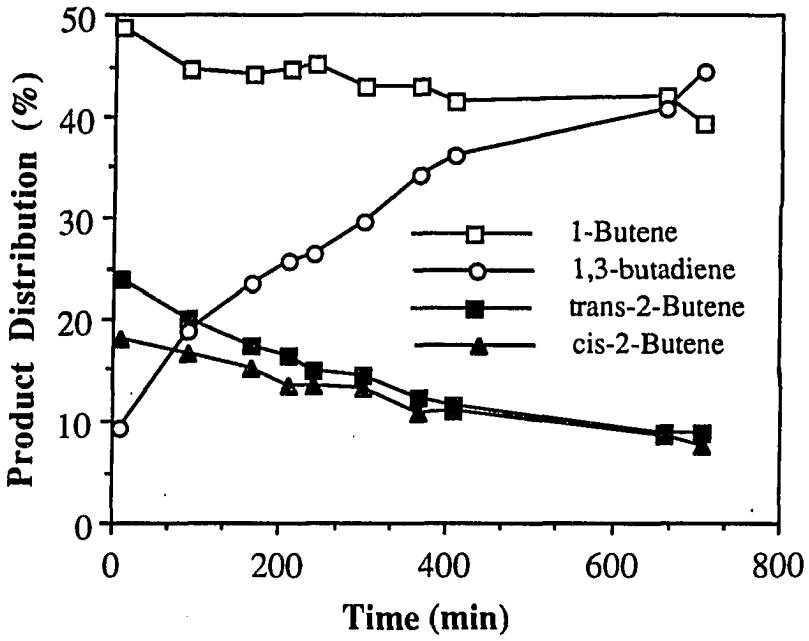

Figure 9. Change in product distribution with time for the reaction of thiophene, 1,3-butadiene and D_2 over $PbMo_{6.2}S_8$ at 400 °C (Experiment E, eq 7).

that most of the deuterium exchanges into the D_B- and D_C-positions. Since the reaction does not achieve a steady state, the catalyst is changing during the course of the reaction, and the results cannot be compared with data from the other reactions that are obtained under steady state conditions.

DISCUSSION OF RESULTS

1,3-Butadiene as the Initial HDS Product

The results of our study of thiophene DDS (Experiment A, eq 4) indicate that BDE is the first desulfurized product, which is subsequently hydrogenated to give the observed C_4 product distribution. This conclusion is supported by the following discussion. First, the relative amount of butadiene (Table 2) increases with decreasing thiophene conversion. This same trend, indicative of a sequential pathway, has been observed over other Chevrel phase catalysts[4] and over MoS_2.[3a] Second, the 1-butene produced during the reaction (Table 2) is always in excess of the equilibrium distribution of butenes[5] at 400 °C; 1-butene is also in excess during the hydrogenation of BDE in a BDE and H_2S mixture (Experiment D) and over MoS_2.[26] Third, hydrogenation of 1-butene over $PbMo_{6.2}S_8$ and other Chevrel phase catalysts[6] does not produce BDE. Thus, the evidence strongly supports the conclusion that the BDE produced in our reactions (Experiment A) is the first product of thiophene DDS.

Deuterium Content in 1,3-Butadiene

The deuterium observed experimentally in BDE formed during thiophene DDS could be incorporated at any of three stages of the reaction (eq 8): in stage (i), thiophene itself could

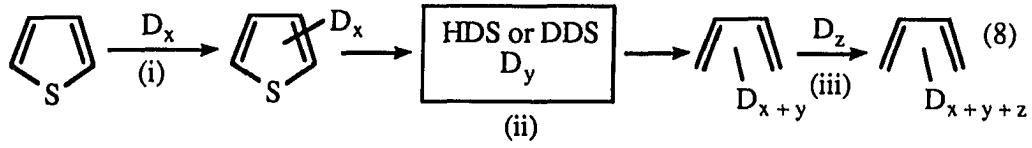

exchange to incorporate x deuterium atoms; in stage (ii), the thiophene undergoes HDS to give BDE, which must incorporate at least two deuteriums in order to form BDE but could contain a total of y deuterium atoms; in stage (iii), the formed BDE may undergo exchange to

incorporate z deuterium atoms. So the total deuterium content in the final BDE is the sum (x + y + z) gained in each of the three stages. We want to know the amount of deuterium (D_y) incorporated in only the DDS stage (ii) of the reaction. In order to establish D_y, the number of deuteriums gained during just the DDS portion of the process (stage ii), it is necessary to determine D_x and D_z in stages (i) and (iii); D_x and D_z are discussed below.

It is entirely possible that deuterium incorporation will occur in stage (i) as thiophene is known to undergo deuterium exchange (eq 9), primarily into the α-position, over a variety of

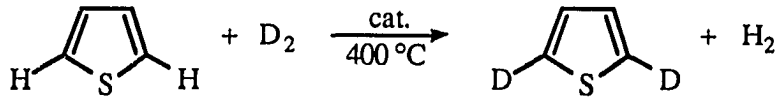

(9)

HDS catalysts,[24, 25] including $PbMo_{6.2}S_8$.[4] In this study, D exchange of the α-protons on thiophene during DDS over $PbMo_{6.2}S_8$ varies with the amount of thiophene conversion (Experiment A, Tables 2 and 3, Figure 7). At the highest conversion of 10.2%, the D.N. is equal to 0.42; this drops to 0.05 at the lowest conversion (0.86%). Thus, deuterium incorporation in stage (i) is relatively small with D_x ranging from $D_{0.4}$ to $D_{0.1}$ or less, and almost all of this deuterium would appear in the D_B and D_C positions (Figure 1) of the BDE product.

Our results indicate that in stage (iii) (eq 8) the BDE does not undergo deuterium exchange; thus, D_z is D_0. The lack of deuterium exchange in the formed BDE appears to result from H_2S/thiophene deactivation of the exchange sites. These conclusions are supported by the following results. (a) At different levels of thiophene conversion, the deuterium content (D.N. = 3.47) of BDE remains virtually constant (Tables 2 and 3, Figure 7). If deuterium were exchanging with the formed BDE, a decrease in D.N. with decreasing thiophene conversion would be expected. Deuterium exchange of thiophene itself shows this trend (Figure 7). (b) Butadiene can be formed *in situ* by passing 2,5-DHT with D_2 over the

$PbMo_{6.2}S_8$ catalyst. This is also known to occur in reactions of 2,5-DHT with H_2 over 5% Re/Al_2O_3 (7b); in addition, BDE is liberated when 2,5-DHT adsorbs to a Mo(110) single crystal surface,[27] and organometallic complexes containing 2,5-DHT as a ligand[7c, 28] liberate BDE when heated. In the present studies, 2,5-DHT (0.12 mL/h, 2.5×10^{-5} mol/min) when passed with D_2 over $PbMo_{6.2}S_8$ gives BDE as the only C_4 hydrocarbon product (Experiment B, Table 4). The BDE formed is 97.4% d_0 (D.N. = 0.04, Table 5) indicating that the BDE does not exchange significantly with deuterium under these conditions. Similar results were obtained for the DDS of 2,5-DHT over 5% Re/Al_2O_3 at 300 °C, where BDE incorporated slightly more deuterium (D.N. = 0.51) (7b). When thiophene, 2,5-DHT and D_2 were reacted (Experiment C, Tables 4, 5), the resulting BDE contains more deuterium (D.N. = 0.33) than that obtained from only 2,5-DHT and D_2 (DN = 0.04). The higher BDE deuterium content in this reaction (Experiment C) appears to result from the BDE produced in the DDS of thiophene. Assuming 5% conversion of thiophene (based on the amount of catalyst), this reaction was run with 10 equivalents of 2,5-DHT for every mole of BDE produced from thiophene. The BDE D.N. of 0.33 is 1/10 of that produced from just thiophene DDS and the ratio D_A:D_B:D_C are similar to those in BDE produced in the DDS of thiophene (Experiment A). This suggests that deuterium is incorporated only into BDE from thiophene DDS, not from 2,5-DHT DDS. (c) H_2S inhibits both the hydrogenation and the deuterium exchange (Experiment D, Tables 4, 5) of BDE over this catalyst. Complete hydrogenation of BDE to butenes is observed over $PbMo_{6.2}S_8$ at 400 °C; however, when H_2S (3.1×10^{-5} mol/min) is added to the feed at a level similar to that of thiophene (2.5×10^{-5} mol/min) and the butadiene flow (2.0×10^{-6} mol/min) is similar to that of the C_4 products obtained from 10% thiophene conversion, 82% of the 1,3-butadiene passes through unhydrogenated and unexchanged (99%-d_0). Results from static reactor studies of BDE and D_2 over MoS_2[26a] and mixtures of D_2S and BDE over MoS_2[26b] also indicate that BDE does not undergo exchange. In these

MoS_2 studies, greater than 94% of the BDE did not exchange. Thus, the above studies indicate that once BDE is formed from thiophene, it is either hydrogenated to 1-butene, or it passes through the catalyst without undergoing exchange. This is not unreasonable as BDE is very active toward hydrogenation, such that, once in contact with an active site, hydrogenation of BDE is faster than deuterium exchange. Thiophene, H_2S and 2,5-DHT all poison the catalyst, inhibiting both the hydrogenation and deuterium exchange of butadiene under these conditions.

The HDS Mechanism

Based on the above discussion, we can estimate that of the 3.47 D atoms found in the BDE resulting from the DDS of thiophene over $PbMo_{6.2}S_8$ at 400 °C, 0.1-0.4 D are introduced in stage (i) (eq 8); this exchange of D into thiophenes before DDS occurs will introduce 0.1-0.4 D into the D_B and D_C positions of the 1,3-butadiene product. Using an average value of 0.3 D for stage (i), this means that of the total 3.47 D observed in the BDE 3.2 D are introduced in the HDS step, stage (ii), of the reaction. Of these 3.2 deuteriums, 0.83 D are in the D_A-position and approximately 1.2 D are in each of the D_B and D_C positions. Any mechanism for HDS must account for this number and distribution of deuterium atoms in the BDE, but it must also account for the fact that there is considerable scrambling of deuterium atoms during HDS that accounts for butadiene with D content ranging from d_0 (1.2%) to d_6 (5.5%) but mostly d_3 (28%) and d_4 (27%) (Table 3). All of the mechanisms discussed in the Introduction and summarized in Table 1 involve processes that give specific numbers of deuteriums in specific positions; none accounts for the formation of d_0 or d_6, for example. Although some of these species are formed in low amounts, there must be a scrambling step in the HDS process that allows their formation. Since the scrambling is likely to involve surface deuterium atoms, any such scrambling will

likely add deuteriums to the number introduced by the DDS process itself. Thus, of the 3.2 deuteriums introduced in stage (ii) most were probably added during the DDS process, but some may have been added by scrambling. Any mechanisms that produce BDE with more than 3.2 D are inconsistent with the results. This eliminates the mechanisms (Table 1) in Figures 4 and 5 as pathways for thiophene HDS over this catalyst ($PbMo_{6.2}S_8$) under these conditions. Both of these mechanisms are also inconsistent with the number of deuteriums at the D_A position, since they both predict 1.5-2.0 D in this position, whereas only 0.83 D are observed.

The mechanism in Figure 3 proposed by Kwart, Schuit and Gates[10] is possibly consistent with our results depending on which pathway (steps *c*, *d*, *f*, *g* and *h* or steps *e*, *f* and *i*) predominates (Table 1). The first pathway (steps *c*, *d*, *f*, *g* and *h*) introduces as many as 3.5 D atoms into BDE with up to 1.5 D atoms in the D_A-position, if one assumes a deuterium isotope effect[9] (C-H bonds are much weaker than C-D bonds). This mechanism would not be consistent with the experimental results as more than 3.2 D are predicted for BDE with more than 0.83 D in the A-position. However, the latter pathway (steps *e*, *f* and *i*) leads to 2.0 D atoms incorporated in the D_B- and D_C-positions of BDE; thus, this mechanism is consistent with our results if a scrambling mechanism is included. Also, if both pathways are involved, they may together account for the observed amount of deuterium in BDE, the amount of deuterium in the D_A-position, as well as provide a mechanism for the scrambling seen in d_2-d_4; yet it still does not account for butadiene-d_0 and -d_1.

The mechanisms in Figures 2 and 6 are also consistent with the BDE deuterium results. Since the mechanism in Figure 2[7] introduces a maximum of 2.8 D atoms during the HDS process, the additional 0.4 D atoms must be added during a scrambling step. That this can occur is supported by the observation[7c] that the DDS of 2,3-DHT (product of step (*b*) in Figure 2) over 5% Re/Al_2O_3 at 300 °C introduces 1.20 D atoms, mainly at the olefinic

positions, into the unconverted 2,3-DHT; the BDE produced from this reaction contains 4.06 D atoms. Thus 2,3-DHT is an intermediate that may account for the extra D incorporation and the scrambling of D atoms which results in the d_0-d_6 distribution in the BDE. It is unlikely however, that scrambling occurs in the 2,5-DHT intermediate (product of step (*c*)) since the BDE produced in the DDS of 2,5-DHT over $PbMo_{6.2}S_8$ (Table 4, Experiments B and C) is 97% d_0, and 2,5-DHT incorporates no deuterium.

Another mechanism that is consistent with the results of this work is shown in Figure 6.[14] The mechanism itself accounts for the incorporation of only two deuterium atoms (Table 1) into BDE (step *f*). Deuterium exchange with one or more of the intermediates in this mechanism would account for the incorporation of D atoms in the D_A-position and the d_0-d_6 distribution. In this case, however, there are no reported studies of D exchange with the intermediates. The other mechanisms[15-18] which result in the addition of two D atoms to the D_B- and D_C-positions are also consistent with the results of this study for the same reasons.

CONCLUSION

The results of this study indicate that a mechanism for thiophene HDS over $PbMo_{6.2}S_8$ must account for a maximum of 3.2 deuterium atoms being incorporated into 1,3-butadiene including 0.83 D in the D_A-position and 1.2 D atoms in each of the D_B- and D_C-positions. Two mechanisms (Figures 4, 5) can be ruled out as they predict more deuterium per butadiene molecule than is found in these studies. Other mechanisms (Figures 2, 3 and 6) which predict fewer than 3.2 deuteriums in each 1,3-butadiene molecule, are consistent with the results of this study, assuming that there is a scrambling step which increases the overall deuterium content and yields the observed d_0-d_6 distribution of deuterated butadiene.

Acknowledgments

We appreciate the help of Chia-Mei Jen-Wang for building the flow reactor and of Jan Beane of the Iowa State University Mass Spectrometry Laboratory for performing the deuterium analyses. We also thank Dr. Mark Ekman and Felix Koo for synthesizing the catalyst. This work was conducted at the Ames Laboratory, which is operated for the U.S. Department of Energy by Iowa State University under Contract No. W-7405-Eng-82. This research was supported by the Office of Basic Energy Sciences, Chemical Sciences Division.

REFERENCES

(1) (a) Gates, B. C.; Katzer, J. R.; Schuit, G. C. A. *Chemistry of Catalytic Processes*, McGraw-Hill, New York, **1979**, Chapter 5.

(b) Sattefield, C. N. *Heterogeneous Catalysis in Industrial Practice*, McGraw-Hill: New York, **1991**, 378.

(c) Girgis, M. J.; Gates, B. C. *Ind. Eng. Chem. Res.* **1991,** *30*, 2021.

(2) Komarewsky, V. I.; Knaggs, E. A. *Ind. Eng. Chem.* **1951,** *43*, 1415.

(3) (a) Kolboe, S.; Amberg, C. H. *Canad. J. Chem.* **1966,** *44*, 2623.

(b) Owens, P. J.; Amberg, C. H. *Adv. in Chem.* **1961,** *Ser. No. 33*, 182.

(c) Owens, P. J.; Amberg, C. H. *Can. J. Chem.* **1962** , *40*, 941.

(d) Owens, P. J.; Amberg, C. H. *Can. J. Chem.* **1962,** *40*, 947.

(4) McCarty, K. F.; Schrader, G. L. *J. Catal.* **1987,** *103*, 261.

(5) These values were calculated from ΔG_f° values found in Rossini, F. D.; Pitzer, K. S.; Arnett, R. L.; Braun, R. M.; Pimentel, G. C. *Selected Values of Physical and Thermodynamic Properties of Hydrocarbons and Related Compounds*; Carnegie Press: Pittsburgh, **1953**, p 737.

(6) (a) Ekman, M. E.; Anderegg, J. W.; Schrader, G. L. *J. Catal.* **1989,** *117*, 246.

(b) McCarty, K. F.; Anderegg, J. W.; Schrader, G. L. *J. Catal.* **1985**, *93*, 375.

(c) McCarty, K. F.; Schrader, G. L. in *Proceedings, 8th International Congress on Catalysis, Berlin,* **1984** Vol. IV, p. 427. Dachema, Frankfurt-am-Main.

(d) McCarty, K.F.; Schrader, G. L. *Ind. Eng. Chem. Prod. Res. Dev.* **1984**, *23*, 519.

(e) Kareem, S. A.; Miranda, J. *J. Mol. Catal.* **1989**, *53*, 275.

(7) (a) Angelici, R. J. *Acc. Chem. Res.* **1988**, *22*, 387.

(b) Sauer, N. N.; Markel, E. J.; Schrader, G. L.; Angelici, R. J. *J. Catal.* **1989**, *117*, 295.

(c) Markel, E. J.; Schrader, G. L.; Sauer, N. N.; Angelici, R. J. *J. Catal.* **1989**, *116*, 11.

(8) (a) Sauer, N. N.; Angelici, R. J. *Inorg. Chem.* **1987**, *26*, 2160.

(b) Glavee, G. N.; Daniels, L. M.; Angelici, R. J. *Organometallics* **1989**, *8*, 1856.

(c) Glavee, G. N.; Daniels, L. M.; Angelici, R. J. *Inorg. Chem.* **1989**, *28*, 1751.

(9) (a) Deuterium isotope effects were not established for individual intermediates in the mechanisms. However, a reasonable estimate of the effect comes from the reaction of $\bullet CH_3$ with CH_3CD_3 at 401 °C, which gives a rate constant ratio (k_H/k_D) of 3.33. Rice, F. O.; Vanderslice, T. A. *J. Am. Chem. Soc.* **1958**, *80*, 291.

(b) An isotope effect estimate (k_H/k_D = 2.3 at 400 °C) can be calculated from the loss of zero-point energy going from C-H to C-D. Lowry, T. H.; Richardson, K. S. *Mechanism and Theory in Organic Chemistry*; Harper Collins: New York, **1987**, 232.

(c) Milander, L.; Saunders, W. H., Jr. *Reaction Rates of Isotopic Molecules*; Wiley: New York, **1980**.

(10) Kwart, H.; Schuit, G. C. A.; Gates, B. C. *J. Catal.* **1980**, *61*, 128.

(11) Delmon, B.; Dallons, J.-L. *Bull. Soc. Chim. Belg.* **1988**, *97*, 473.

(12) (a) Chen, J.; Angelici, R. J. *Organometallics* **1990**, *9*, 849.

(b) Chen, J.; Angelici, R. J. *Organometallics* **1989**, *8*, 2277.

(c) Chen, J.; Daniels, L. M.; Angelici, R. J. *J. Am. Chem. Soc.* **1990**, *112*, 199.

(d) Chen, J.; Angelici, R. J. *Organometallics* **1990**, *9*, 879.

(e) Luo, S.; Ogilvy, A. E.; Rauchfuss, T. B.; Rheingold, A. L.; Wilson, S. R. *Organometallics* **1991**, *10*, 1002.

(f) Ogilvy, A. E.; Skaugset, A. E.; Rauchfuss, T. B. *Organometallics* **1989**, *8*, 2739.

(13) Kolboe, S. *Canad. J. Chem.* **1969**, *47*, 352.

(14) Chen, J.; Daniels, L. M.; Angelici, R. J. *J. Am. Chem. Soc.* **1991**, *113*, 2544.

(15) Desikan, P.; Amberg, C. H. *Canad. J. Chem.* **1964**, *42*, 843.

(16) Lipsch, J. M. J. G.; Schuit, G. C. A. *J. Catal.* **1969**, *15*, 179.

(17) Curtis, M. D.; Penner-Hahn, J. E.; Schwank, J.; Baralt, O.; McCabe, D. J.; Thompson, L.; Waldo, G. *Polyhedron* **1988**, *7*, 2411.

(18) Cowley, S. W. *Ph.D. Thesis*, Southern Illinois University, **1975**.

(19) Spies, G. H.; Angelici, R. J. *Organometallics* **1987**, *6*, 1897.

(20) Everhardus, R. H.; Gräfing, R.; Brandsma, L. *J. R. Neth. Chem. Soc.* **1976**, *95*, 153.

(21) (a) Davis, S. M.; Somorjai, G. A. *J. Phys. Chem.* **1983**, *87*, 1545.

(b) Biemann, K. *Mass Spectrometry--Organic Chemical Application*; McGraw-Hill: New York, **1962**.

(22) Smith, I. P. C. in *NMR of Newly Accessible Nuclei*" (P. Laszlo, Ed.), Vol. 2, p. 1. Academic Press, New York, **1983**.

(23) Brevard, C.; Krutzinger, J. P. *NMR and the Periodic Tabl*" (R. K. Harris and B. E. Mann, Eds.), p. 107. Academic Press, New York, **1978**.

(24) Kieran, P.; Kimball, C. *J. Catal.* **1965**, *4*, 394.

(25) Behbahany, F.; Sheikhrezai, Z.; Djalali, M.; and Salajegheh, S. *J. Catal.* **1980**, *63*, 285.

(26) (a) Blake, M. R.; Eyre, M.; Moyes, R. B.; Wells, R. B. *Std. Surf. Sci. Catal.* **1981**, *7*, 591 .

(b) Barbour, J.; Cambell, K. C. *J. Chem. Soc. Chem. Commun.* **1982**, 1371.

(27) (a) Liu, A. C.; Friend, C. M. *J. Am. Chem. Soc.* **1991**, *113*, 820.

(b) Friend, C. M.; Wiegand, B. C. *Chem. Rev.* **1992**, *92*, 491.

(c) Friend, C. M.; Roberts, J. T. *Acc. Chem. Res.* **1988**, *21*, 394.

(28) Choi, M.-G.; Daniels, L. M.; and Angelici, R. J. *Inorg. Chem.* **1991**, *30*, 3647.

APPENDIX

The microreactor in 2311 Gilman Hall is designed for the study of gas phase reactions of heterogeneously-catalyzed reactions. This appendix is designed to be a detailed guide for operation of the microreactor[1] as well as an aid in calculating the deuterium distribution from the mass spectra and calculating the amount of deuterium at each position in 1,3-butadiene, thiophene and 2,5-dihydrothiophene.

Microreactor Design

The microreactor system is illustrated schematically in Figure 1. Listings of equipment manufacturers and feed component sources are shown in Tables 1 and 2. Hydrogen, deuterium and helium gases are purified by 5Å molecular sieves to remove H_2O, activated charcoal to remove residual hydrocarbons and copper/oxygen traps to remove O_2, and a 5 μm filter. The reactor is designed to allow the simultaneous flow of up to four gases (e.g. H_2, He, 1,3-butadiene and H_2S). Flow of each gas is controlled separately by a needle valve and controlled and monitored on rotameters (calibrated with a bubble meter); the manifold system of 3-way valves allows the selection of any combination of the four feed gasses plus the purging of the manifold dead volumes. A three-way valve allows immediate switching of H_2 to D_2 during the reaction, while only H_2 is used to run the flame ionization detector (FID) on the G.C.. Thiophene is injected into the system using a Sage 341A syringe pump equipped with a 2.5 mL gas-tight syringe. Thiophene is vaporized and mixed with the carrier gas in the saturator, a 0.5 in x 6 in stainless steel (s.s.) tube packed with 5 mm glass beads. In order to ensure that the thiophene is vaporized, all of the feed lines leading to and from the reactor furnace as well as the valves and the saturator are heated using heating tape .

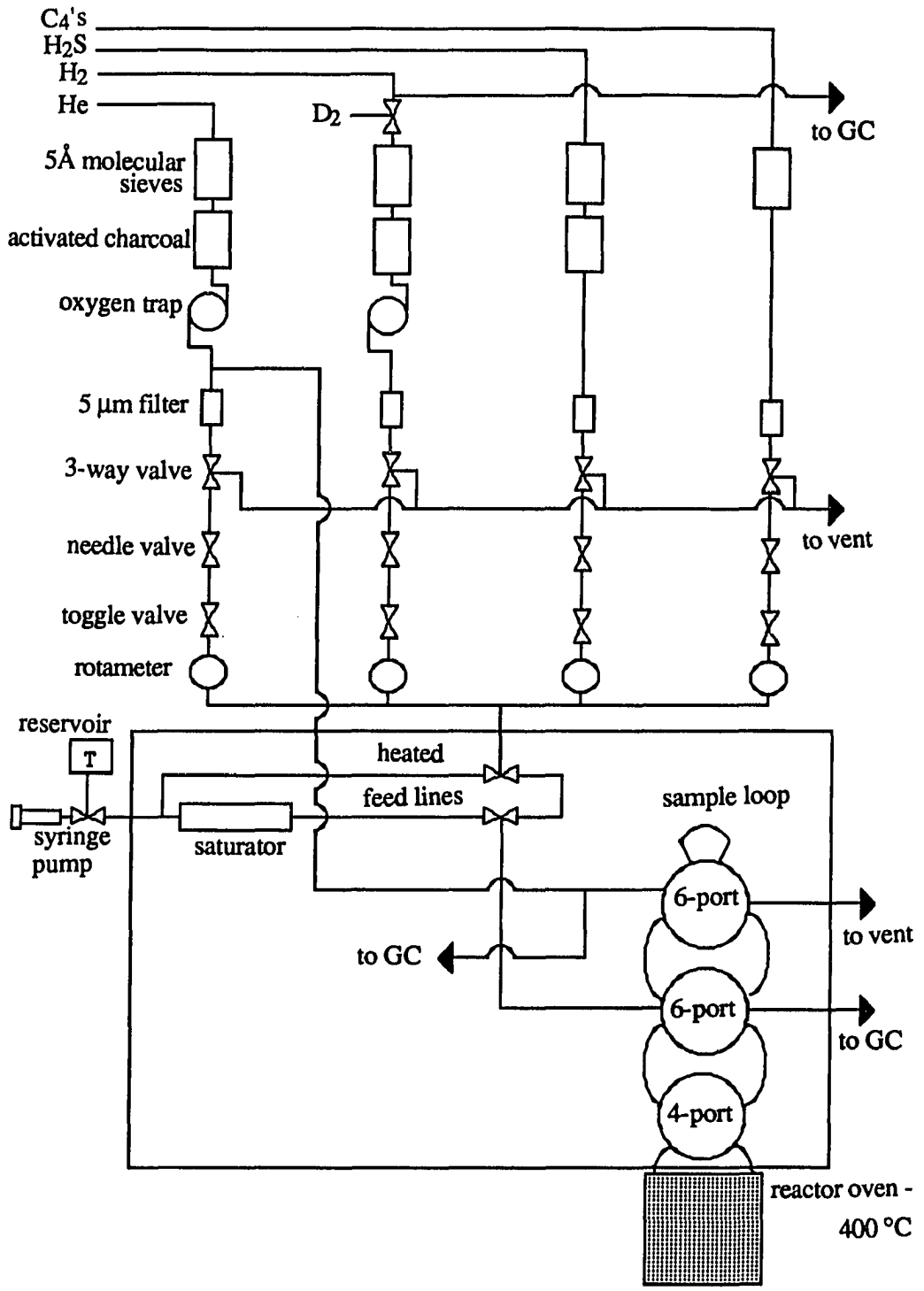

Figure 1. Schematic of the Fixed Bed Flow Microreactor

Table 1. Microreactor Equipment

Part Name (Catalog No.)	Source	1987-88 Unit Price
5Å molecular sieve trap (8125)	Alltech	$55.00
activated charcoal trap (8129)	Alltech	$58.00
oxy-trap (4002)	Alltech	$49.50
5μm filter (SS-4F-7)	Swagelok	$30.80
pressure regulator (2-3748)	Supelco, Inc.	$48.00
3-way ballvalve (SS-43XS4)	Swagelok	$47.60
3-way ballvalve (SS-41XS2)	Swagelok	$48.70
needle valve (SS-4MG)	Swagelok	$52.60
toggle valve (SS-1GS4)	Swagelok	$33.30
2.5 mL syringe (A1161)	Anspec	$35.00
Sage syringe pump 341A (14-831-40)	Fisher	$750.00
4-port valve (39104)	Alltech	$175.00
6-port valve (39110)	Alltech	$275.00
10-port valve (39120)	Alltech	$300.00
Rotameter, He (7910)	Alltech	$140.00
Rotameter, H_2 (7912)	Alltech	$140.00
Rotameter, N_2 (7912)	Alltech	$140.00
1 mL sample loop (91102)	Alltech	$10.00
0.19% picric acid column	Alltech	$72.00
Porapak Q column	Alltech	$40.00
Temperature Controller	Omega	$300

Table 2. Feed Components

Feed (purity)	Source
Hydrogen (99.997 %)	Air Products
Helium (99.997 %, <0.5 ppm total hydrocarbons)	Air Products
1,3-butadiene (99.0 %)	Matheson
Air (< 1 ppm total hydrocarbon)	Air Products
Deuterium (99.99 %)	Air Products
Thiophene (99 %)	Aldrich
Hydrogen Sulfide (99.5%) Matheson	

controlled by variacs and monitored with thermocouples. The reactor bed is heated in a furnace controlled by a variac and a temperature controller

Microreactor Function

Switching of the gases in the reactor is accomplished using two 6-port valves and one 4-port valve that are enclosed and heated. The diagrams in Figure 2 are of the flow through the 6-port valves in the different valve positions. The arrows on the lines outside of the valve circle indicate the flow direction in and out of the valves. The arrow in the center of the individual valve diagram indicates the direction of the valve handle. (Note: there is no mid-valve position; the manufacturer suggests that the valve never be left in a mid, or partially,

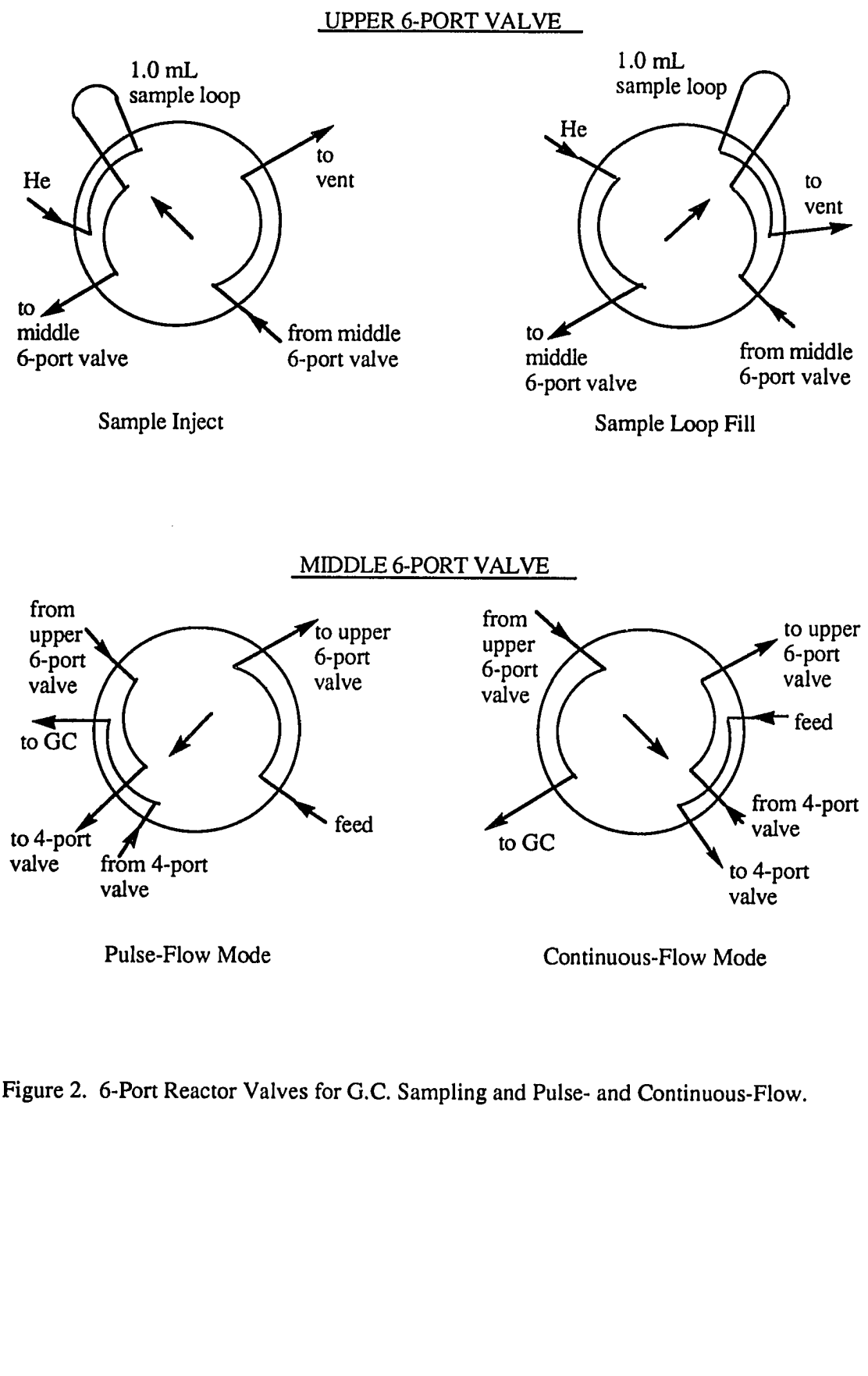

Figure 2. 6-Port Reactor Valves for G.C. Sampling and Pulse- and Continuous-Flow.

actuated positions.) The middle 6-port valve switches the system between pulse- and continuous-flow modes. In the continuous-flow mode, the upper 6-port valve allows 1.0 mL samples of the reaction products to be injected from the sample loop onto the G.C. Helium gas passing through the valves acts to inject the sample onto the G.C. column when the upper 6-port valve handle is moved from right to left. When the middle 6-port valve is moved to the left to the pulse flow mode, the upper 6-port valve injects a 1.00 mL pulse of the feed stream through the reactor when the handle is moved from right to left (pulses of feed flow through the reactor at the same flow rate as the G.C. column, not the rate of the feed stream) and into the G.C.. When switching from continuous-flow to pulse-flow, all lines below the middle 6-port valve contain reactants, which are flushed directly into the G.C. column being used at that time. It is easier to use the shorter Poropak Q column to make this valve switch.

Figure 3 shows the lower 4-port valve of the reactor and the reactor bed. This valve is used to shut off and bypass flow from the reactor. This valve with the reactor bed can then be removed to allow the catalyst to be loaded and unloaded in a dry box. The catalyst bed is a 1.5 in x 1/4 in (o.d.) section of stainless steel tubing. The catalyst is held in place between two pads of quartz wool (quartz wool is used due to its higher melting point compared to glass wool). The reactor bed is mounted to the 4-port valve, extending below the heated valve box and into the furnace.

On-Line Gas Chromatography

Figure 4 shows the two valves in the analytical section of the G.C. These valves are mounted directly on the side of a Varian 3400 gas chromatograph equipped with a flame ionization detector (FID). Peaks were detected on a Varian 4270 integrator. The upper 4-port valve allows the column flow to be reversed, or backflushed. The lower 10-port valve

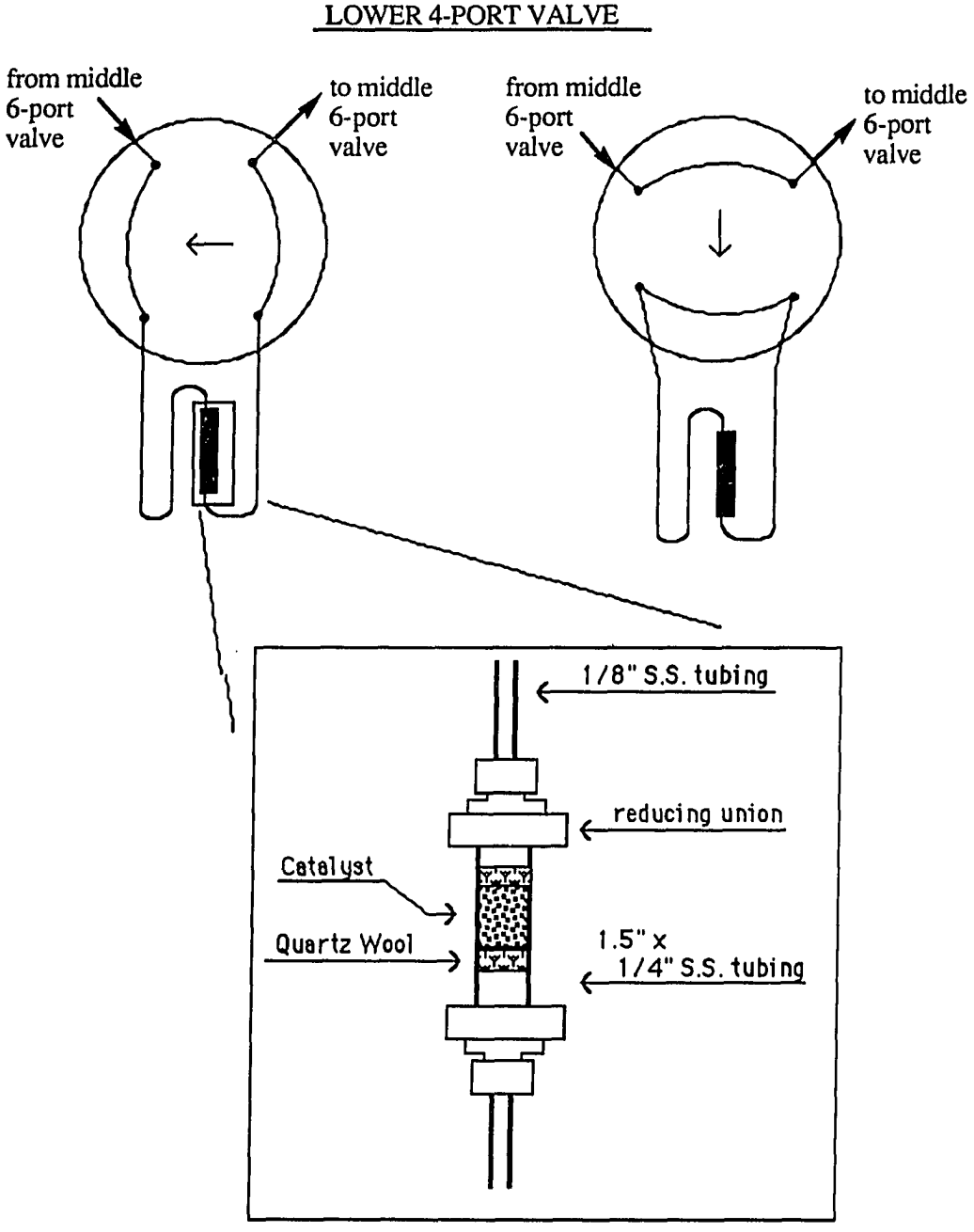

Figure 3. Lower 4-port Reactor Valve and Reactor Bed Diagram

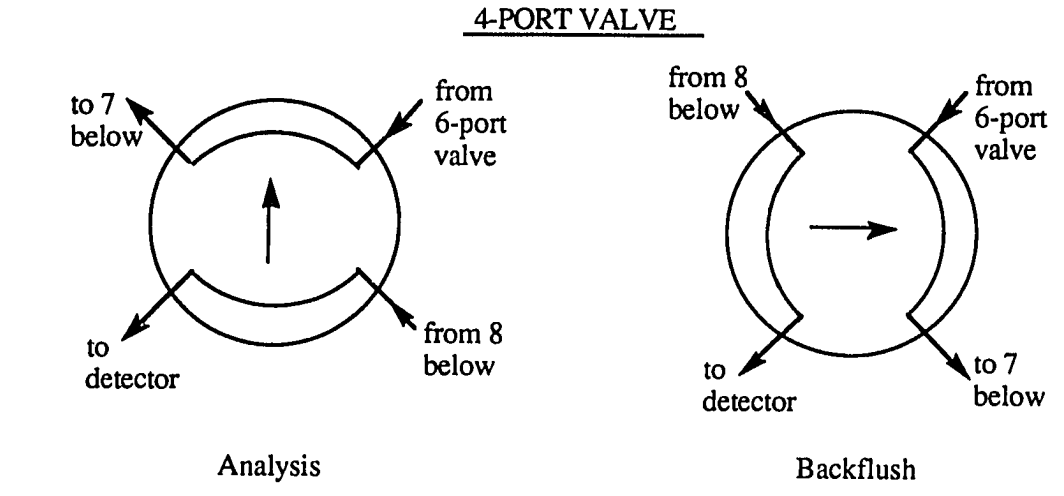

Figure 4. 4-port and 10-port G.C. switching valves which enable intercolum switching and backflush options.

switches between two available columns, either the picric acid column or the poropak Q column. With this design the column not being used maintains a He flow at all times.

Figure 5 shows a typical gas chromatogram from the reaction of thiophene with either H_2 or D_2 over $PbMo_{6.2}S_8$. The chromatogram was obtained from a 6 ft x 1/8 in stainless steel, 0.19% picric acid on Graphpak C column. The column was held at 40 °C for 5 min followed by a 35 ° / min ramp to 65 °C. This temperature was held for 2 min. The column temperature was then ramped to 85 °C. When this second ramp started, the 4-port valve was used to backflush the column, driving off thiophene. The C_4 gasses separated in the following order: 1-butene (rt =3.4) > cis-2-butene (rt = 4.6) > trans-2-butene (rt = 5.2) > 1,3-butadiene (rt =6.1).

Deuterium Distribution Calculations

Products from the microreactor were trapped at the 6-port valve vent (Figures 1 and 2) in a pyrex tube containing 5 mm glass beads and immersed in liquid nitrogen. Following the reaction, the trapped products are vacuum transferred into a 5 mm NMR tube containing 0.50 mL of $CHCl_3$ (dried over CaH_2 and distilled under nitrogen) for analysis by ^2H NMR and mass spectrometry. The ^2H NMR spectrum of each sample was recorded on a Varian VXR-300 spectrometer using $CHCl_3$ as the internal lock and standard (δ 7.24 ppm). The resolved 1,3-butadiene and thiophene peaks were integrated (see Figure 2, Section 5).

The sample was then submitted to the mass spectrometry lab for deuterium analysis. The analyses were carried out on a Finnigan 4000 G.C.-M.S. data system. The C_4 products separated on a GS-Alumina megabore column (J and W Scientific). The ionization energy of the mass spectrometer was reduced to 13 - 16 eV to minimize fragmentation of the parent ion (M-1).

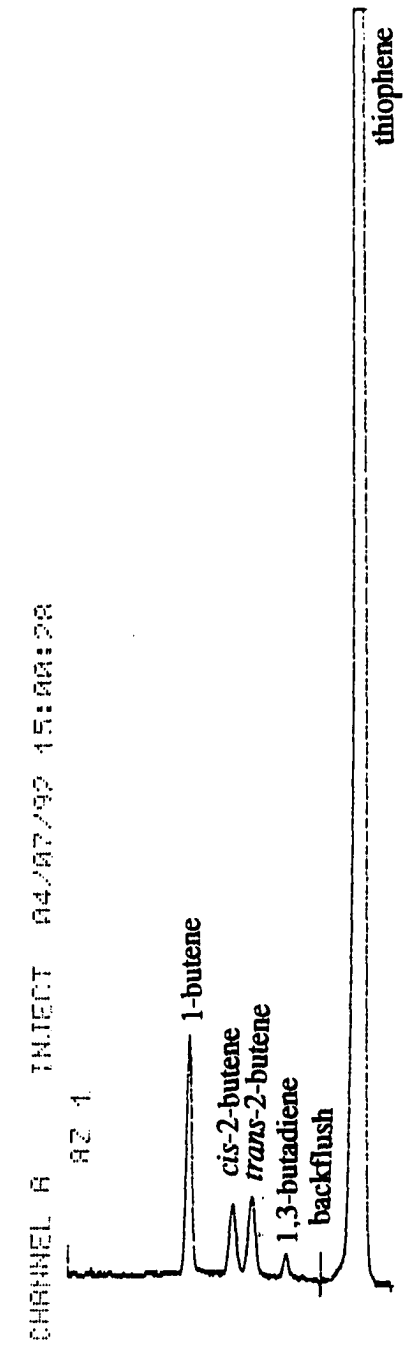

CHANNEL A INJECT 04/07/92 15:00:28
AZ 1

JWB 04/07/92 15:00:28 CH= "A" PS= 1.

FILE 1. METHOD A. BIN 17 INDEX 17

PEAK#	AREA%	RT	AREA	AR
1	3.974	3.42	1640	A1
2	1.526	4.66	630	A1
3	1.904	5.21	786	A1
4	0.373	6.18	154	A1
5	92.222	8.17	38062	A1
TOTAL	100.		41272	

Figure 5. Gas Chromatogram Obtained During Thiophene HDS Using the Picric Acid Column.

The mass spectrum of 1,3-butadiene, thiophene and 2,5-dihydrothiophene from the HDS reactions provide a distribution of deuterated products, d_0, d_1, . . . , d_n. These data have to be corrected, however, for the fragmentation of the parent ion and the natural abundance of heavy isotopes, ^2H, ^{13}C and ^{34}S. Each time samples from the reactor were submitted, an authentic standard sample of 1,3-butadiene, thiophene and 2,5-dihydrothiophene in $CHCL_3$ was also submitted to determine the following correction factors.

The fragmentation factor, α, is a ratio of the intensity of the M-1 peak (loss of H) to the intensity of the parent ion, M (eq 1):

$$\alpha = \frac{\text{M-1 peak intensity}}{\text{M peak intensity}} \qquad (1)$$

Typical values for α are shown in Table 3. The actual value of α depends upon

Table 3. Mass Spectral Correction Factors for 1,3-Butadiene, Thiophene and 2,5-Dihydrothiophene

Product	α	β_1	β_2
1,3-butadiene	0.090	0.045	
thiophene	0	0.056	0.048
2,5-dihydrothiophene	0.088	0.068	0.051

spectrometer operation conditions, and thus varied somewhat. No M-1 was ever detected for T. The peaks for M-2 were always less than 0.5 % and thus, neglected.

The correction factors, β_1 (for naturally occurring ^2H and ^{13}C) and β_2 (for naturally occurring ^{34}S) for naturally occurring heavy isotopes, is the ratio of the intensity of the M+1 and M+2 peaks to the intensity of the parent ion (eq 2 and 3):

$$\beta_1 = \frac{\text{M+1 peak intensity}}{\text{M peak intensity}} \qquad (2)$$

$$\beta_2 = \frac{\text{M+2 peak intensity}}{\text{M peak intensity}} \qquad (3)$$

Typical values for β_1 and β_2 are found in Table 3.

While the following discussion describes a common method for correcting the deuterium distribution,[2] (this same method is used by McCarty and Schrader.[3]) it is based on two critical assumptions, which may be a source of error. First, it is assumed that ^1H and ^2H are lost with equal probability; a qualitative argument suggests, however, that protium is lost preferentially.[4] Second, the molar mass intensities at all deuterated isomers are assumed to be equal. Significant error may also be introduced using these assumptions.[5] However, the only alternative would be to determine the mass spectrum for each of the deuterated isomers, a Ph.D. project in itself.

The mass spectral data for 1,3-butadiene is corrected as follows. Let Φ_i be the uncorrected intensity for the isomer containing i deuterium atoms, and let Θ_i be the corrected intensity. For i = 6 and 5, this gives eq 4 and 5.

$$\Theta_6 = \Phi_6 - \Theta_5\beta \qquad (4)$$

$$\Theta_5 = \Phi_5 - \Theta_4\beta \qquad (5)$$

Combining these two equations and dropping the second order terms gives eq 6.

$$\Theta_6 = \Phi_6 - \Phi_5\beta \qquad (6)$$

The intensity correction for i = 4 (eq 7) includes the fragmentation factor, α.

$$\Theta_4 = \Phi_4 - \Phi_3\beta - (1/6)\Theta_5\alpha - (6/6)\Theta_6\alpha \qquad (7)$$

Substitution into eq (2) gives eq (8) after dropping second order terms.

$$\Theta_5 = \Phi_5 - \Phi_4\beta \qquad (8)$$

Following this pattern of dropping second order terms gives a general equation (eq 9) for correction of i = 4, 3, 2 and 1.

$$\Theta_i = \Phi_i - \Phi_{i-1}\beta - (5-i/6)\Theta_{i+1}\alpha - (i+2/6)\Theta_{i+2}\alpha \qquad (9)$$

for i = 4,3,2,1

The peak for i = 0 is corrected using equation (10).

$$\Theta_0 = \Phi_0 - (5/6)\Theta_1\alpha - (2/6)\Theta_2\alpha \qquad (10)$$

Once the peak intensities have been corrected, the relative amounts of deuterium, d_i, for each fragment is calculated using equation (11). The numbers

$$d_i = \frac{\Theta_i}{\Sigma \Theta_i} \tag{11}$$

d_0 - d_6 make up the deuterium distribution, the relative amounts of deuterium contained in each isomer. From this distribution of d_i, the average amount of deuterium per molecule of 1,3-butadiene, or the Deuterium Number (D. N.), is calculated using equation (12).

$$D.\ N. = \Sigma\, i d_i \tag{12}$$

Table 4. Mass Spectral Correction Data for 1,3-Butadiene from the Deuterodesulfurization of Thiophene at 400 °C over $PbMo_{6.2}S_8$.

i	Φ_i	Θ_i	β	α	d_i	D.N.
6	5686	4988	0.0451	0.0903	0.07270	3.76
5	15460	14461			0.21076	
4	22124	20534			0.29926	
3	20424	18229			0.26566	
2	10837	8640			0.12592	
1	3054	1690			0.02463	
0	462	75			0.00109	

Plugging the uncorrected mass data into these equations, starting with eq 1, gives a typical distribution as shown in Table 4.

The corrections for thiophene and 2,5-dihydrothiophene are similar. In both these cases the correction for ^{34}S (β_2) is required. However, no M-1 peak was ever detected for thiophene. The equations for thiophene correction follow (eq 13 - 16).

$$\Theta_i = \Phi_i - \Phi_{i-1}\beta_1 - \Phi_{i-2}\beta_2 \qquad (13)$$

i=4, 3, 2 for thiophene

$$\Theta_1 = \Phi_1 - \Phi_0\beta_1 \qquad (14)$$

$$\Theta_0 = \Phi_0 \qquad (15)$$

The equations for 2,5-dihydrothiophene are as follows (eq 16 - 19).

$$\Theta_i = \Phi_i - \Phi_{i-1}\beta_1 - \Phi_{i-2}\beta_2 \qquad (16)$$

i=6, 5

$$\Theta_i = \Phi_i - \Phi_{i-1}\beta_1 - \Phi_{i-2}\beta_2 - (5-i/6)\Theta_{i+1}\alpha - (i+2/6)\Theta_{i+2}\alpha \qquad (17)$$

i = 4, 3, 2

$$\Theta_1 = \Phi_1 - \Phi_0\beta_1 - (4/6)\Theta_2\alpha - (3/6)\Theta_3\alpha \qquad (18)$$

$$\Theta_0 = \Phi_0 - (5/6)\Theta_1\alpha - (2/6)\Theta_2\alpha \qquad (19)$$

The deuterium distributions for both thiophene and 2,5-dihydrothiophene are calculated using equation (11) and the D. N. is calculated using equation (12).

Once the DN is calculated, this number is combined with the integrals from the ^2H NMR in order to determine the number of D atoms at each position on each 1,3-butadiene molecule. The deuterium at each position A, B and C is determined from equation (20), where X = A, B and C and I is the integral of each peak in the ^2H NMR spectrum.

$$D_X = \frac{I_X}{\Sigma I_X} (DN) \qquad (20)$$

References

(1) For more details see McCarty, K. F. *Ph.D. Thesis*, Iowa State University, **1985**.

(2) (a) Biemann, K. *Mass Spectrometry--Organic Chemical Applications*; McGraw-Hill: New York, **1962**.

(b) Davis, S. M.; Somorjai, G. A. *J. Phys. Chem.* **1983**, *87*, 1545.

(3) McCarty, K. F.; Schrader, G. L. *J. Catal.* **1987**, *103*, 261.

(4) Stevenson, D. P.; Wagner, C. D. *J. Chem. Phys.* **1951**, *19*, 11.

(5) (a) Amenomiya, Y.; Pottie, R. F. *Can. J. Chem.* **1968**, *46*, 1735.

(b) Amenomiya, Y.; Pottie, R. F. *Can. J. Chem.* **1968**, *46*, 1741.

GENERAL SUMMARY

This research indicates that, although thiophene and its methyl- and benzo-substituted derivatives are weakly binding ligands in organometallic complexes, stable η^1(S)-bound complexes, $Cp(CO)_2Ru(\eta^1(S)\text{-Th})^+$ and $Cp(CO)(PPh_3)Ru(\eta^1(S)\text{-Th})^+$ (Th = T, 2-MeT, 3-MeT, 2,5-Me_2T, Me_4T, BT and DBT), are formed. Once synthesized, these complexes are used to determine the relative binding strengths of the substituted thiophenes through equilibrium and kinetic studies of thiophene replacement. In general, increasing the number of methyl groups on thiophene increases its ability to bind through the S atom to the $Cp(CO)_2Ru^+$ fragment (T < 2-MeT < 3-MeT < 2,5-Me_2T < Me_4T). Thus, there is no steric interaction between the α-methyl groups on thiophene and metal center, as was previously suggested. However, replacing one CO at the metal center with a bulky PPh_3 ligand creates a steric interaction between the α-methyl groups on thiophene and the phenyl rings on phosphine, reducing the relative binding abilities of 2,5-Me_2T and Me_4T.

These studies also indicate that the binding of η^1(S)-thiophenes increases with benzo-substitution as well (T < BT < DBT). The η^1(S)-BT complexes, $Cp(PMe_3)_2Ru(\eta^1(S)\text{-BT})^+$ and $Cp(CO)(PPh_3)Ru(\eta^1(S)\text{-BT})^+$, are also synthesized by protonation of the corresponding benzothienyl complexes with CF_3SO_3H.

In the reactor studies of thiophene deuterodesulfurization, the first desulfurized product, 1,3-butadiene, incorporates 3.47 D atoms during the reaction at 400 °C at $PbMo_{6.2}S_8$. Between 0.1 and 0.4 D atoms are incorporated during deuterium exchange of thiophene before desulfurization. The 1,3-butadiene, however, does not exchange after it is formed on the catalyst, as indicated by the constant deuterium number (D.N.) over a range of thiophene conversions. Reactions of 2,5-DHT with D_2 also produces butadiene with almost no deuterium. Reactions of 1,3-butadiene with H_2S and D_2 indicate that H_2S inhibits both butadiene hydrogenation and deuterium exchange.

ADDITIONAL REFERENCES

(1) (a) Gates, B. C.; Katzer, J. R.; Schuit, G. C. A. *Chemistry of Catalytic Processes*; McGraw-Hill: New York, 1979, Chapter 5.

(b) Schuman, S. C.; Shalit, H. *Catalysis Rev.* **1970**, *4*, 245.

(c) Satterfield, C. N. *Heterogeneous Catalysis in Industrial Practice*; McGraw-Hill: New York, **1991**, P. 378.

(d) McCulloch, D.C. In *Applied Industrial Catalysis*; Vol 1, Leach, B. E. Ed; Academic: New York **1983**, p. 69.

(e) *Geochemistry of Sulfur in Fossil Fuels*; Orr, W. L.; White, C. M., Eds.; ACS Symposium Seried 429, American chemical Society: Washington D. C. **1990**.

(2) Desulfurization was found under two catagories: Catalytic Hydrorefining (7.8 million barrels/day) and Catalytic Hydrotreating (19.4 million barrels/day) in Thrash, L.A. *Oil and Gas J.* **1991**, *89(51)*, 39.

(3) (a) Speight, J. G. *The Desulfurization of Heavy Oil and Residua*; Marcel Dekker: New York, 1981.

(b) Lyapina, N. K. *Russian Chem. Rev.* **1982**, *51(2)*, 189.

(4) Girgis, M. J.; Gates, B. C. *Ind. Eng. Chem. Res*, **1991**, *30*, 2021.

(5) (a) Parham, T. G.; Merrill, R. P. *J. Catal.* **1984**, *85*, 295.

(b) Clausen, B. S.; Topsøe, H.; Candia, R.; Villadsen, J.; Lengeler, B.; Als-Nielsen, J.; Christensen, F. *J. Phys. Chem.* **1981**, *85*, 3868.

(6) Schrader, G. L.; Cheng, C. P. *J. Catal.* **1983**, *80*, 369.

(7) Pollack, S. S.; Mokovsky, L. E.; Brown, F. R. *J. Catal.* **1979**, *59*, 452.

(8) (a) Li, C. P.; Hercules, D. M. *J. Phys. Chem.* **1984**, *88*, 456.

(b) Zingg, D. S.; Makovsky, L. E.; Tisher, R. E.; Brown, F. R.; Hercules, D. M. *J. Phys. Chem.* **1980**, *84*, 2898.

(c) Patterson, T. A.; Carver, J. C.; Leyden, D. E.; Hercules, D. M. *J. Phys. Chem.* **1976**, *80*, 1700.

(9) Topsøe, H.; Clausen, B. S.; Candia, R.; Wivel, C.; Mørup, S. *J. Catal.* **1981**, *68*, 433.

(10) (a) Angelici, R. J. *Coord. Chem. Rev.* **1990**,*105*, 61.

(b) Rauchfuss, T. B. *Prog. Inorg. Chem.* **1991**, *39*, 259.

(11) (a) Prins, R.; de Beer, V. H. J.; Somorjai, G. A. *Catal. Rev.-Sci. Eng.* **1989**, *31*, 1.

(b) Friend, C. M.; Wiegard, B. C. *Chem. Rev.* **1992**, *92*, 491.

(c) Zdrazil, M. *Appl. Catal.* **1982**, *4*, 107.

(d) Kemball, C. *Chem. Soc. Rev.* **1984**, *13* , 375.

(12) Sauer, N. N. *Ph. D. Thesis*, Iowa State University, 1986.

(13) Moldavski, B. L.; Prokoptscuk, J. *J. Appl. Chem. U. S. S. R.* **1932**, *5*, 619.

(14) Griffith, R. H.; Marsh, J. D. F.; Newling, W. B. S. *Proc, Roy. Soc. London* **1949**, *A197*, 194.

(15) (a) Kieran, P.; Kemball, C. *J. Catal.* **1965**, *4*, 380.

(b) Kieran, P.; Kemball, C. *J. Catal.* **1965**, *4*, 394.

(16) Kwart, H.; Schuit, G. C. A.; Gates, B. C. *J. Catal.* **1980**, *61*, 128.

(17) Daudel, P.; Daudel, R.; Ng, P. B.-H.; Martin, M. *Bull. Soc. Chim.* **1948**, *15*, 1202.

(18) Komarewski and Knaggs *Ind. Eng. Chem.* **1951**, *43*, 1415

(19) (a) Owens, P. J.; Amberg, C. H. *Adv. in Chem.* **1961**, *Ser. No. 33*, 182.

(b) Owens, P. J.; Amberg, C. H. *Can. J. Chem.* **1962**, *40*, 941.

(c) Owens, P. J.; Amberg, C. H. *Can. J. Chem.* **1962**, *40*, 947.

(20) (a) Desikan, P.; Amberg, C. H. *Can. J. Chem.* **1963**, *41*, 1966.

(b) Desikan, P.; Amberg, C. H. *Can. J. Chem.* **1964**, *42*, 843.

(21) Kolboe, S.; Amberg, C. H. *Can. J. Chem.* **1966**, *44*, 2623.

(22) Kolboe, S. *Can. J. Chem.* **1969**, *47*, 352.

(23) Ratnasamy, P.; Fripiat, J. J. *Trans. Faraday. Soc.* **1974**, *66*, 2897.

(24) Lipsch, J. M. J. G.; Schuit, G. C. A. *J. Catal.* **1969**, *15*, 179.

(25) (a) Nickolson, D. E. *Anal. Chem.* **1960**, *32*, 1365.

(b) Nickolson, D. E. *Anal. Chem.* **1962**, *34*, 370.

(26) Mikovsky, R. J.; Silvestri, A. J.; Heineman, J. *J. Catal.* **1974**, *34*, 324.

(27) McCarty, K. F.; Schrader, G. L. *J. Catal.* **1987**, *103*, 261.

(28) Cowley, S. W. Ph.D. Thesis, Southern Illinois University, 1975.

(29) Blake, M. R.; Eyre, M.; Moyes, R. B.; Wells, P. B. *Stud. Surf. Sci. Catal.* **1981**, *7*, 591.

(30) Zdrazil, M. *Coll. Czech. Chem. Commun.* **1977**, *42*, 1484.

(31) Devanneaux, J.; Maurin, J. *J. Catal.* **1981**, *69*, 202.

(32) Zdrazil, M. *Coll. Czech. Chem. Commun.* **1975**, *40*, 3491.

(33) (a) Angelici, R. J. *Acc. Chem. Res.* **1988**, *22*, 387.

(b) Sauer, N. N.; Markel, E. J.; Schrader, G. L.; Angelici, R. J. *J. Catal.* **1989**, *117*, 295.

(34) Lee, C. C.; Iqbal, M.; Gill, U. S.; Sutherland, R. G. *J. Organomet. Chem.* **1985**, *288*, 89.

(35) (a) Spies, G. H.; Angelici, R. J. *J. Am. Chem. Soc.* **1985**, *107*, 5569.

(b) Spies, G. H.; Angelici, R. J. *Organometallics* **1987**, *6*, 1897.

(36) Fischer, E. O.; Öfele, K. *Chem. Ber.* **1958**, *91*, 2395.

(37) (a) Singer, H. *J. Organomet. Chem.* **1967**, *9*, 135.

(b) Lesch, D. A.; Richardson, J. W.; Jacobson, R. A.; Angelici, R. J. *J. Am. Chem. Soc.* **1984**, *106*, 2901.

(38) Huckett, S. C.; Miller, L. L.; Jacobson, R. A.; Angelici, R. J. *Organometallics* **1988**, *7*, 686.

(39) Sanchez-Delgado, R. A.; Marquez-Silva, R. L.; Puga, J.; Tiripicchio, A.; Camellini, M. T. *J. Organomet. Chem.* **1986**, *316*, C35.

(40) (a) Sauer, N. N.; Angelici, R. J. *Inorg. Chem.* **1987**, *27*, 2160.

(b) Glavee, G. N.; Daniels, L. M.; Angelici, R. J. *Organometallics* **1989**, *8*, 1856.

(c) Glavee, G. N.; Daniels, L. M.; Angelici, R. J. *Inorg. Chem.* **1989**, *28*, 1751.

(41) Markel, E. J.; Schrader, G. L.; Sauer, N. N.; Angelici, R. J. *J. Catal.* **1989**, *116*, 11.

(42) Chalconer, P. A. *Handbook of Coordination Catalysis in Organic Chemistry*; Butterworths: London, 1986; p. 403.

(43) Choi, M.-G.; Daniels, L. M.; Angelici, R. J. *Inorg. Chem.* **1991**, *30*, 3647.

(44) Chen, J.; Daniels, L. M.; Angelici, R. J. *J. Am. Chem. Soc.* **1990**, *112*, 199.

(45) (a) Jones, W. D.; Dong, L. *J. Am. Chem. Soc.* **1991**, *113*, 559.

(b) Dong, L.; Duckett, S. B.; Ohman, K. F.; Jones, W. D. *J. Am. Chem. Soc.* **1992**, *114*, 151.

(46) Oglivy, A. E.; Skaugset, A. E.; Rauchfuss, T. B. *Organometallics* **1989**, *8*, 2739.

(47) Jones, W. D.; Chen, R. M. *Organometallics* **1992**, *11*, 2698.

(48) Curtis, M. D.; Penner-Hahn, J. E.; Schwank, J.; Baralt, O.; McCabe, D. J.; Thompson, L.; Waldo, G. *Polyhedron* **1988**, *7*, 2411.

(49) Delmon, B.; Dallons, J.-L. *Bull. Soc. Chim. Belg.* **1988**, *97*, 473.

(50) Chen, J.; Angelici, R. J. *Organometallics* **1990**, *9*, 849.

ACKNOWLEDGMENTS

There are a number of people who deserve an acknowledgment as they have contributed to this dissertation, whether they know it or not. At this time, I would like to take the opportunity to thank

Jill, my wife, for her continued support, patience and an unlimited supply of chocolate chip cookies.

Professor Robert J. Angelici for his guidance, encouragement and support during my graduate career. It has been a pleasure to work in the Angelici group.

My Mom and Dad for encouraging me to continue my education.

Dr William H. Gong for his advice, interest and long-distance pep talks.

Past and present members of the A-Team: Dr. Ruth Doyle, Dr. Dave Miller, Dr. Moon-Gun Choi, Dr. John Sowa, Dr. Jiabi Chen, Dr. Valerio Zanotti, Dr. K. Mohan Rao, Chia-Mei Jen-Wang, Mary Rottink, Mitch Robertson, Hyoung Jun, Carter White, Mike Sanger, Dongmei Wang and Chip Nataro. A special thanks to Mary and Mitch for their friendship, their sense of humor and for keeping me from taking myself and my research too seriously.

This work was performed at Ames Laboratory under contract no. W-7405-eng-82 with the U. S. Department of Energy. The United States Government has assigned the DOE Report number IS-T 1632 to this thesis.